



University of Natural Resources
and Life Sciences, Vienna



MASTER THESIS

BIOTECHNOLOGICAL PRODUCTION OF FLAVOURINGS

Marcel Hans
0940817

**In partial fulfilment of the requirements
for the degree of
Diplom-Ingenieur**

Master's programme: Biotechnology

Supervisor: Prof. Dr. Diethard Mattanovich

Co-Supervisor: Dr. Michael Hofer

Vienna, 08 February 2016

ACKNOWLEDGEMENT

I would like to thank everyone who supported me during the development of this master thesis.

First, I want to acknowledge Prof. Dr. Diethard Mattanovich of the Department of Biotechnology at the University of Natural Resources and Life Sciences in Vienna, Austria as my thesis advisor. He was always available whenever I had questions about my research, writing and the organisation of the graduation.

My sincere appreciation goes to my supervisor Dr. Michael Hofer of the project group BioCat of the Fraunhofer Institute for Interfacial Engineering and Biotechnology in Straubing, Germany. I am very grateful for his patience and his very valuable advice during the experiments and writing of this thesis.

I also want to thank all the co-workers of the BioCat group for the kind working environment, especially Christina Faltl and Patricia Huber for the introduction to the lab and continuous help during the experiments.

Finally, I want to express my profound gratitude to my parents for supporting and encouraging me throughout my whole studies, which would not have been possible without them. Thank you.

Table of Contents

1	Introduction.....	1
1.1	Flavourings	1
1.1.1	Flavouring production and the food law	1
1.2	Carotenoids	2
1.2.1	ϵ -Carotene biosynthesis	4
1.3	Carotenoid Cleavage Dioxygenases.....	6
1.3.1	The carotenoid cleavage dioxygenase 1 of <i>Vitis vinifera</i> (VvCCD1)	7
1.3.2	Ionones.....	9
2	Aims of the work	11
3	Material	12
3.1	Equipment	12
3.2	Chemicals.....	13
3.3	Media and buffers	14
3.4	Enzymes.....	14
3.5	Microorganisms.....	15
3.6	Vectors and Plasmids	15
3.7	Kits	15
3.8	Oligonucleotides.....	16
3.9	Ladders	17
4	Methods	18
4.1	Microbiological Methods	18
4.1.1	Cultivation of <i>E. coli</i> strains	18
4.1.2	Optical density.....	19
4.1.3	Expression of VvCCD1.....	19
4.1.4	Protein expression analysis by SDS-PAGE	19
4.1.5	Reducing background expression of VvCCD1.....	20
4.1.6	Estimation of theoretical α -ionone concentrations	20
4.2	Product purification.....	24
4.2.1	α -ionone stability	24
4.2.2	Two-phase system with n-Hexane	25
4.2.3	Direct extraction of α -ionone from the supernatant	25
4.2.4	Exhaust air collection.....	26
4.3	Analytical Methods.....	27
4.3.1	Carotene extraction.....	27

4.3.2	Carotene analysis by HPLC-PDA	27
4.3.3	Volatile analysis by GC-MS	28
4.4	Cloning of VvCCD1 from pET22b-VvCCD1 to pBAD-A	29
4.4.1	Amplification of VvCCD1 by Phusion-PCR	31
4.4.2	Agarose gel electrophoresis	32
4.4.3	Gel extraction of DNA.....	32
4.4.4	Determination of the DNA Concentration	32
4.4.5	Restriction digest.....	33
4.4.6	Ligation	34
4.4.7	Transformation by electroporation.....	35
4.4.8	Selection of transformants.....	35
4.4.9	Colony PCR.....	35
4.4.10	Glycerol stock	36
4.4.11	Sequencing	36
4.5	<i>In vitro</i> experiment.....	37
5	Results	38
5.1	Carotene analysis of <i>E. coli</i> BL21(DE3) pAC-Epsilon	38
5.1.1	Carotene identification.....	38
5.2	Carotene and apocarotene analysis of <i>E. coli</i> BL21(DE3) pAC-Epsilon + pET22b-VvCCD1....	40
5.3	Influence of pET22b on the carotene production	42
5.4	Background expression	43
5.5	Cloning of VvCCD1 from pET22b-VvCCD1 into pBAD (Method 4.4)	45
5.6	Carotene and apocarotene analysis of <i>E. coli</i> BL21(DE3) pAC-Epsilon + pBAD-VvCCD1.....	46
5.7	Unspecific carotene degradation	48
5.8	<i>In vitro</i> experiments	50
6	Discussion	51
6.1	Carotene identification.....	51
6.2	Carotene production and analysis.....	51
6.2.1	Influence of pET22b.....	51
6.3	Background expression	51
6.4	Apocarotene production and analysis.....	52
6.4.1	Unspecific carotene degradation	53
6.4.2	VvCCD1 functionality.....	54
6.5	Cloning.....	55
6.6	<i>In vitro</i> experiments	56

7	Summary and future prospect	57
8	References.....	59
9	Appendix.....	64
9.1	Standard measurements	64
9.1.1	Carotene analysis by HPLC-PDA	64
9.1.2	Ionone analysis by GC-MS	65
9.2	Vector maps	66
9.2.1	pET22b.....	66
9.2.2	pBAD-A	68
9.3	Sequence alignment.....	71
10	Affirmation	78

Abbreviations

ABA	Abscisic acid
Amp	Ampicillin
CCD	Carotenoid cleavage dioxygenase
Cm	Chloramphenicol
DCM	Methylene chloride
DMAPP	Dimethylallyl diphosphate
dNTP	Deoxyribose nucleoside triphosphate
DTT	Dithiothreitol
<i>E. coli</i>	<i>Escherichia coli</i>
EthAc	Ethyl acetate
FPP	Farsenyl diphosphate
G3P	Glyceraldehyde-3-phosphate
GC	Gas chromatography
GGPP	Geranyl geranyl diphosphate
Glc	D-Glucose
GMO	Genetically modified organism
GPP	Geranyl diphosphate
HPLC	High pressure liquid chromatography
IPP	Isopentenyl diphosphate
IPTG	Isopropyl β -D-1-thiogalactopyranoside
KOH	Potassium hydroxide
L-Ara	L-Arabinose
LB	Lysogeny broth
MEP/DOXP	2-C-methyl-D-erythritol 4-phosphate / 1-deoxy-D-xylulose 5-phosphate
MS	Mass spectrometry
NCED	9-cis-epoxycarotenoid dioxygenase
OD	Optical density
PDA	Photo diode array
PTFE	Polytetrafluoroethylene
Pyr	Pyruvate
RT	Room temperature
SPME	Solid phase micro extraction
VvCCD1	Carotenoid cleavage dioxygenase 1 of <i>Vitis vinifera</i>

Figure index

Figure 1: General carotenoid structure (Lycopene); the dashed lines indicate the formal division into isoprenoid units.....	3
Figure 2: General carotenoid structure with atom numbering.....	3
Figure 3: β -carotene: a very common carotene and a vitamin A precursor in humans	3
Figure 4: Zeaxanthin: a xanthophyll and the abscisic acid precursor in plants	3
Figure 5: ϵ -carotene: rarely found in nature.....	4
Figure 6: The non-mevalonate pathway for the biosynthesis of the C5 precursors to isoprenoids, IPP and DMAPP. ADP: adenosine 5'-diphosphate, ATP: adenosine 5'-triphosphate, CDP-ME: 4-diphosphocytidyl-2C-methyl-d-erythritol, CDP-ME2P: 4-diphosphocytidyl-2C-methyl-d-erythritol-2-phosphate, DMAPP: dimethylallyl diphosphate, DXS: 1-deoxy-d-xylulose 5-phosphate synthase, IPP: isopentenyl diphosphate, MECDP: 2C-methyl-d-erythritol-2,4-cyclodiphosphate. (Crane, et al., 2008)4	4
Figure 7: Schematic overview of the ϵ -carotene synthesis.....	5
Figure 8: Reaction scheme of VvCCD1 activity on ϵ -carotene (1). The arrows indicate the cleavage at the 9,10(9',10') double bond positions. This activity produces two molecules of α -ionone (2) and a central C14-dialdehyde (3).....	7
Figure 9: Quick Load, 1 kb DNA Ladder 50 μ g/ μ L, New England Biolabs	17
Figure 10: Protein Ladder (10-250 kDa), New England Biolabs.....	17
Figure 11: β -carotene calibration.....	21
Figure 12: Estimation of the extinction coefficient of ϵ -carotene at 450 nm from its absorbance spectrum.	23
Figure 13: Scheme of the exhaust air collection setup.	26
Figure 14: Scheme of the cloning procedure. The VvCCD1 gene was amplified from pET22b-VvCCD1, digested with HindIII and BsaI and inserted into the previously NcoI and HindIII digested pBAD-A vector. With BsaI being an exocutter, it was possible to design the complementary sticky end to the NcoI sticky end of the vector.....	30
Figure 15: Scheme of the ligation of the complementary sticky ends of the vector and insert DNA... 34	34
Figure 16: Chromatogram of <i>E. coli</i> BL21(DE3) pAC-Epsilon grown at 16 °C for 48 hours.	38
Figure 17: Chromatogram of <i>E. coli</i> BL21(DE3) pAC-Epsilon + pET22b-VvCCD1 grown at 30 °C for 41 hours.....	40
Figure 18: GC-MS chromatogram of the direct extraction of α -ionone from the culture suspension. 41	41
Figure 19: Typical carotene profile for <i>E. coli</i> BL21(DE3) pAC-Epsilon (6 data points)	42
Figure 20: Typical carotene profile for <i>E. coli</i> BL21(DE3) pAC-Epsilon + pET22b. (3 data points)	42
Figure 21: SDS-PAGE of the protein expression analysis of <i>E. coli</i> BL21(DE3). The arrow indicates an overexpressed protein of about 60 kDa in both clones containing the VvCCD1 gene. 1: pAC-Epsilon; 2: pAC-Epsilon + pET22b; 3: pAC-Epsilon + pET22b-VvCCD1; 4: pAC-Epsilon + pET22b-VvCCD1 + 0.1 mM IPTG.	43
Figure 22: Carotenes in cultures with and without glucose as catabolite repressor.....	44
Figure 23: Effect of glucose addition on the amount of carotenes in cultures with VvCCD1	44
Figure 24: Typical carotene profile for <i>E. coli</i> BL21(DE3) pAC-Epsilon (6 data points)	45
Figure 25: Carotene profile for <i>E. coli</i> BL21(DE3) pAC-Epsilon + pBAD grown at 30 °C for 24 hours. (2 data points)	45
Figure 26: Pellets of <i>E. coli</i> BL21(DE3) 1: pAC-Epsilon + pBAD; 2: pAC-Epsilon + pBAD + 0.1 % L-Arabinose; 3: pAC-Epsilon + pBAD-VvCCD1; 4: pAC-Epsilon + pBAD-VvCCD1 + 0.1 % L-Arabinose	46

Figure 27: Pellet colour comparison of <i>E. coli</i> BL21(DE3) with different plasmids. 1: pAC-Epsilon, 2: pAC-Epsilon + pET22b, 3: pAC-Epsilon + pBAD, 4: pAC-Epsilon + pBAD-VvCCD1	46
Figure 28: SDS-PAGE of <i>E. coli</i> BL21(DE3) pAC-Epsilon + pBAD-VvCCD1 with L-Arabinose concentrations from 0.00002% to 0.2%. The arrow indicates an overexpressed protein of about 60 kDa in clones containing the VvCCD1 gene. 1: negative (<i>E. coli</i> BL21(DE3) pAC-Epsilon + pBAD); 2: <i>E. coli</i> BL21(DE3) pAC-Epsilon + pBAD-VvCCD1 without L-Arabinose; 3: 0.00002 % L-Arabinose; 4: 0.0002 % L-Arabinose; 5: 0.002 % L-Arabinose; 6: 0.02 % L-Arabinose; 7: 0.2 % L-Arabinose; 8: <i>E. coli</i> BL21(DE3) pAC-Epsilon + pBAD in M9; 9: <i>E. coli</i> BL21(DE3) pAC-Epsilon + pBAD-VvCCD1 in M9	47
Figure 29: Zoomed in Chromatogram of SPME measurements. From top to bottom: <i>E. coli</i> BL21(DE3) pAC-Epsilon and <i>E. coli</i> BL21(DE3) pAC-Epsilon + pET22b-VvCCD1 + 0.25 mM IPTG.....	48
Figure 30: Further zoomed in Chromatogram of SPME measurement of <i>E. coli</i> containing different plasmids. From top to bottom: pAC-Epsilon; pAC-Epsilon + pBAD; pAC-Epsilon + pET22b; pAC-Epsilon + pET22b-VvCCD1; pAC-Epsilon + pET22b-VvCCD1 + 0.25 mM IPTG	48
Figure 31: Amount of α -ionone in ϵ -carotene oxidation test. The sample which was grown with nitrogen in the headspace of the SPME vial has about 5 times less α -ionone present.....	49
Figure 32: Chromatogram of the <i>in vitro</i> assay 1. From top to bottom: 1 mL samples of the reaction suspension were taken at t=0 h; 1 h; 17.5 h; 24 h; 96 h. The last row shows the extracted reaction suspension after 96 hours which was concentrated by vacuum distillation.	50
Figure 33: β -carotene standard.....	64
Figure 34: Chromatogram of the lycopene standard.....	64
Figure 35: Chromatogram of the α -ionone and β -ionone standards.....	65
Figure 36: pET22b vector map (Novagen TB038 12/98)	66
Figure 37: Vector map of pET22b-VvCCD1.....	67
Figure 38: pBAD vector map (Invitrogen pBAD User Manual, 2010)	68
Figure 39: pBAD vector multiple cloning site. Row 301 shows the initiation ATG where VvCCD1 was cloned into.....	69
Figure 40: Vector map of pBAD-VvCCD1.....	70
Figure 41: Overview of the alignment. The arrows display the forward and reverse sequencing runs. The filled red part of the arrows resembles the aligned sequences.....	71

Table index

Table 1: Reported VvCCD1 reactions.	8
Table 2: Odour properties and odour detection thresholds of ionones.....	9
Table 3: List of used equipment.....	12
Table 4: List of used chemicals.....	13
Table 5: List of used media and buffer solutions.....	14
Table 6: List of used Enzymes.....	14
Table 7: List of used strains.....	15
Table 8: List of used vectors.....	15
Table 9: List of used plasmids.....	15
Table 10: List of used DNA purification kits.....	15
Table 11: List of used oligonucleotides.....	16
Table 12: Growing conditions of <i>E. coli</i> BL21(DE3) clones.....	18
Table 13: SDS-PAGE settings.....	19
Table 14: Weighed masses of standards.....	21
Table 15: β -carotene calibration points.....	21
Table 16: Standard preparation inaccuracy.....	22
Table 17: Injector inaccuracy.....	22
Table 18: Extinction coefficients of carotenes in petroleum ether.....	22
Table 19: HPLC eluent gradient.....	27
Table 20: GC-MS measurement parameter.....	28
Table 21: GC-MS temperature gradient.....	28
Table 22: PCR reaction mixture for VvCCD1 amplification from pET22b-VvCCD1.....	31
Table 23: Thermocycler setup for VvCCD1 amplification from pET22b-VvCCD1.....	31
Table 24: PCR reaction mixture for the amplification of the VvCCD1-Amplicon.....	32
Table 25: Expected fragment sizes after the restriction digest.....	33
Table 26: Calculation of the enzyme units for the restriction digest.....	33
Table 27: Restriction digest reaction mixture.....	34
Table 28: Calculation of the volume of DNA needed for ligation.....	35
Table 29: Electroporator settings for different <i>E. coli</i> strains.....	35
Table 30: PCR reaction mixture for colony PCR.....	36
Table 31: Thermocycler setup for colony PCR.....	36
Table 32: Absorbance spectra of the extracted compounds of <i>E. coli</i> BL21(DE3) pAC-Epsilon.....	39
Table 33: Absorbance maxima of selected carotenoids in different solvents.....	40
Table 34: Sizes of genes and corresponding proteins.....	56

Abstract

The extraction of flavourings from nature is often not feasible due to low concentrations in the raw material. Though many flavourings can be chemically synthesised, they cannot be labelled as a “natural flavouring substance” which reduces their market value. The biotechnological production using whole cells or enzymes is generating compounds allowed to be labelled as a “natural flavouring substance”.

The flavouring of interest of this work is rarely found in nature and usually only present in trace amounts. Enzymes producing this flavouring from a precursor compound have already been identified and isolated, but it has not been described which of the two symmetrical varieties (enantiomers) is generated, both varieties showing different aroma properties.

The main objective of this work was to establish the biotechnological production of the flavouring. The optimisation of this process towards high yield and easy purification as well as the identification of the actual enantiomer being produced were further objectives.

A plasmid containing the gene of interest was introduced into an *E. coli* strain accumulating the precursor. The cells were grown in shaking flasks under various conditions. Alternatively, the gene was cloned into another vector. Analytical methods were HPLC-PDA for the investigation of the precursor and SPME-GC-MS for volatile products of the cleaving reaction.

The enzyme was highly expressed without induction in both vector systems. Due to its broad substrate specificity it was cleaving compounds involved in the biosynthesis of the precursor, therefore preventing the generation of the flavouring itself. Attempts to reduce the background expression were not successful.

The production of the flavouring of interest could not be established because of the highly background expressed enzyme. Further objectives could therefore not be followed. Further cloning work is needed to achieve a controllable enzyme expression and thereby flavouring production.

Zusammenfassung

Die Extraktion von Aromastoffen aus der Natur ist aufgrund ihrer zumeist geringen Konzentrationen im Rohmaterial nicht sinnvoll. Obwohl viele Aromastoffe auch chemisch synthetisiert werden können, dürfen diese, im Gegensatz zu biotechnologisch produzierten, nicht als „natürlicher Aromastoff“ bezeichnet werden, was ihren Marktwert verringert.

Der Aromastoff im Fokus dieser Arbeit kommt nur selten und nur in Spuren in der Natur vor. Enzyme zur Produktion des Stoffes wurden bereits identifiziert und isoliert. Welches der zwei symmetrischen Stoffe (Enantiomere) mit unterschiedlichen Geruchseigenschaften bei der Reaktion entsteht, wurde jedoch nicht gezeigt.

Das Hauptziel dieser Arbeit war die biotechnologische Produktion des Aromastoffes zu etablieren. Die Optimierung des Prozesses in Richtung hoher Ausbeuten und einfacher Aufreinigung, sowie die Identifikation des Enantiomers waren weitere Ziele.

Ein *E. coli* Stamm, der den Ausgangsstoff bereits anreichert, wurde mit einem weiteren Plasmid modifiziert. Nach Induktion wandelt das Enzym den Ausgangsstoff in den Aromastoff um. Die Zellen wurden in Schüttelkolben unter verschiedenen Wachstumsbedingungen wachsen gelassen. Alternativ wurde das Gen in einen anderen Vektor kloniert. Die analytischen Methoden umfassten HPLC-PDA zur Untersuchung des Ausgangsstoffes und SPME-GC-MS zur Analyse der flüchtigen Reaktionsprodukte.

Bei beiden Vektorsystemen wurde das Enzym auch ohne Induktion stark exprimiert. Durch die breite Substratspezifität wurden Vorstufen des Ausgangsstoffes kontinuierlich zerstört, wodurch die Produktion des Aromastoffes verhindert wurde. Versuche, die Hintergrundexpression zu verringern waren nicht erfolgreich.

Aufgrund der hohen Hintergrundexpression konnte die Produktion des Aromastoffes nicht etabliert werden. Weitere Ziele konnten daher nicht verfolgt werden. Es sind weitere Klonierungsarbeiten nötig, um eine kontrollierbare Genexpression und damit Aromastoffproduktion zu gewährleisten.

1 Introduction

1.1 Flavourings

The term "flavourings" is defined in Article 3, paragraph 2 of Regulation (EC) No 1334/2008 on flavourings:

“(a) ‘flavourings’ shall mean products:

(i) not intended to be consumed as such, which are added to food in order to impart or modify odour and/or taste;“

Hence flavourings are usually added to food or cosmetic products to alter or improve the perceptible taste and smell of these products, also called “aroma”. The aroma of a product was found to be one of the most important parameter regarding their perceived quality and consumer acceptance. The most common characteristic is their volatility and low odour thresholds to be perceived (Bicas, et al., 2010).

First unaware about the scientific background, humanity was consciously altering and improving the taste and smell of food for thousands of years beginning with the control of fire, leading to cooked and smoked food products, the gathering and use of aromatic plants and spices for seasoning and the extracts and aromatic oils of such as fragrances. Even without any knowledge about microbiology mankind was using microbiological systems in fermentation products like bread, cheese, wine and beer. The first distillation processes lead to the first separation of chemical compounds and to the production of ethanol.

With the rapid increase in knowledge about organic chemistry in the early 19th century the chemical structure of isolated aromatic compounds could be identified. The first isolated flavouring compounds were cinnamaldehyde (1834) and benzaldehyde (1837). Only a few years later the first flavouring compound Benzaldehyde (1845) followed by other important flavouring agents like vanillin (1870), coumarin (1874) and β -ionone (1893) could be chemically synthesised and used in the food and cosmetic industry. With the identification of microbes and the understanding of molecular biology humans began to consciously use, improve and genetically design microbes for the production of fermented foods and biopharmaceutical products like human insulin or as biocatalysts for the production of specific chemical compounds as an alternative to chemical transformation.

1.1.1 Flavouring production and the food law

A flavouring is a *chemically defined substance*. “The scientifically unfounded opinion of the average consumer that natural chemicals are somehow healthier than synthetics is reflected by food laws...” (Krings & Berger, 1998). Before 2009 flavouring substances have been discriminated between:

- “natural” (compounds which have been identified in nature and were obtained from nature)
- “nature identical” (compounds which have been identified in nature but were chemically synthesized)
- “artificial” (compounds which have not been identified in nature which were chemically synthesized)

The new regulation only discriminates between “flavouring substance” and “natural flavouring substance”. The label “natural flavouring substance” can be applied when the “substances are

naturally present and have been identified in nature” and which are “obtained by appropriate physical, enzymatic or microbiological processes from material of vegetable, animal or microbiological origin either in the raw state or after processing for human consumption.” (REGULATION (EC) No 1334/2008).

Flavouring production

There are three basic methods to obtain an aroma compound:

- Extraction from nature
- Chemical transformation
- Biotechnological production (de-novo-synthesis and biotransformations)

In nature, aroma compounds are usually present in low concentration, which increases the extraction and purification needs. The availability and quality of the raw material is dependent on seasonal, climatic and respective political changes. The potential toxicity of solvents contains additional ecological risks.

In chemical transformations, the reaction rates are fast and the product yields in high concentration. However these reactions are often conducted under pressure at high temperatures, requiring suitable safety measurements regarding the reactor design. Chemical transformations are also usually not regio- and stereospecific, leading to a mixture (racemate) of compounds, resulting in different aroma properties than the intended product. Furthermore they cannot be labelled as “natural flavouring substance”, decreasing their economic value due to the increase in the consumers environmental and health awareness, which increased the use of natural flavours obtained from natural sources.

In biotechnological production, whole cells and/or free enzymes are used. These biocatalysts can completely synthesise a complex product from simple molecules through a cascade of reactions (de-novo-synthesis) or fulfil only one or a few reactions (biotransformation). In comparison to chemical transformations reactions are stereo- and regiospecific only requiring mild reaction conditions but do not reach as high concentrations, requiring more effort in purification. Flavouring compounds produced by cells or enzymes can be labelled as “natural flavouring substance”, increasing its economic value. (Bicas, et al., 2010)

Genetically modified organisms (GMO’s) are considered as production aids when they are only used during the production process of a compound and are no longer present in the final product. [REGULATION (EC) No 1829/2003] Flavouring substances which were produced by GMO’s are therefore also considered as “natural flavouring substances”.

“The global flavour and fragrance market...” including flavour compounds of both natural and synthetic origin “...totaled \$23.9 billion in 2013. This market is expected to grow to \$25.3 billion in 2014 and \$35.5 billion in 2019, a compound annual growth rate (CAGR) of 5.8 %.” (BBC Research, 2014).

1.2 Carotenoids

Carotenoids are hydrophobic C₄₀ terpenoids consisting of eight isoprene units having a long central chain of conjugated double bonds. The general carotenoid structure is shown in Figure 2. All carotenoids can be derived from this structure by hydrogenation, dehydrogenation, cyclisation or oxidation or a combination of all. There are two groups of carotenoids, the carotenes which are

purely hydrocarbons and their oxygenated derivatives are called xanthophylls (IUPAC, 1974). They are widely distributed in nature of which more than 700 have been identified (Britton, et al., 2004).

They are mainly produced by phototrophic organisms such as algae, plants and some bacteria in which they act as accessory pigments for the energy transfer and antioxidants for protection against photooxidative damage in photosynthesis and as visual pigments such as in yellow, orange and red fruits, roots and leaves to attract insects and animals for pollination and seed distribution (Rosati, et al., 2009). Plants change their carotenoid composition and localisation in response to stress and during plastid differentiation (Biswal, 1995).

Carotenes can also have some health benefits for humans. Lycopene, responsible for the red colour of tomatoes, has been associated with a decreased risk of prostate cancer (Ansari & Ansari, 2005).

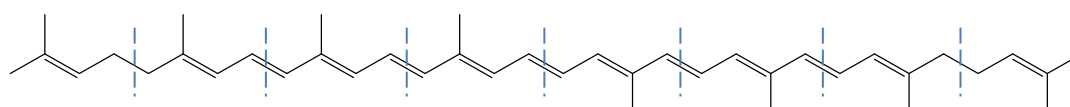


Figure 1: General carotenoid structure (Lycopene); the dashed lines indicate the formal division into isoprenoid units

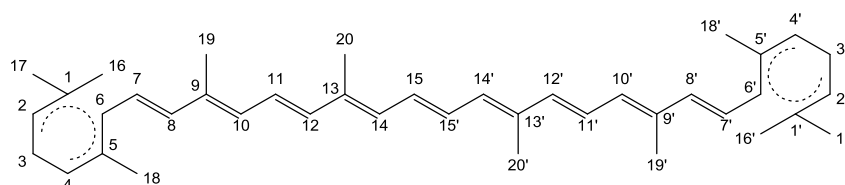


Figure 2: General carotenoid structure with atom numbering

The introduction of two β -rings at both ends of lycopene leads to the formation of β -carotene, which is present in high amounts in orange carrots. Carotenes with β -rings act as precursors to the essential vitamin A. Due to its strong colour, antioxidant activity and possible health advantages it is widely used as additive in food products.

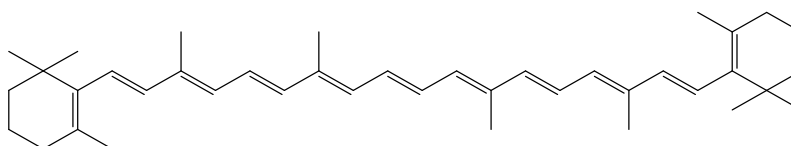


Figure 3: β -carotene: a very common carotene and a vitamin A precursor in humans

The oxygenated derivative of β -carotene, the xanthophyll called zeaxanthin is the precursor for the important growth hormone abscisic acid (ABA) in plants.

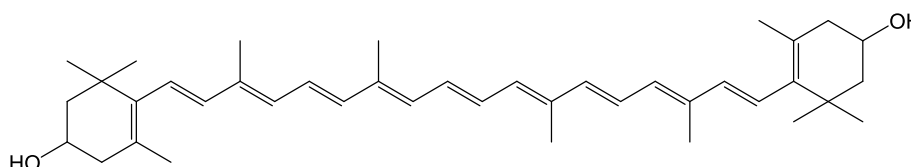


Figure 4: Zeaxanthin: a xanthophyll and the abscisic acid precursor in plants

While carotenoids with two β -rings are quite common in nature, carotenes with two ϵ -rings like ϵ -carotene are rarely found and usually only present in trace amounts in most plants (Meckenstock, 2005), (Cunningham, et al., 1996), (Barbosa-Filho, et al., 2008). Extraction of this compound from nature is therefore not economic.

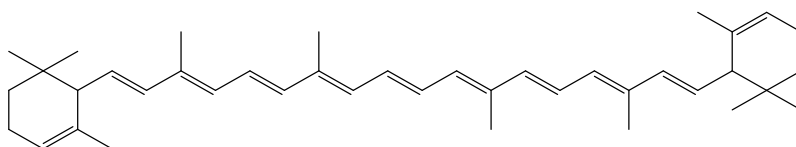


Figure 5: ϵ -carotene: rarely found in nature

In 1994, Cunningham engineered *E. coli* cells accumulating the carotenes ζ -carotene, neurosporene and lycopene (Cunningham, et al., 1994). These clones and similar carotenoid accumulating clones are commonly used to investigate the functions of enzymes involved in the biosynthesis of carotenoids or their cleavage. Two years later a plasmid introducing one ϵ -ring to lycopene, resulting in the accumulation of δ -carotene was constructed by Sun (Sun, et al., 1996). Another nine years later, Cunningham constructed the plasmid pAC-Epsilon able to introduce two ϵ -rings on lycopene resulting in the accumulation of ϵ -carotene (Cunningham & Gantt, 2005). These genetically modified organisms can be used as a readily available natural source for the otherwise rarely found ϵ -carotene.

1.2.1 ϵ -Carotene biosynthesis

“There are two biosynthetic pathways, the mevalonate pathway and the non-mevalonate pathway or the MEP/DOXP pathway for the terpenoid building blocks: isopentenyl diphosphate (IPP) and dimethylallyl diphosphate (DMAPP). The action of prenyltransferases then generates higher-order building blocks: geranyl diphosphate (GPP), farnesyl diphosphate (FPP), and geranylgeranyl diphosphate (GGPP), which are the precursors of monoterpenoids (C10), sesquiterpenoids (C15), and diterpenoids (C20), respectively. Condensation of these building blocks gives rise to the precursors of sterols (C30) and carotenoids (C40).” (Kanehisa Laboratories, 2015)

The clone *E. coli* BL21(DE3) pAC-Epsilon provided by Cunningham (Cunningham & Gantt, 2005) uses the MEP pathway shown in Figure 6 to synthesize IPP and DMAPP from pyruvate (Pyr) and glyceraldehyde 3-phosphate (G3P). FPP is then generated from two molecules of IPP and one molecule of DMAPP by the farnesyl diphosphate synthase in a two-step reaction. (Kanehisa Laboratories, 2015)

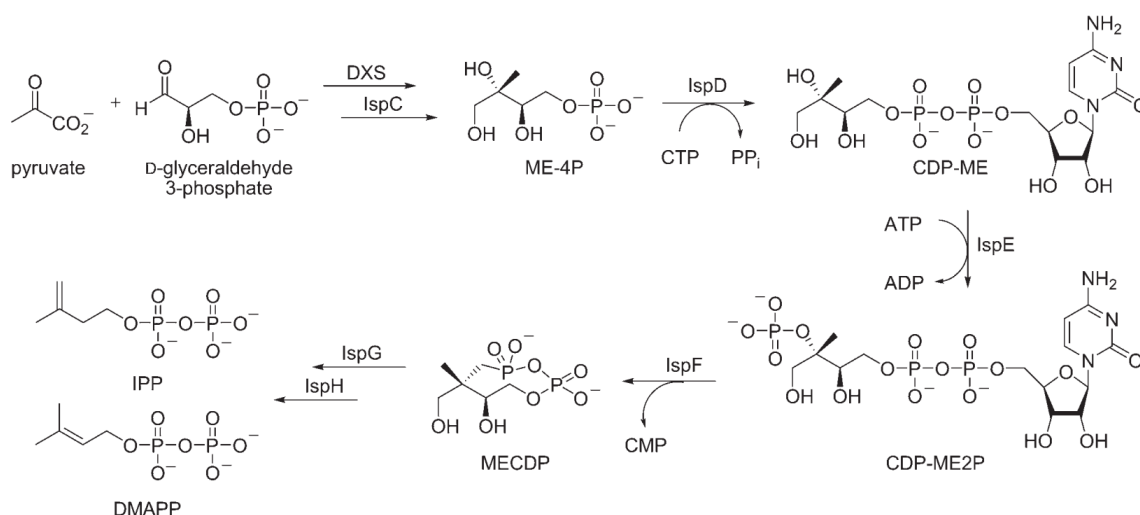


Figure 6: The non-mevalonate pathway for the biosynthesis of the C5 precursors to isoprenoids, IPP and DMAPP. ADP: adenosine 5'-diphosphate, ATP: adenosine 5'-triphosphate, CDP-ME: 4-diphosphocytidyl-2C-methyl-d-erythritol, CDP-ME2P: 4-diphosphocytidyl-2C-methyl-d-erythritol-2-phosphate, DMAPP: dimethylallyl diphosphate, DXS: 1-deoxy-d-xylulose 5-phosphate synthase, IPP: isopentenyl diphosphate, MECDP: 2C-methyl-d-erythritol-2,4-cyclodiphosphate. (Crane, et al., 2008)

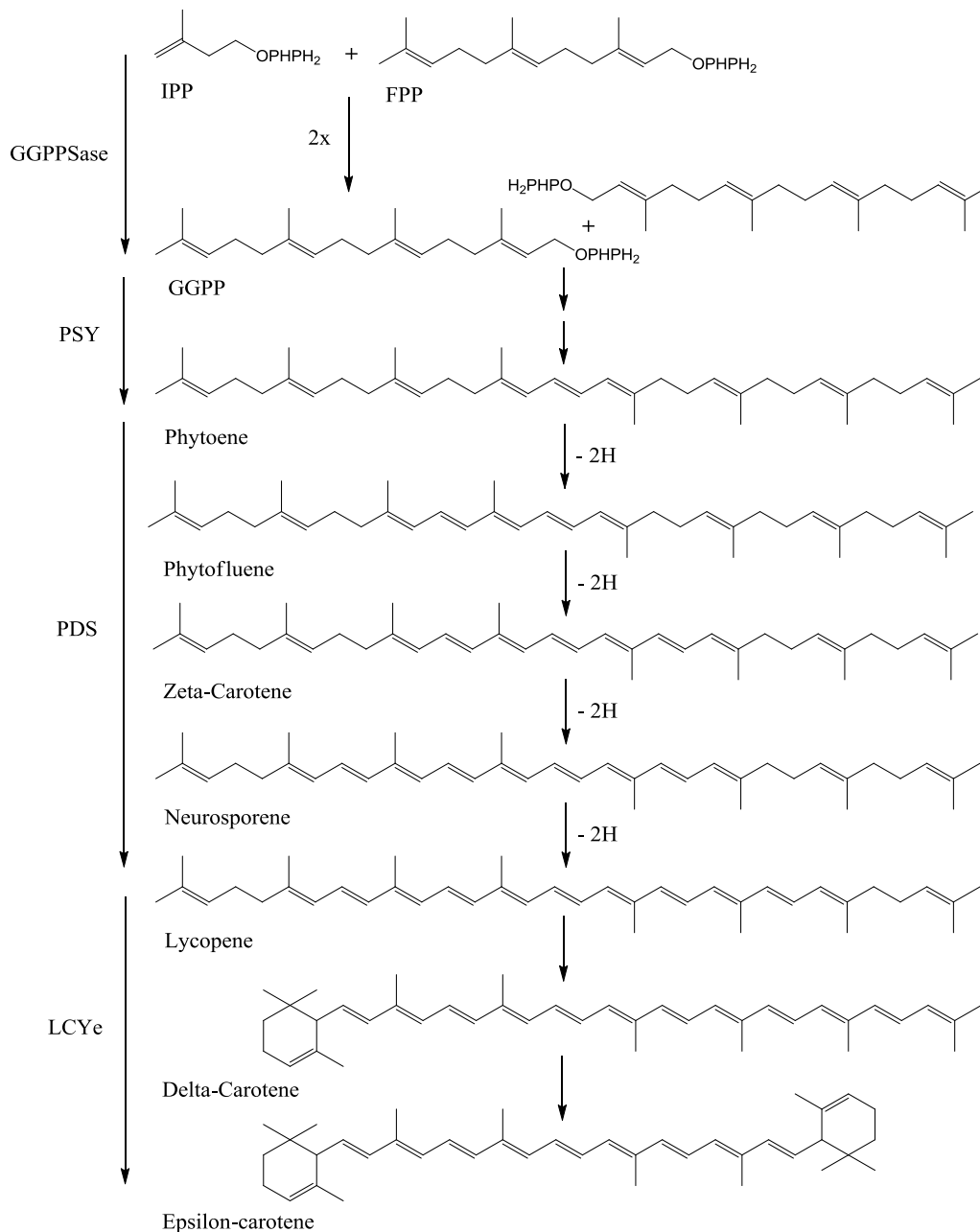


Figure 7: Schematic overview of the ϵ -carotene synthesis.

IPP: isopentenyl pyrophosphate; FPP: farnesyl pyrophosphate; GGPP: geranylgeranylpyrophosphate, GGPPSase: GGPP synthase, PSY: phytoene synthase, PDS: phytoene desaturase, LCYe: lycopene- ϵ -cyclase

The ϵ -carotene synthesis with the genes on the pAC-Epsilon plasmid is displayed in Figure 7. By the addition of one more IPP unit to FPP geranylgeranyl diphosphate (GGPP) is created by the GGPP Synthase (GGPPSase). Phytoene as the first C₄₀ molecule is synthesised from the condensation of two C₂₀ GGPP by Phytoene-Synthase (PSY). Four subsequent desaturation steps, catalysed by the phytoene desaturase (PDS) result in lycopene (Rosati, et al., 2009). The enzyme lycopene- ϵ -cyclase (LCYe) then introduces ϵ -ring groups at both linear Ψ -end groups of lycopene yielding ϵ -carotene.

1.3 Carotenoid Cleavage Dioxygenases

Carotenoids can be cleaved by oxidation due to various chemical, photochemical and enzymatic mechanisms (Boon, et al., 2010). When molecular oxygen is introduced at any of the double bond positions, an aldehyde or ketone is generated depending on the reaction site, leading to a large number of possible products known as apocarotenoids. These products are widespread in nature and fulfil important biological functions, such as the important growth hormones abscisic acid (ABA) and strigolactone in plants and the essential vitamin A in mammals, reviewed in (Auldrige, et al., 2006). Though cleavage can occur non-specifically, biologically active apocarotenoids are commonly produced by selective cleavage of carotenoids catalysed by a large class of non-heme iron (II) dependent enzymes called carotenoid cleavage dioxygenases (CCDs) (Auldrige, et al., 2006).

In *Arabidopsis thaliana*, the model plant in plant research, nine different CCDs have been identified (Auldrige, et al., 2006). Five 9-cis-epoxycarotenoid dioxygenases (NCEDs), which primarily cleave xanthophylls asymmetrically at the 11,12 double bond position are involved in the biosynthesis of ABA ((Tan, et al., 2003), (Auldrige, et al., 2006)). NCEDs have also been identified in other plant species, though varying in the number of NCED enzymes needed for ABA production ((Tan, et al., 1997), (Qin & Zeevaart, 2002), (Thompson, et al., 2000), (Qin & Zeevaart, 1999)).

The remaining four CCD members (CCD1, CCD4, CCD7 and CCD8) show more diverse cleavage activities. CCD7 and CCD8 are involved in the formation of the shoot-branching inhibition hormone strigolactone (Dun, et al., 2009) , whereas CCD1 and CCD4 catalysis leads to a variety of flavour and aroma compounds (Huang, et al., 2009) often with very low detection thresholds.

The CCD1 enzymes in plants are highly homologue to each other and were found to be localised in the cytosol instead of the plastids as the only CCD class (Lashbrooke, et al., 2013). They contribute to the flavour and aroma of many flowers and fruits producing aroma compounds such as β -ionone, pseudoionone, geranylacetone (Simkin, et al., 2004), β -cyclocitral, α - and β -damascenone and geranial (Rodríguez-Ávila, et al., 2011). Several CCD1 enzymes of different plants such as *Arabidopsis thaliana* (AtCCD1), maize (ZmCCD1), carrot (DcCCD1), tomato (LeCCD1), melon (CmCCD1), damask rose (RdCCD1), or grapes (VvCCD1) have been characterized, all showing slightly different substrate specificities and cleavage activities on the carotenoids ((Schwartz, et al., 2001), (Sun, et al., 2008), (Yahyaa, et al., 2013), (Ilg, et al., 2014), (Ibdah, et al., 2006), (Huang, et al., 2009), (Lashbrooke, et al., 2013)).

1.3.1 The carotenoid cleavage dioxygenase 1 of *Vitis vinifera* (VvCCD1)

The CCD1 of *Vitis vinifera* (common grape wine) was identified and isolated in 2005 by Mathieu (Mathieu, et al., 2005). Most studies report that VvCCD1 primarily cuts at the positions 9,10 (9',10') of cyclic ends of some carotenes and xanthophylls and the 5,6 (5',6') of the linear carotene lycopene and the linear end of δ -carotene reviewed in (Lashbrooke, et al., 2013). The cleavage reaction on ϵ -Carotene is displayed in Figure 8.

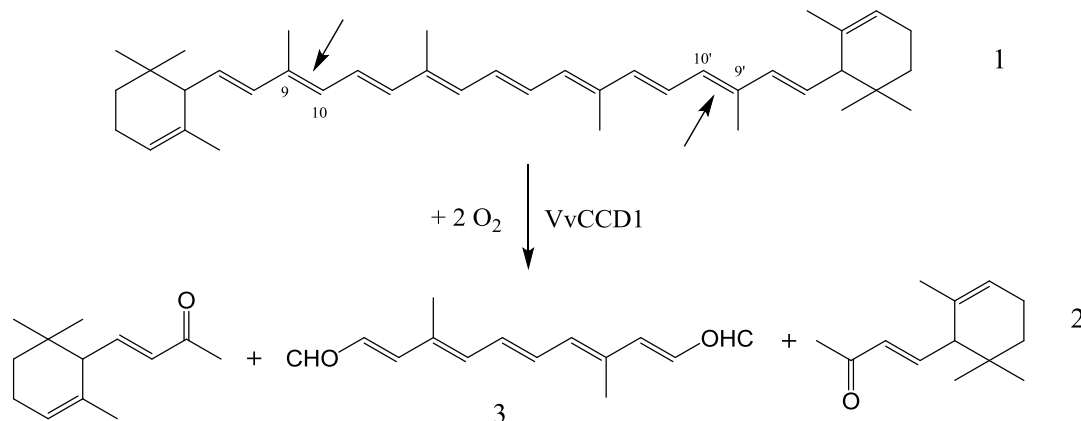


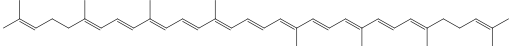
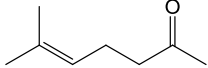
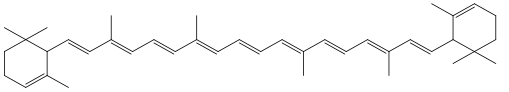
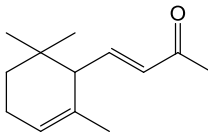
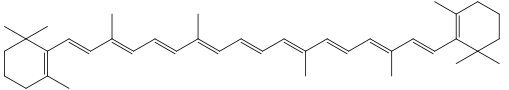
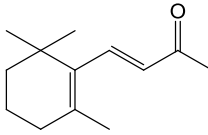
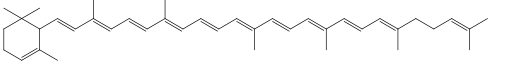
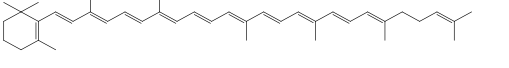
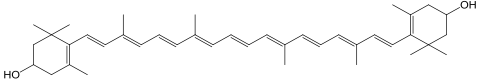
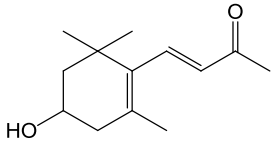
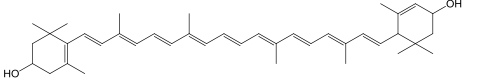
Figure 8: Reaction scheme of VvCCD1 activity on ϵ -carotene (1). The arrows indicate the cleavage at the 9,10(9',10') double bond positions. This activity produces two molecules of α -ionone (2) and a central C14-dialdehyde (3)

The enzyme VvCCD1 cleaves ϵ -carotene at the 9,10(9',10') positions yielding two molecules of α -ionone and one molecule of a central C14-dialdehyde (Mathieu, et al., 2005).

Though VvCCD1 has shown a broad substrate range, cross-comparing the results between studies is difficult due to different types of assays given the fact that VvCCD1 isolated from *V. vinifera* L. cv Shiraz could not cleave β -carotene *in vitro* (Mathieu, et al., 2005) but VvCCD1 isolated from *V. vinifera* L. cv Pinotage could cleave β -carotene *in vivo*. (Lashbrooke, et al., 2013). The VvCCD1 used in this work is the one isolated from *V. vinifera* L. cv Pinotage, which sequence has been optimised for codon usage in *E. coli* the vector pET22b in a previous work of Fraunhofer IGB.

The hypothesis that cleavage by CCD enzymes only occurs when there is a double bond next to the cleaving double bond position present (Vogel, et al., 2008) was currently strengthened (Lashbrooke, et al., 2013). For example, when cleaving at the 9,10(9',10') positions there must be a double bond at the 7,8(7'8') or 11,12(11',12') positions. Reported cleaving reactions of VvCCD1 are collected in Table 1.

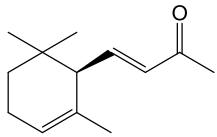
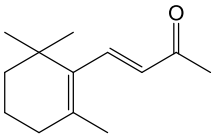
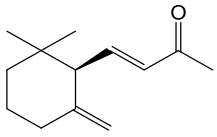
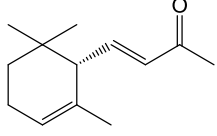
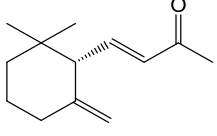
Table 1: Reported VvCCD1 reactions.

Cleavage positions	Substrate	Products	Reference
Carotenes			
5,6 (5',6')	Lycopene 	2x MHO (6-methyl-5-hepten-2-one) 	(Lashbrooke, et al., 2013)
9,10 (9',10')	ϵ -Carotene 	2x α -ionone 	
9,10 (9',10')	β -Carotene 	2x β -ionone 	
9,10 (9',10')	δ -Carotene 	1x α -ionone	(Lin, 2013)
5,6 (5',6')		1x MHO	
9,10 (9',10')	α -zeacarotene 	1x β -ionone	
5,6 (5',6')		1x MHO	
Xanthophylls			
9,10 (9',10')	Zeaxanthin 	2x 3-hydroxy- β -ionone 	(Mathieu, et al., 2005)
9,10 (9',10')	Lutein 	2x 3-hydroxy- β -ionone	

1.3.2 Ionones

One interesting class of these flavour and aroma compounds generated by the cleavage of carotenes by CCDs are ionones, a major compound responsible for the aroma of violets. Depending on which carotene is cleaved, the corresponding ionone is formed. For example, the cleavage of β -Carotene leads to the formation of two molecules of β -ionone, whereas the cleavage of ϵ -Carotene leads to the formation of two molecules of α -ionone. In nature they often occur in a mixture of regioisomers (α , β , γ) and their enantiomers/stereoisomers (*R*, *S*). Although the production of α -ionone from ϵ -carotene by VvCCD1 has been shown it has not been examined which enantiomer of α -ionone the reaction yields. This is of particular interest since both enantiomers possess different flavours.

Table 2: Odour properties and odour detection thresholds of ionones

<p>(<i>R</i>)-α-ionone</p>  <p>- Violet like, fruity, raspberry like, flowery odour [1] - Floral-woody note, with an additional honey aspect. Slightly weaker than the (<i>S</i>) isomer [2]</p> <p>3.2 ng/L of air [2]</p>	<p>β-ionone</p>  <p>- Woody violet like odour [1] - Typical floral-woody note [2]</p> <p>0.12 ng/L of air [2]</p>	<p>(<i>R</i>)-γ-ionone</p>  <p>- Weak green, fruity, pineapple-like odour with metallic aspects, - quite different from the typical ionone odour; however, slightly woody, ionone-type nuances are also present [2]</p> <p>11 ng/L of air [2]</p>
<p>(<i>S</i>)-α-ionone</p>  <p>- Woody, cedarwood-like, fruity, raspberry like and β-ionone like odour [1] - Floral-woody note, with an additional honey aspect. Slightly more powerful than the (<i>R</i>) isomer. [2]</p> <p>2.7 ng/L of air [2]</p>		<p>(<i>S</i>)-γ-ionone</p>  <p>- Linear, very pleasant, floral, green, woody odour with a very natural violet tonality; - The most powerful and pleasant isomer [2]</p> <p>0.07 ng/L of air [2]</p>

[1] (Schaefer, 2007, p. 73)

[2] (Brenna, et al., 2002)

Ionones could be extracted from boronia oils mainly containing β -ionone and only small amounts of α -ionone (Menary & Garland, 1999). Though ionones can also be produced by chemical transformation, this often leads to a racemic mixture of the ionone isomers and enantiomers. They can be synthesized from citral and acetone with pseudoionone as intermediate, forming a mixture of α -ionone and β -ionone after cyclization (Noda, et al., 1998).

These cheap ionone mixtures are often used in soap products (Poucher & Jouhar, 1991, p. 187). The most common ionone used as a fragrance is β -ionone, which is often added to oils to enhance their quality (Menary & Garland, 1999, p. 5). Having a fruity-woody odour, which is reminiscent of cedarwood and raspberries, it is often used in jasmine perfumes. The less commonly used α -ionone is used in violet perfumes (Poucher & Jouhar, 1991, p. 187).

The application of ionones is not only limited by their aroma properties. β -ionone has shown chemo preventive effects in rats (Cardozo, et al., 2011), as well have ionone derivatives shown anti prostate-cancer (Zhou, et al., 2009), neuroprotective (Srivastava, et al., 2010) and antimicrobial (Sharma, et al., 2012) effects

2 Aims of the work

The main goal of this work was to produce α -ionone biotechnologically through the conversion of ϵ -carotene by the enzyme VvCCD1, producing two molecules of α -ionone from one molecule of ϵ -carotene. Since ϵ -carotene is rare in nature the extraction of this substrate from plants is not feasible. Using ϵ -carotene accumulating *E. coli* strains for the production of the α -ionone precursor can circumvent this issue. These *E. coli* cells could then be further genetically engineered by introducing VvCCD1 to directly produce α -ionone from the accumulated ϵ -carotene (de-novo-synthesis). The substrate and the enzyme could also be produced independently in two different *E. coli* clones, be purified and brought to reaction outside the cells (biotransformation).

After establishing the α -ionone production, the next steps would be to optimise the production towards a high yield of product and to develop and optimise the downstream processing towards a preferably easy and cheap purification of the product.

Though VvCCD1 has already been characterised and has shown to be regioselective it has not been shown if the reaction is also stereoselective. The analysis of the α -ionone enantiomer produced by the cleavage reaction of VvCCD1 was therefore another aim of the work.

3 Material

3.1 Equipment

Table 3: List of used equipment

Name	Manufacturer
Balance P-4002	Denver Instrument
C1301B	neoLab, Heidelberg, Germany
Dark Hood DH-40	Biostep GmbH, Jarndorf, Germany
Electro Cell Manipulator 630	BTX Harvard Apparatus, Holliston, U.S.A.
Extend Balance ED124S	Sartorius Weighing Technology GmbH, Goettingen, Germany
Haake A 10 Refrigerated Bath Circulator	Thermo Scientific
HERA Therm Incubator	Thermo Scientific
IKA HB10 control	VWR International
IKA RCT-classic	IKA®-Werke GmbH & Co. KG, Staufen, Germany
IKA RV10 control	VWR International
ImageSystem Felix 6000	biostep GmbH, Burkhardtsdorf, Germany
Innova 40 Incubator Shaker Series	New Brunswick Scientific
Innova 42 R Incubator Shaker Series	New Brunswick Scientific
Mastercycler personal	Eppendorf
Milli-Q Integral 15	Millipore
MP-3 AP Power Supply	Major Science, Saratoga, U.S.A.?
MP-300 V Power Supply	Major Science, Saratoga, U.S.A.?
MR Hei-Tec Biorührer	Heidolph
NanoDrop Spectrophotometer ND-Lite TE-66	Thermo Scientific
pHenomenal pH 1000 L	VWR International
Rotavapor R-3	Buchi
RV 10 C S40 rotary evaporater	IKA
Safe 2020 Class II Biological Safety Cabinets	Thermo Scientific, Langensfeld, Germany
Safety Stand 630B	BTX Harvard Apparatus, Holliston, U.S.A
Scotsman AF 80 Ice Flaker	Hubbard systems
SDS-Gel electrophoresis chamber GH102	Biostep GmbH, Jahnsdorf, Germany
Sonopuls HD 2200	Bandelin electronic
SPME Fiber Assembly 85 µm Polyacrylate, Fused Silica 24 Ga, Autosampler (white)	Supelco, Bellefonte, U.S.A.
Thermomixer comfort	Eppendorf
Titanium probe micro tip MS 73	Bandelin electronic
TS 0.75 kW Benchtop French Press	Constant Systems
Ultraspec 10 Cell Density Meter	Amersham Biosciences
Vent Filter MPK01	Millipore
Vortex Genie 2	Scientific Industries Inc., U.S.A.
GCMS-QP2010 Plus	Shimadzu Corp.
GC Autosampler AOC-5000	Jain (Combipal)
Sigma 1-14	Sigma Laborzentrifugen GmbH, Osterode a.H.
Sigma 1-15PK	Sigma Laborzentrifugen GmbH, Osterode a.H.
Avanti J-E centrifuge (JA-25.50, JLA-10.500, JS-5.3)	Beckman Coulter

3.2 Chemicals

Table 4: List of used chemicals

Substance	Manufacturer
1-Octanol > 99 %	Sigma Aldrich, St. Louis, USA
Acetic acid	Sigma Aldrich, St. Louis, USA
Aceton puriss. (Barrell)	The Geyer GmbH Renningen, Germany
Acrylogel 30 % Solution	VWR International, Radnor, USA
Agar Kobe 1	AppliChem GmbH, Darmstadt
Agarose Basic	AppliChem GmbH, Darmstadt
Amberlite XAD 2	Supelco, Bellfonte, U.S.A.
Ammonium sulfate	AppliChem GmbH, Darmstadt
Ampicillin sodium salt	AppliChem GmbH, Darmstadt
Bromophenol blue sodium salt	AppliChem GmbH, Darmstadt
Chloramphenicol	AppliChem GmbH, Darmstadt
Coomassie Brilliant Blue R 250	VWR International, Radnor, USA
D-(+)-Glucose	Sigma Aldrich, St. Louis, USA
Diethyl ether	VWR International, Radnor, USA
Di-Sodium hydrogen phosphat dihydrate	AppliChem GmbH, Darmstadt
Dodecane ReagentPlus > 99 %	Sigma Aldrich, St. Louis, USA
DTT Molecular biology grade	AppliChem GmbH, Darmstadt
EDTA disodium salt dihydrate	VWR International, Radnor, USA
Ethanol > 99.5%	AppliChem GmbH, Darmstadt
Ethanol abs. p.a. > 99.9 %	The Geyer GmbH Renningen, Germany
Ethidium bromide	VWR International, Radnor, USA
Ethyl acetate	VWR International, Radnor, USA
Glycerol Rotipuran > 99,5 %, p.a., anhydrous	Carl Roth GmbH & Co. KG, Karlsruhe
Iron (II) sulphate heptahydrate	VWR International, Radnor, USA
Kanamycin sulfate	AppliChem GmbH, Darmstadt
Lycopene	Sigma Aldrich, St. Louis, USA
Methanol ROTISOLV HPLC	Carl Roth GmbH & Co. KG, Karlsruhe
Methylene chloride Rotipuran > 99.5 %	Carl Roth GmbH & Co. KG, Karlsruhe
Potassium chloride	BDH Laboratory Supplies, Poole, UK
Potassium dihydrogen phosphate p.a. > 99 %	Carl Roth GmbH & Co. KG, Karlsruhe
Sodium chloride	VWR International, Radnor, USA
Sodium dihydrogen phosphate dihydrate	AppliChem GmbH, Darmstadt
Sodium dihydrogen phosphate monohydrate	VWR International, Radnor, USA
Sodium dodecyl sulfate (SDS) solution	Sigma Aldrich, St. Louis, USA
Tert-Butyl methyl ether for HPLC > 99.8 %	The Geyer GmbH Renningen, Germany
TRIS hydrochloride p.a. > 99 %	Carl Roth GmbH & Co. KG, Karlsruhe
Triton X-100 Electron	VWR International, Radnor, USA
Tryptone/Peptone ex casein	Carl Roth GmbH & Co. KG, Karlsruhe
Water (Milli-Q)	
Yeast extract	Carl Roth GmbH & Co. KG, Karlsruhe
α -ionone > 90 %	Sigma Aldrich, St. Louis, USA
β -carotene	Sigma Aldrich, St. Louis, USA
β -ionone > 96 %	Sigma Aldrich, St. Louis, USA

3.3 Media and buffers

Table 5: List of used media and buffer solutions

Name	Ingredients
10 x D	20 % (w/v) Glucose
10 x M9	6 % (w/v) Na ₂ HPO ₄ , 3 % (w/v) KH ₂ PO ₄ , 1 % (w/v) NH ₄ Cl, 0.5 % (w/v) NaCl
10 x SDS running buffer	0.25 M Tris Base, 1.92 M glycine, 1 % (w/v) SDS
4 x SDS-lower gel Puffer	1.5 M Tris/HCl (pH 8.8)
4 x SDS-upper gel Puffer	0.5 M Tris/HCl (pH 6.8), 2 mg bromophenol blue
Agarose gel (1 %)	1 g agarose, 100 mL 1x TAE
Ampicillin stock solution	100 mg/mL
Chloramphenicol stock solution	34 mg/mL
Coomassie Brilliant Blue staining solution	50 % (w/v) methanol, 10 % (w/v) acetic acid, 0.05 % (w/v) Coomassie Brilliant Blue R-250 100 mM (pH 7.5)
Destain solution	TAE buffer
EtBr staining solution	0.1 % (w/v) EtBr [10 ng/mL], TAE buffer
HPLC Eluent A	83 % (v/v) MeOH + 17 % (v/v) MTBE
HPLC Eluent B	10 % (v/v) MeOH + 89 % (v/v) MTBE
<i>In vitro</i> buffer 1	0.1 M TRIS/HCl pH 7.2, 50 µM FeSO ₄ , 0.1 g/L catalase, 0.05 % (v/v) Triton-X 100, 20 % (v/v) glycerol
<i>In vitro</i> buffer 2	50 mM TRIS/HCl pH 7.0, 300 mM NaCl, 10 mM DTT, 500 µM FeSO ₄ , 0.05 % (v/v) Triton-X 100
Kanamycin stock solution	30 mg/mL
LB agar	1 % (w/v) Tryptone, 0.5 % (w/v) yeast extract, 1 % (w/v) NaCl, 1.5 % (w/v) agar-agar
LB medium	1 % (w/v) Tryptone, 0.5 % (w/v) yeast extract 1 % (w/v) NaCl
M9 medium	10 % (v/v) 10 x M9, 2 mM MgSO ₄ , 2 % (v/v) 10 x D, 25 µM CaCl ₂ , 0.0001 % (w/v) Thiamin
SOC medium	2 % (w/v) Tryptone, 0.5 % (w/v) yeast extract, 0.05 % (w/v) NaCl, 0.03 % (w/v) KCl, 10 % (v/v) 10x Glucose (200 mM), 10 % (v/v) 10x MgCl ₂ (100 mM)
Sonication buffer	50 mM sodium phosphate buffer, pH 7.0
TAE buffer	40 mM TRIS, 1 mM EDTA, 5,7 % (w/v) acetic acid, 2 % (w/v) TRIS, 0.05 % (w/v) EDTA

3.4 Enzymes

Table 6: List of used Enzymes

Enzyme	Concentration [U/mL]	Manufacturer
Phusion DNA Polymerase	2000	Thermo Scientific, Waltham, USA
Rapidozym Taq Polymerase	5000	Rapidozym GmbH, Berlin, Germany
Restriction enzyme BsaI	20000	New England Biolabs, Ipswich, USA
Restriction enzyme HindIII	20000	New England Biolabs, Ipswich, USA
Restriction enzyme NcoI	20000	New England Biolabs, Ipswich, USA
T4 DNA Ligase	400000	New England Biolabs, Ipswich, USA

3.5 Microorganisms

Table 7: List of used strains

Species	Strain	Plasmids	Genotype	Supplier
<i>Escherichia coli</i>	DH10B		F- <i>mcrA</i> Δ(<i>mrr-hsdRMS-mcrBC</i>) Φ80 <i>lacZ</i> ΔM15 Δ <i>lacX74 recA1 endA1 araD139</i> Δ(<i>ara leu</i>) 7697 <i>galU galK rpsL nupG</i> λ-	Invitrogen
<i>Escherichia coli</i>	BL21(DE3)		F- <i>dcm ompT hsdS</i> (r _B ⁻ m _B ⁻) <i>gal</i> λ(DE3)	Novagen

3.6 Vectors and Plasmids

Table 8: List of used vectors

Name	Resistance gene	Antibiotic used	Inducer used	Source
pAC derived plasmid	<i>Cm</i>	Chloramphenicol	IPTG	Cunningham [2005 A study in scarlet]
pET22b	<i>lacZ</i>	Ampicillin	IPTG	Life Technologies, Thermo Scientific Waltham, USA
pBAD	<i>lacZ</i>	Ampicillin	L-Arabinose	Life Technologies, Thermo Scientific Waltham, USA

Table 9: List of used plasmids

Plasmid name	Gene names	Protein names	Reaction	Source organisms	Source
pAC-Epsilon	<i>crtE, crtB, crtI</i>	GGPP Synthase (GGPPSase) Phytoene-Synthase (PSY) Phytoene Desaturase (PDS)	FPP + IPP → GGPP GGPP →→ Phytoene	<i>Erwinia herbicola</i> <i>Eho10</i>	(Cunningham & Gantt, 2005)
	<i>lcyE</i>	Lycopene-ε-cyclase		<i>Lactuca sativa</i>	
pET22b-VvCCD1	<i>VvCCD1</i>	Carotenoid Cleavage Dioxygenase I	Lycopene → δ-carotene → ε-carotene	<i>Vitis vinifera</i>	Previous work of Fraunhofer IGB
pBAD-VvCCD1	<i>VvCCD1</i>	Carotenoid Cleavage Dioxygenase I	Lycopene → δ-carotene → ε-carotene	<i>Vitis vinifera</i>	This work

3.7 Kits

Table 10: List of used DNA purification kits

Kit Name	Manufacturer
GeneJet Gel Extraction Kit	Life Technologies, Thermo Scientific Waltham, USA
GeneJet Plasmid Miniprep Kit	Life Technologies, Thermo Scientific Waltham, USA

3.8 Oligonucleotides

All required primers were designed using Clonemanager 9.

Table 11: List of used oligonucleotides

Nr.	Name	Type	Sequence	Tm [°C]	Manufacturer
730	VvCCD1-fwd2	PCR-Primer for VvCCD1 amplification from pET22b-VvCCD1	5'-TCCTCAGCTTCCTTCGGGCTTTG-3'	65	MWG Eurofins, Ebersberg, Germany
731	VvCCD1-rev2		5'- GGTCTC CCATGAAATACCTGCTGCCGACC-3' ¹	64	MWG Eurofins, Ebersberg, Germany
732	pBAD-A-fwd	PCR-Primer for VvCCD1 amplification from pBAD-VvCCD1 and sequencing of pBAD-VvCCD1 and	5'-GGCGTCACACTTTGCTATGC-3'	64	MWG Eurofins, Ebersberg, Germany
733	pBAD-A-rev		5'-CAGACCGCTTCTGCGTTCTG-3'	65	MWG Eurofins, Ebersberg, Germany
760	pBAD-A-fwd-seq	Sequencing Primer for sequencing of amplified pBAD-VvCCD1	5'-AGATTAGCGGATCCTACCTG-3'	57	MWG Eurofins, Ebersberg, Germany
761	pBAD-A-rev-seq		5'-CAGACCGCTTCTGCGTTCTG-3'	63	MWG Eurofins, Ebersberg, Germany

¹Primer 731 possesses the Bsal recognition sequence "GGTCTC" and a NcoI overhang "CCATG"

3.9 Ladders

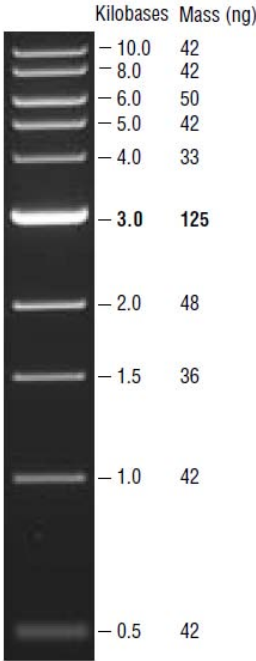


Figure 9: Quick Load, 1 kb DNA Ladder 50 µg/µL,
New England Biolabs

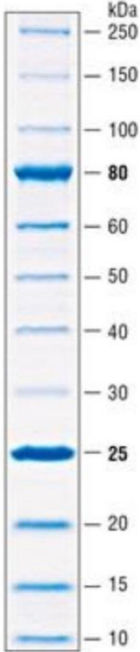


Figure 10: Protein Ladder (10-250 kDa),
New England Biolabs

4 Methods

4.1 Microbiological Methods

4.1.1 Cultivation of *E. coli* strains

All strains were plated on 1 % LB agar plates containing the respective antibiotics and incubated at 37 °C for 24 to 48 hours. The plates were renewed every four weeks to ensure viable colonies. The precultures of usually 25 mL LB medium were inoculated with one colony and incubated at 30 °C and 125 rpm in the dark overnight.

E. coli BL21(DE3) strains were usually grown in LB medium containing the respective antibiotics at 30 °C with some exceptions, 125 rpm with different incubation times ranging from 17 hours to 72 hours.

For cloning work *E. coli* DH10b was grown at 37 °C and 125 rpm.

4.1.1.1 Carotene profiles

The growing conditions of the measurements to investigate the carotene profiles are shown in the following table.

Table 12: Growing conditions of *E. coli* BL21(DE3) clones

<i>E. coli</i> BL21(DE3)	Measurement	Temperature [°C]	Incubation time [h]
pAC-Epsilon	1	30	17
	2	30	41
	3	30	65
	4	16	48
	5	30	72
	6	30	35
pAC-Epsilon + pET22b	1	30	24
	2	30	48
	3	30	72
pAC-Epsilon + pBAD	1	30	24
	2	30	24

4.1.1.2 Colour comparison of *E. coli* BL21(DE3) pAC-Epsilon + pBAD and *E. coli* BL21(DE3) pAC-Epsilon + pBAD-VvCCD1

Two shaking flasks with 25 mL of LB (Cm + Amp) each were inoculated with *E. coli* BL21(DE3) pAC-Epsilon + pBAD and *E. coli* BL21(DE3) pAC-Epsilon + pBAD. Incubation at 37 °C and 125 rpm in the dark for 8 hours. Each culture was then split in two shaking flasks and refilled to 30 mL of LB (Cm + Amp). One of each culture was induced with 0.01 % of L-Arabinose. Incubation at 37 °C and 125 rpm in the dark overnight. The cells were centrifuged (4000 g, 4 °C, 15 min.) and a picture of the pellets was taken.

4.1.1.3 Colour comparison of various clones

Four shaking flasks with 25 mL of LB with the respective antibiotics were inoculated with

- *E. coli* BL21(DE3) pAC-Epsilon
- *E. coli* BL21(DE3) pAC-Epsilon + pET22b
- *E. coli* BL21(DE3) pAC-Epsilon + pBAD
- *E. coli* BL21(DE3) pAC-Epsilon + pBAD-VvCCD1

Incubation at 30 °C and 125 rpm in the dark for 24 hours. One mL of each culture was centrifuged in a microcentrifuge tube (13000 g, 3 min.) and a picture was taken.

4.1.2 Optical density

To monitor the growth behaviour of the cells the optical density was measured at 600 nm by blanking with the respective medium and when necessary diluting the culture in a range of an OD of 0.2 to 1.

The absorbance of a specific substance is given by the law of Lambert-Beer. The Absorbance of substances of light at a specific wavelength is given by:

$$A_{\lambda} = \epsilon_{\lambda} * c * d$$

c: Molar concentration of the substance in the solution [mol L⁻¹]

ϵ_{λ} : Molar extinction coefficient of the substance at that specific wavelength [m² mol⁻¹]

d: Thickness of the measuring container [cm⁻¹]

4.1.3 Expression of VvCCD1

For protein expression of VvCCD1 in *E. coli* BL21(DE3) the cells were grown at 30 °C with some exceptions, 125 rpm and shielded from light. The pET22b-vectors and pBAD-vectors were induced in mid-log phase an OD value of about 0.6 with 0.1 mM IPTG or 0.01 % L-Arabinose respectively.

4.1.4 Protein expression analysis by SDS-PAGE

For protein expression analysis a culture suspension volume of 500/OD [μL] was taken and centrifuged (13000 g, 3 min.). The pellet was resuspended in 100 μL of water and 100 μL of SDS loading buffer by vortexing. The electrophoresis chamber was filled with 1x SDS-buffer. Prior loading 10 μL of the protein ladder and 20 μL of each sample to the gel, the samples were cooked for 5 minutes at 95 °C and 500 rpm.

Table 13: SDS-PAGE settings

	Voltage [V]	Current [mA]	Power [W]	Time [min]
12 % SDS gel	300	30 per gel	300	45

The gel was then shortly cooked in water and stained with Coomassie Blue staining solution for 12.5 minutes and then decolourized by shortly cooking in water and letting dissolve in warm water several times until enough contrast could be gained. A picture was then taken in the Dark Hood.

4.1.4.1 Protein expression analysis of *E. coli* BL21(DE3) pAC-Epsilon + pET22b-VvCCD1

Cultures of

- *E. coli* BL21(DE3) pAC-Epsilon
- *E. coli* BL21(DE3) pAC-Epsilon + pET22b
- *E. coli* BL21(DE3) pAC-Epsilon + pET22b-VvCCD1
- *E. coli* BL21(DE3) pAC-Epsilon + pET22b-VvCCD1 + 0.25 mM IPTG

were grown overnight at 30 °C, 125 rpm in the dark.

4.1.4.2 Protein expression analysis of *E. coli* BL21(DE3) pAC-Epsilon + pBAD-VvCCD1

For VvCCD1 expression analysis 10 mL LB (Cm + Amp) were inoculated to an OD of 0.2 and grown at 30 °C, 125 rpm in the dark. The cells were induced with L-Arabinose concentrations ranging from

0.00002 % to 0.2 % at an OD of 0.76. *E. coli* BL21(DE3) pAC-Epsilon + pBAD was used as negative control. The cells were incubated at 30 °C and 125 rpm in the dark for 24 hours. Samples for the SDS-PAGE were taken after 6.5 hours and 24 hours.

4.1.5 Reducing background expression of VvCCD1

One attempt to reduce the basal expression of VvCCD1 is to add glucose to the medium. By adding 1 % of glucose as a good carbon source to the medium, the cAMP levels are reduced which again reduces the level of the CAP complex hence reducing the expression of T7 Polymerase which recognises and expresses the VvCCD1 gene on the pET22b vector.

4.1.5.1 Reducing background expression of pET22b-VvCCD1

Five 200 mL shaking flasks of the following cultures were inoculated to an OD of 0.2 with an overnight culture grown at 30 °C and 125 rpm in the dark for 65 hours.

Organism	V [mL]	Medium	Antibiotics
<i>E. coli</i> BL21(DE3) pAC-Epsilon	200	LB	Cm
<i>E. coli</i> BL21(DE3) pAC-Epsilon	200	LB + 1 % Glc	Cm
<i>E. coli</i> BL21(DE3) pAC-Epsilon + pET22b-VvCCD1	200	LB	Cm + Amp
<i>E. coli</i> BL21(DE3) pAC-Epsilon + pET22b-VvCCD1	200	LB + 1 % Glc	Cm + Amp
<i>E. coli</i> BL21(DE3) pAC-Epsilon + pET22b-VvCCD1	200	LB + 1 % Glc + 0.1 mM IPTG	Cm + Amp

Samples were taken at the time of inoculation and after 17, 41 and 65 hours.

4.1.5.2 Reducing background expression of pBAD-VvCCD1

Each three samples of 60 mL LB (Cm + Amp) + 1 % Glc were inoculated with *E. coli* BL21(DE3) pAC-Epsilon + pBAD and *E. coli* BL21(DE3) pAC-Epsilon + pBAD-VvCCD1 to an OD of 0.2 and incubated overnight at 30 °C, 125 rpm in the dark. 25 mL of each sample was centrifuged (4000 g, 15 min., 4 °C) and frozen at -20 °C for later carotene extraction and HPLC-PDA analysis. The data was compared to measured samples of experiment 0.

For volatile analysis by HS-SPME-GC-MS another 25 mL of each sample was centrifuged (4000 g, 15 min., 4 °C) and resuspended in 6 mL of LB (Cm + Amp) + 1 % Glc. The three samples with pBAD-VvCCD1 were induced with 0.01 % L-Arabinose. Incubation overnight at 30 °C and 125 rpm in the dark. The reactions were stopped with 5 mL of 5 M NaCl solution and the samples measured by HS-SPME-GC-MS.

4.1.5.2.1 M9 medium

The M9 medium is a defined medium containing glucose as the only carbon source. It should therefore reduce background expression levels. In addition any other possible influences of the compounds of the complex LB medium on the cells can be excluded.

Two samples of 30 mL of M9 (Cm + Amp) medium were inoculated with *E. coli* BL21(DE3) pAC-Epsilon + pBAD and *E. coli* BL21(DE3) pAC-Epsilon + pBAD-VvCCD1. Incubation at 30 °C, 125 rpm in the dark for 48 hours. The cells were then analysed for protein expression by SDS-PAGE.

4.1.6 Estimation of theoretical α -ionone concentrations

To give a rough estimation about the possible amount of α -ionone produced from ϵ -carotene by VvCCD1 a calibration with β -carotene was conducted.

4.1.6.1 β -Carotene calibration

In this matter three standards of 5 mM β -carotene were prepared. Three portions of 10.7 mg of β -carotene were dissolved in 4 mL of DCM and diluted 1:100 to a final concentration of 50 μ M β -carotene.

Table 14: Weighed masses of standards

Standard #	Mass [mg]
1	10.5
2	10.2
3	10.6

Six calibration points of the first standard were measured and a standard calibration curve was plotted.

Table 15: β -carotene calibration points

V [μ L]	c [μ M]
10	50
8	40
6	30
4	20
2	10
0.1	0.5

Since the upper injection volume of the standard calibration is half of the usual sample injection volume of 20 μ L, the concentration of the plot was halved to provide a fast visual determination of the concentrations.

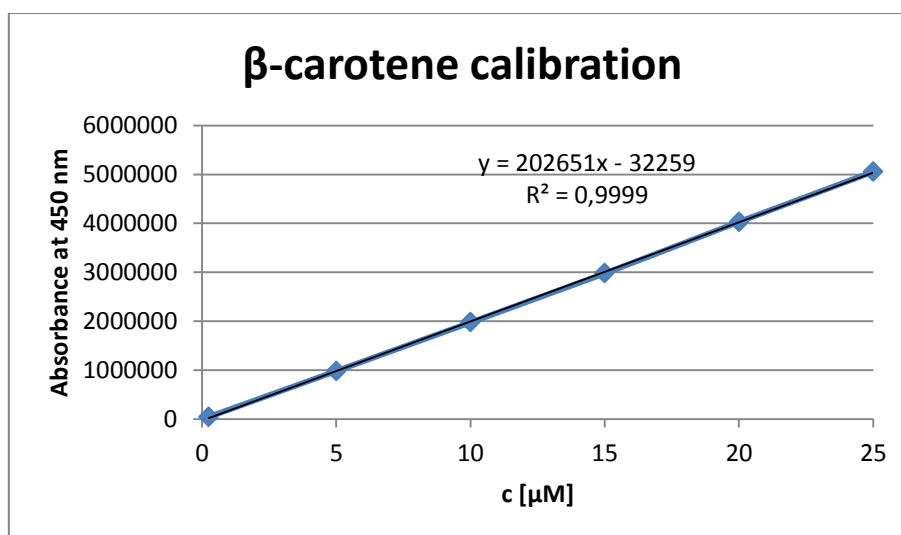


Figure 11: β -carotene calibration

The concentration of β -carotene can also be calculated with equation of the linear regression in Figure 11.

$$c [\mu M] = \frac{\text{Absorbance} + 32259}{202651}$$

4.1.6.1.1 Standard preparation inaccuracy

To assess the inaccuracy of the standard preparation procedure, 5 μL of all standards were injected and compared to the standard calibration curve.

The theoretical absorbance of 5 μL in the 10.5 mg sample would be:

$$\text{Absorbance (theoretical)} = 202067 * 12.5 - 21336$$

$$\text{Absorbance (theoretical)} = 2504501$$

Table 16: Standard preparation inaccuracy

Weighed portion [mg]	Injection volume [μL]	Absorbance	A/theor. A [%]	rel. sd [%]
10.5	5	2578274	102.9	0.18
10.2	5	2576556	102.9	
10.6	5	2569420	102.6	

All samples deviate by about plus 3 percent but are very accurate among one another.

4.1.6.1.2 Injector inaccuracy (Repeatability)

To assess the inaccuracy of the injector, the upper (10 μL) and lower (0.1 μL) injection volumes of the calibration sample #1 (10.5 mg) were measured two more times.

Table 17: Injector inaccuracy

Sample	Injection volume [μL]	Absorbance	rel. sd [%]
upper volume 1	10	5054865	0.33
upper volume 2	10	5025651	
upper volume 3	10	5027392	
lower volume 1	0.1	43598	2.96
lower volume 2	0.1	43973	
lower volume 3	0.1	46047	

The injector has an inaccuracy of 0.33 % at the upper injection volume of 10 μL and an inaccuracy of 2.96 % at the lower injection volume of 0.1 μL .

4.1.6.2 Estimation of the extinction coefficient of ϵ -carotene

The absorbance of a substance depends on the applied wavelength [nm] and the solvent the compound is dissolved in. The extinction coefficient of ϵ -carotene was estimated by comparing the extinction coefficients and absorbance maxima of similar compounds.

Table 18: Extinction coefficients of carotenes in petroleum ether

Compound	Solvent	Ext. coefficient [$\text{L g}^{-1} \text{cm}^{-1}$]	Abs. max. [nm]	Source
β -carotene (β - β -carotene)	Petroleum ether	256	453	(Isler, et al., 1956)
α -carotene (β - ϵ -carotene)	Petroleum ether	280	444	(Schwieter, 1965)
ϵ -carotene (ϵ - ϵ -carotene)	Petroleum ether	301	440	(Schwieter, 1965)

The replacement of the β -rings with ϵ -rings leads to a stronger absorption with an absorption maximum at a lower wavelength.

For simplification the extinction coefficient of β -carotene at 450 nm was assumed as $256 \text{ L g}^{-1} \text{ cm}^{-1}$. The extinction coefficient of ϵ -carotene at 450 nm was estimated from its absorbance spectrum.

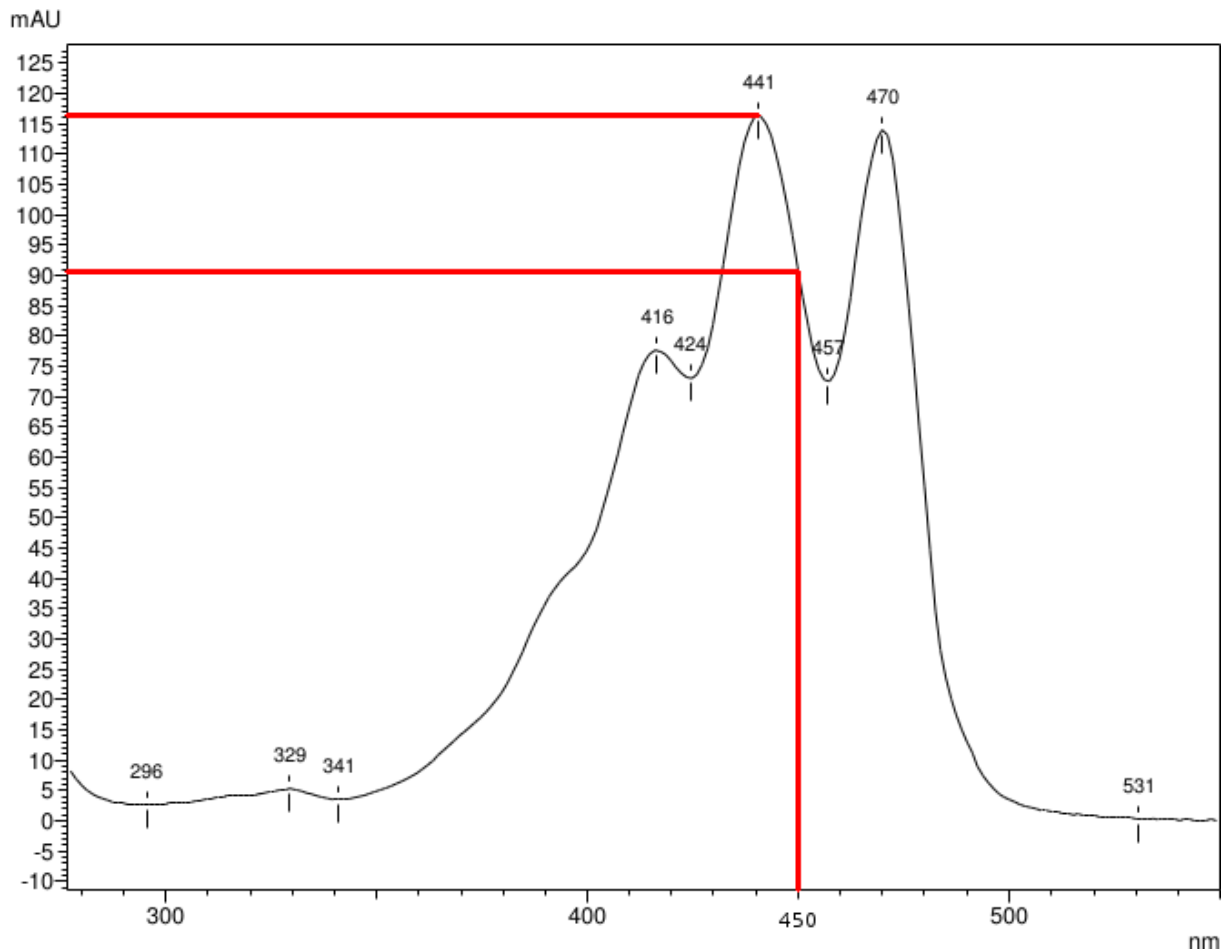


Figure 12: Estimation of the extinction coefficient of ϵ -carotene at 450 nm from its absorbance spectrum.

The ratio of absorbance can be read off in Figure 12. The absorbance at 450 nm is about 91 mAU, which is 78.4 % of the absorbance of 116 mAU at the absorbance maximum. Multiplying the extinction coefficient of ϵ -carotene at 440 nm with the ratio of the absorbance at 440 nm over the absorbance at 450 nm equals the extinction coefficient at 450 nm.

$$\begin{aligned}
 E_{450\text{nm}}(\epsilon - \text{carotene}) &= E_{440\text{nm}}(\epsilon - \text{carotene}) * \frac{A_{450\text{nm}}}{A_{440\text{nm}}} \\
 &= 301 \text{ L} * \text{g}^{-1} * \text{cm}^{-1} * \frac{91 \text{ mAU}}{116 \text{ mAU}} = 235 \text{ L} * \text{g}^{-1} * \text{cm}^{-1}
 \end{aligned}$$

The extinction factor of ϵ -carotene in petroleum ether at 450 nm is therefore $235 \text{ L g}^{-1} \text{ cm}^{-1}$.

$$\text{Ratio [\%]} = \frac{E_{450 \text{ nm}}(\epsilon - \text{carotene})}{E_{450 \text{ nm}}(\beta - \text{carotene})} = \frac{235 \text{ L} * \text{g}^{-1} * \text{cm}^{-1}}{256 \text{ L} * \text{g}^{-1} * \text{cm}^{-1}} = 91.8 \%$$

Finally ϵ -carotene absorbs about 92 % as much as β -carotene does at 450 nm.

4.1.6.3 Calculation of the estimated α -ionone amount

The average absorbance of ϵ -carotene per gram wet biomass of five measurements of *E. coli* BL21(DE3) pAC-Epsilon was 6135079 (sd= 987017). Using the equation of the β -carotene calibration multiplied by the previously estimated absorbance ratio of ϵ -carotene to β -carotene equals the ϵ -carotene concentration.

$$c(\epsilon - \text{carotene}) = \frac{6135079 + 32259}{202651} * 0.922 = 28.06 \mu\text{M} (\pm 4.64 \mu\text{M})$$

Since the extracted carotenes were dissolved in 1 mL of solvent the molar amount in the HPLC sample can be easily concluded.

$$\begin{aligned} n(\epsilon - \text{carotene}) \text{ per HPLC sample} &= 28.06 \mu\text{M} = \frac{\mu\text{mol}}{\text{L}} = \frac{\text{nmol}}{\text{mL}} * 1 \text{ mL} \\ &= 28.06 \text{ nmol} (\pm 4.64 \text{ nmol}) \end{aligned}$$

In average there were 28.06 nmol (\pm 4.64 nmol) of ϵ -carotene present per HPLC sample. Only 5 mL of 12.5 mL of the ether phase was used for HPLC analysis during the extraction. The actual amount of ϵ -carotene in one sample was therefore 2.5 times higher.

$$n(\epsilon - \text{carotene}) \text{ per sample taken} = 28.06 \text{ nmol} * 2.5 = 70.15 \text{ nmol} (\pm 11.6 \text{ nmol})$$

There are in average 70.15 nmol (\pm 11.6 nmol) of ϵ -carotene in 1 gram of wet biomass. Since one molecule of ϵ -carotene is cleaved into two molecules of α -ionone the molar amount of α -ionone is doubled.

$$n(\alpha - \text{Ionone}) = n(\epsilon - \text{carotene}) * 2 = 70.15 \text{ nmol} * 2 = 140.30 \text{ nmol} (\pm 23.2 \text{ nmol})$$

Multiplying by the molar mass of α -ionone equals the mass of α -ionone per mass of wet biomass.

$$m(\alpha - \text{Ionone})[\text{ng}] = n(\alpha - \text{Ionone})[\text{nmol}] * M(\alpha - \text{Ionone}) \left[\frac{\text{nmol}}{\text{ng}} \right]$$

$$m(\alpha - \text{Ionone}) = 140.30 \text{ nmol} * 192.30 \frac{\text{nmol}}{\text{ng}} = 26979 \text{ ng} = 26.98 \mu\text{g} (\pm 4.46 \mu\text{g})$$

The dry biomass was assumed to be a fifth of the wet biomass. The amount of α -ionone is therefore multiplied by five.

$$\frac{m(\alpha - \text{Ionone})}{m(\text{dry biomass})} = \frac{m(\alpha - \text{Ionone})}{m(\text{wet biomass})} * 5 = 26.98 \frac{\mu\text{g}}{\text{g wet biomass}} * 5 = 134.9 \mu\text{g} (\pm 22.3 \mu\text{g})$$

4.2 Product purification

4.2.1 α -ionone stability

To assess the volatility and general handling properties of α -ionone some experiments on the stability were conducted.

4.2.1.1 Evaporation test

50 mL of LB were inoculated with *E. coli* BL21(DE3) to an OD of 0.2 and 5.2 μL (500 μM) of α -ionone were added. The culture was thoroughly mixed and 25 mL of the suspension frozen at -20°C . Incubation at 30°C , 125 rpm in the dark for 48 hours.

After 48 hours both samples were extracted twice with 10 mL of purified EthAc. 6 mL of the first extract were removed and 9 mL of the second which results in 15 mL of sample. The pooled extracts were evaporated in the rotary evaporator and dissolved in 1.5 mL of EthAc. 1 mL of the samples were filtered through a PTFE filter, diluted 1:10 and measured by GC-MS.

4.2.1.2 Heat stability

To ensure that α -ionone is not degraded over the time of incubation or during adsorption onto the SPME fiber at 80 °C during HS-SPME-GC-MS measurement α -ionone and β -ionone standards were added to SPME samples. 100 mM of each standard were added to 6 mL of LB medium, incubated at 30 °C for 72 hours and measured by HS-SPME-GC-MS.

As negative controls 100 mM of α -ionone and β -ionone were added to 1 mL of EthAc in a 20 mL SPME vial and immediately measured by HS-SPME-GC-MS.

4.2.1.3 Oxidation stability

In order to create a ϵ -carotene standard with the autosampler of the HPLC ϵ -carotene must sustain the evaporation of the eluent and the exposure of oxygen while stored dry on air overnight.

For this purpose a previously measured extract of *E. coli* BL21 (DE3) pAC-Epsilon + pBAD was opened, weighed and let evaporate overnight in the dark. The next morning the evaporated DCM was supplemented until the previous weight was achieved and measured again by HPLC-PDA.

4.2.2 Two-phase system with n-Hexane

100 mL of LB medium (Cm + Amp) were inoculated to an OD value of 0.2 with *E. coli* BL21(DE3) pAC-Epsilon + pET22b-VvCCD1 and incubated at 30 °C, 125 rpm in the dark for 6 hours. The suspension was then filled into the two-neck round-bottom flask connected to a reflux condenser, sealed with a septum and placed on a magnetic stirrer. The suspension was overlaid with 25 mL (20 %) of n-Hexane. The other neck was closed with a septum where pressurised air was pumped directly into the suspension through a needle. Incubation at RT (~ 24 °C), 1000 rpm for 16 hours. The suspension was centrifuged (4000 g, 15 min., 4 °C) and 15 mL of the n-hexane phase were concentrated by a vacuum distillation and taken for volatile analysis by GC-MS. The cultures were filled back into the two-neck round-bottom flask, induced with 0.1 mM IPTG and substituted with new 15 mL of n-hexane and further incubated for another 16 hours again taking 15 mL of the n-hexane phase for volatile analysis by GC-MS.

4.2.3 Direct extraction of α -ionone from the supernatant

100 mL of LB medium (Cm + Amp) was inoculated to an OD of 0.2 with *E. coli* BL21(DE3) pAC-Epsilon + pET22b-VvCCD1. Pressurised air was pumped into the suspension just underneath the surface. The culture was incubated for 48 hours at RT (~24 °C) and 500 rpm on a magnetic stirrer.

The culture was then centrifuged (4000 g, 15 min., 4 °C) and 75 mL of the supernatant were shaken out with DCM. The DCM phase was pipetted off, washed with 10 mL of 5 M NaCl, dried under a nitrogen flow, dissolved in 1 mL of EthAc, filtered through a PTFE filter and measured by GC-MS.

The other 25 mL were extracted with 5 mL of diethyl ether and prepared the same way for GC-MS measurement.

4.2.4 Exhaust air collection

Since α -ionone is often described as a volatile compound it was tried to collect α -ionone from the exhaust air by the following experimental setup.

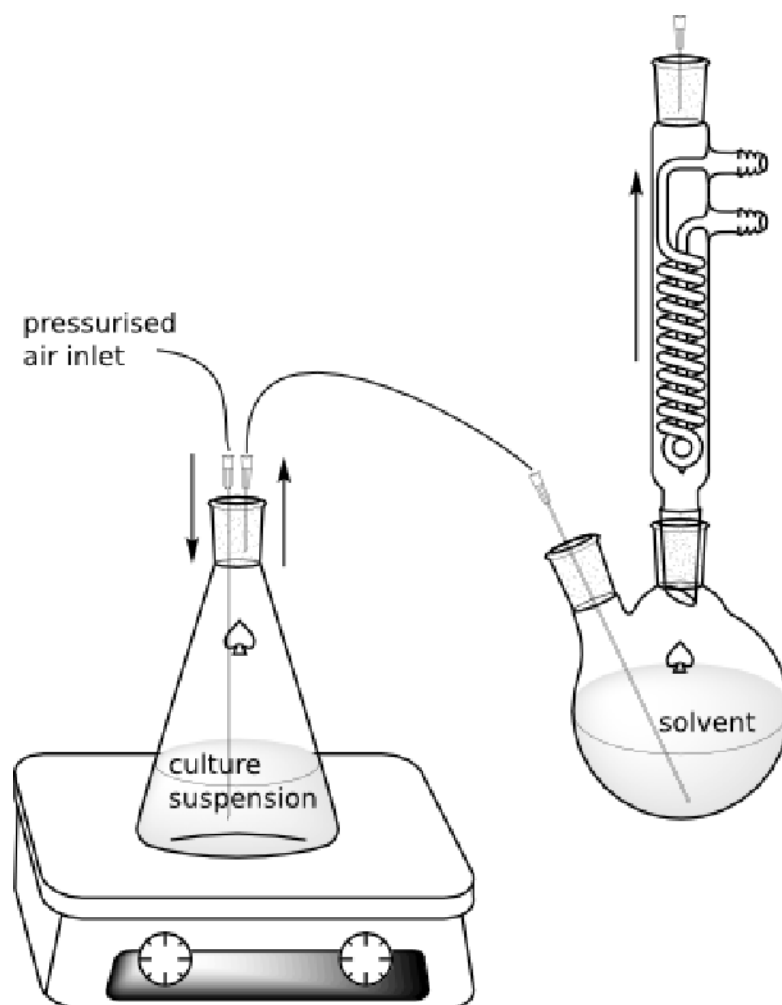


Figure 13: Scheme of the exhaust air collection setup.

E. coli cultures in shaking flasks of Figure 13 were sealed with a rubber septum and placed on a magnetic stirrer. Pressurised air was pumped directly into the suspension through a needle pushing the exhaust air into a two-neck round-bottom flask containing ethyl acetate where the volatile compounds were absorbed. The two-neck round-bottom flask was connected to a reflux condenser to prevent evaporation of both the solvent and product. The reflux condenser was also sealed with a rubber septum to prevent contamination with dust from the surrounding air. A needle was used for pressure compensation. This experiment was performed using different types of tubes.

4.2.4.1 Tygon F-4040 A tube 1

100 mL of LB (Amp + Cm) were inoculated with *E. coli* BL21 (DE3) pAC-Epsilon + pET22b-VvCCD1 to an OD of 0.2 and incubated at 37 °C, 135 rpm in the dark until an OD of 0.6 was reached. The culture was then sealed with a septum and placed on a magnetic stirrer and induced with 0.1 mM IPTG. The two-neck round-bottom flask was filled with 50 mL of EthAc. The culture was incubated at 37 °C, 600 rpm in the dark for 25 hours. Samples were taken at after 1, 3.5, 18.5 and 23.5 hours. After 25 hours the culture was heated to 100 °C for 10 minutes, concentrated by vacuum distillation until a volume of 1 mL was reached, filtered through a PTFE filter and measured by GC-MS.

4.2.4.2 Tygon F-4040 A tube 2

150 mL of LB (Cm + Amp) were inoculated with *E. coli* BL21(DE3) pAC-Epsilon + pET22b-VvCCD1 to an OD of 0.2. The exhaust air was lead through 40 mL of EthAc. Incubation at RT (23 °C), 500 rpm in the dark for 48 hours.

4.2.4.3 Teflon tube

150 mL of LB (Amp + Cm) were inoculated with *E. coli* BL21(DE3) pAC-Epsilon + pET22b-VvCCD1 to an OD of 0.2 and incubated at 30 °C, 125 rpm until an OD of 1.7 was reached. The culture was then placed on a magnetic stirrer and incubated at RT (24 °C), 400 rpm for 48 hours. The culture was then induced with 0.1 mM IPTG and incubated for another 24 hours.

4.3 Analytical Methods

4.3.1 Carotene extraction

The Carotenes were extracted according to an optimised version of Cunningham.

[1996_CUNNINGHAM_FUNCTIONAL ANALYSIS OF THE B AND E LYCOPENE CYCLASE] Since this extraction protocol requires a lot of time it was found that the incubation time, the 6 % KOH and one extraction step could be excluded from the extraction without having a negative impact on the carotene extraction (data not shown).

For carotene analysis 25 mL cell suspension was centrifuged (4000 g, 15 min., 4 °C). The pellet was vortexed in 1 mL of methanol until properly resuspended, 4 mL of diethyl ether were added and mixed by inversion or short vortexing. After centrifugation (4000 g, 15 min. 4 °C) the extract was collected, kept on ice and shielded from direct light exposure. The pellet was again resuspended in 1 mL of methanol and 8.5 mL of diethyl ether were added and mixed by inversion. After centrifugation (4000 g, 15 min., 4 °C) the extracts were pooled. The extract was then washed three times with 10 mL of 5 M NaCl. 5 mL of the diethyl ether phase were dried under a nitrogen gas flow, dissolved in 1 mL of DCM and kept on ice for 10 minutes before being filtered through a PTFE filter and measured by HPLC-PDA.

4.3.2 Carotene analysis by HPLC-PDA

The Carotene analysis was performed on a Shimadzu Corporation system. The software used was Labsolutions version 5.10 SP1.

The carotenes were separated on a reversed phase YMC C30 Carotenoid S-3 µm column (250 x 4.6 mmI.D.) using an isocratic gradient with an eluent flow rate of 1 mL per minute. The oven temperature was held at 25 °C.

Table 19: HPLC eluent gradient

Time [min]	Eluent B [%]
5	0
45	100
50	100
55	0
60	0

The absorbance spectrum was acquired from 250 nm to 500 nm. Carotenes were displayed at 450

nm. The resulting C14-dialdehyde of carotenoid degradation by VvCCD1 can be detected at 414 nm (2005 MATHIEU).

4.3.3 Volatile analysis by GC-MS

For the analysis of volatile compounds the samples were either extracted using various solvents and concentrated by vacuum distillation, filtered through a PTFE filter and directly measured using GC-MS injecting 1 µL of sample or by incubating HS-SPME-GC-MS.

4.3.3.1 Measurement parameters

The GC-MS measurements were performed on a GCMS-QP2010 Plus system of the Shimadzu Corporation which is equipped with a quadrupole mass spectrometer. The used software was GCMSsolution 2.12.

The volatile compounds were separated on a BPX 5 column (Length: 30m; I.D. 0.25mm; Film: 0.25 µm; by SGE Analytical Science). The required hydrogen was provided by a Hydrogen Generator NMH, 250 by SL Schmidlin, Schwäbisch Gmünd, Germany. The compounds were ionized by Electron Ionisation (EI).

Table 20: GC-MS measurement parameter

GC measurement parameter	Value
Column oven temp. [°C]	60
Injection temperature [°C]	290
Injection Mode	Split
Split Ratio	25
Carrier Gas	He
He Gas primary pressure [kPa]	500-900
Flow control Mode	Linear Velocity
Pressure [kPa]	72.8
Total Flow [mL/min]	41.3
Column Flow [mL/min]	1.20
Linear Velocity [cm/sec]	40
Purge Flow [mL/min]	10
Ion source Temp. [°C]	200
Interface Temp. [°C]	250

Table 21: GC-MS temperature gradient

Temperature rate [°C/min]	Final Temperature [°C]	Hold Time [min]
-	60	1
7	170	0
70	280	2
0	0	0

Total program time of one measurement was 20.29 minutes. The mass to charge ratio (m/z) was scanned from 27 to 350 with a scan speed of 1250 starting from 4.10 minutes.

4.3.3.2 HS-SPME-GC-MS

For the analysis of volatile compounds 25 mL of cell suspensions were centrifuged (4000 g, 15 min. 4 °C) and resuspended in 6 mL LB medium containing the respective antibiotics and filled in 20 mL SPME glass vials. The samples were then induced with 0.1 mM IPTG or 0.01 % L-Arabinose for pET22b and pBAD plasmids respectively and incubated at 30 °C and 125 rpm and different incubation times.

Prior to measurement the samples were placed in the heating block by the autosampler where the volatile compounds were adsorbed onto the SPME fiber at 80 °C for 10 minutes.

4.4 Cloning of VvCCD1 from pET22b-VvCCD1 to pBAD-A

The VvCCD1 gene was transferred from the donor plasmid pET22b-VvCCD1 to the recipient plasmid pBAD by restriction cloning. Figure 14 gives an overview of the cloning procedure. The VvCCD1 region of pET22b-VvCCD1 was amplified by Phusion-PCR using primer *VvCCD1-fwd2* and *VvCCD1-rev2*. After amplification of VvCCD1 both the insert DNA and the vector pBAD were digested by the restriction enzymes HindIII and BsaI as well as NcoI and HindIII respectively creating linear DNA with complementary sticky ends. After ligation of these DNA strands *E. coli* DH10b was transformed with the newly created pBAD-VvCCD1 plasmids and plated on LB (Cm + Amp) plates. The resulting colonies were then screened for positive clones by colony PCR.

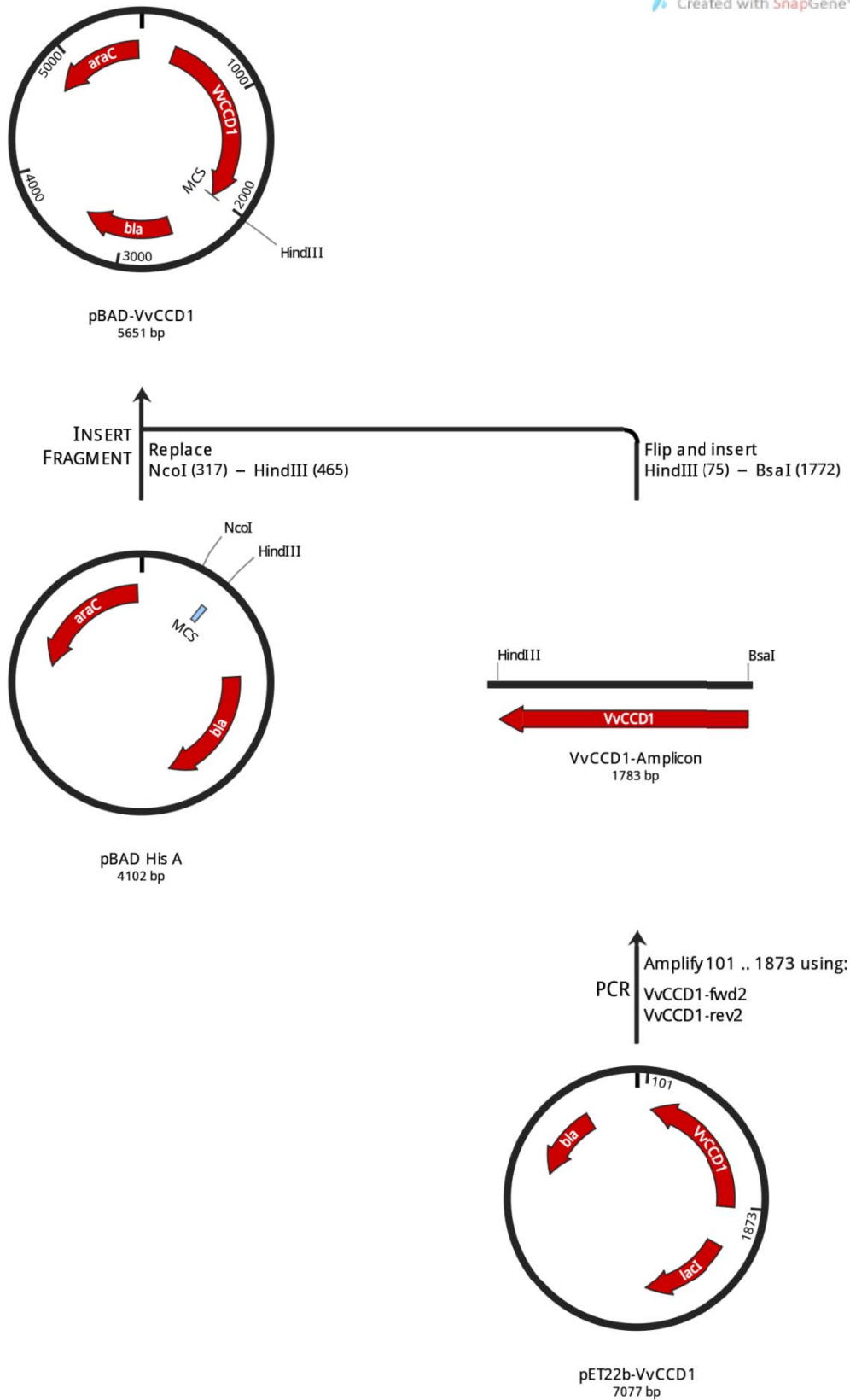


Figure 14: Scheme of the cloning procedure. The VvCCD1 gene was amplified from pET22b-VvCCD1, digested with *HindIII* and *BsaI* and inserted into the previously *NcoI* and *HindIII* digested pBAD-A vector. With *BsaI* being an exocutter, it was possible to design the complementary sticky end to the *NcoI* sticky end of the vector.

4.4.1 Amplification of VvCCD1 by Phusion-PCR

To amplify VvCCD1 from the pET22b vector a PCR reaction with the respective primers was conducted. The PCR reaction mixture was prepared according to Table 22.

Table 22: PCR reaction mixture for VvCCD1 amplification from pET22b-VvCCD1

PCR reaction components	Volume [μ L]
Water	36.5
5x HF buffer	10
10 mM dNTPs	1
Primer1: VvCCD1-fwd [100 μ M]	0.5
Primer2: VvCCD1-rev [100 μ M]	0.5
pET22b-VvCCD1 MiniPrep	1 = 66 ng
Phusion DNA Polymerase	0.5
Total volume	50

To avoid unspecific primer binding and therefore increase the total yield of the PCR product the annealing temperature was increased by 3 °C.

Table 23: Thermocycler setup for VvCCD1 amplification from pET22b-VvCCD1

Step	Temperature [°C]	Time [s]	Repeats
Initial denaturation	98	60	1
Denaturation	98	20	30
Annealing	67	30	
Extension	72	120	
Final extension	72	200	1

The PCR-product was purified by gel extraction. The DNA was eluted in 30 μ L of water, the concentration was measured and another Phusion-PCR of the purified VvCCD1-Amplicon was conducted to gain enough DNA for the subsequent restriction digest.

Table 24: PCR reaction mixture for the amplification of the VvCCD1-Amplicon

PCR reaction components	Volume [μ L]
Water	35.5
5x HF-Puffer	10
10 mM dNTPs	1
Primer 1: VvCCD1-fwd [100 μ M]	0.5
Primer 2: VvCCD1-rev [100 μ M]	0.5
VvCCD1-Amplicon	2 = 11.8 ng
Phusion DNA Polymerase	0.5
Total volume	50

The Thermocycler settings were the same as in Table 23. The PCR product was purified by gel extraction. The DNA was eluted in 30 μ L of water, the concentration of the DNA was measured and stored at -20 °C.

4.4.2 Agarose gel electrophoresis

After the PCR reaction was finished, the different sized DNA fragments were separated by agarose gel electrophoresis to verify the appropriate DNA sizes and quality of PCR reaction. The DNA samples were mixed with 6 x gel loading buffer prior loading the gel. The gel was run at 100 volts for 60 minutes.

After the electrophoresis the gels were stained in ethidium bromide staining solution for 12.5 minutes and shortly rinsed TAE buffer afterwards. A picture was then taken in the Dark Hood.

4.4.3 Gel extraction of DNA

To purify a PCR-product the DNA was run on an agarose gel and then purified by using the GeneJET Gel Extraction Kit. In detail the stained gel was exposed to UV light (365 nm) to identify the appropriate gel bands. To minimize the probability of mutations this working step must be conducted fast. The gel bands of appropriate size were then cut out and weighed in a pre weighed micro centrifuge tube. According to the weight of the band in milligram the same amount of binding buffer in microliters was added. The gel was dissolved by heating to 60 °C for 10 minutes and shaking (500 rpm) or until dissolved. The solution was then transferred to the purification column and centrifuged (13000 g, 1 min). For sequencing samples another 100 μ L of loading buffer was added to the column. After the flow through was discarded, 700 μ L of washing buffer was added to the purification column and centrifuged twice. In the end the DNA concentration was measured.

4.4.4 Determination of the DNA Concentration

The DNA concentration was determined with the NanoDrop system. Double stranded DNA is measured at 260 nm. The undiluted DNA solution was blanked twice against 1 μ L of water before 1 μ L of each DNA sample was measured.

4.4.5 Restriction digest

After a sufficient amount of the VvCCD1-Amplicon was obtained the VvCCD1-Amplicon and the vector pBAD-A were ready for the restriction digest. The amount of the vector pBAD-A was taken from a previous MiniPrep.

Table 25: Expected fragment sizes after the restriction digest

Name	DNA size [bp]
pBAD-A	4102
pBAD-A cut with HindIII and NcoI	3954
VvCCD1-Amplicon	1783
VvCCD1-Amplicon cut with HindIII and BsaI	1697

The units of restriction enzymes necessary for the digest were calculated:

$$U = \frac{\text{size of assay} - \text{DNA}[bp] * \text{nr. of cutting positions at target} - \text{DNA}}{\text{size of target} - \text{DNA}[bp] * \text{nr. of cutting positions at assay} - \text{DNA}} * \frac{m(\text{DNA})[\mu\text{g}]}{\text{reaction time [h]}} * x - \text{fold digest}$$

Table 26: Calculation of the enzyme units for the restriction digest

	Vector: pBAD-A		Insert: VvCCD1-Amplicon	
Enzyme Number	1: NcoI	2: HindIII	1: BsaI	2: HindIII
Assay DNA	λ-DNA			
Size of assay DNA [bp]	48502			
Number of cutting positions	4	7	2	7
Size DNA [bp]	4102		1783	
Number of cutting positions	1	1	1	1
Amount of DNA [μg]	5		1.39	
Required Units for 4x digest after 2 h	30	17		
Required Units for 1.5x digest after 2 h			14	4
Enzyme amount in stock solution [U/mL]	20000	20000	20000	20000
Required amount of enzyme [μL]	1.5	0.85	0.7	0.2

After the units were calculated the reaction mixtures were prepared.

Table 27: Restriction digest reaction mixture

Restriction digest components	Vector: pBAD-A	Insert: VvCCD1
	[μL]	[μL]
Water	27.31	16.1
10x Cutsmart buffer	5	5
DNA	27.31 = 5 μg	28 = 1.39 μg
Enzyme 1	1.5	0.7
Enzyme 2	0.85	0.2
Total volume	50	50

The restriction digest was incubated for 2 hours at 37 °C followed by inactivation at 80 °C for 20 minutes. The corresponding sizes of the DNA are. After inactivation the DNA samples were purified by gelexttraction and the DNA concentration was measured.

4.4.6 Ligation

After the restriction digest both the vector DNA and insert DNA were linearised and now possess complementary sticky ends which are shown in Figure 15. Both DNA strands were now ready for ligation.

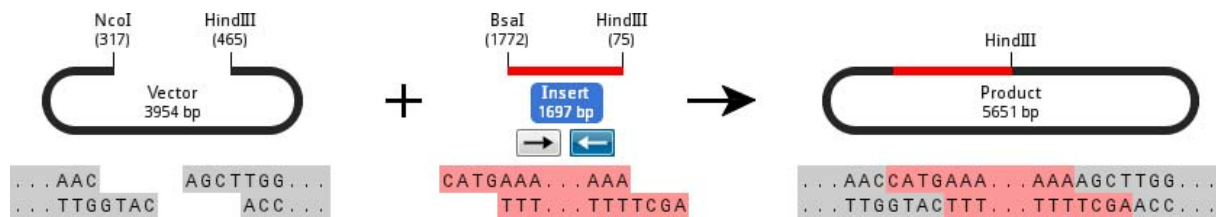


Figure 15: Scheme of the ligation of the complementary sticky ends of the vector and insert DNA.

For ligation a 1:3 ratio of the molar amount of the vector and insert DNA is taken. Therefore the measured mass concentration [$\text{ng}/\mu\text{L}$] must be converted to the molar concentration [$\text{fmol}/\mu\text{L}$]. For that purpose the average molecular weight of one basepair was estimated as 660 g/mol which equals 0.00066 ng/fmol.

$$V(\text{DNA})[\mu\text{L}] = \frac{n(\text{DNA})[\text{fmol}] * M(\text{DNA}) \left[\frac{\text{ng}}{\text{fmol}} \right] * \text{size of DNA} [\text{bp}]}{c(\text{DNA}) \left[\frac{\text{ng}}{\mu\text{L}} \right]}$$

Table 28: Calculation of the volume of DNA needed for ligation

	Vector: pBAD-A	Insert: VvCCD1
c (DNA) [ng/μL]	14.1	15.3
n (DNA ideal) [fmol]	200	600
n (DNA reduced 1:3) [fmol]	66.67	200
m (DNA) [ng]	173.98	224
Volume [μL]	12.34	14.64

Usually 200 fmol of vector DNA and 600 fmol of insert DNA are chosen for ligation. Since the concentration of the insert DNA was too low the molar amounts were reduced to one third of the standard amount.

Incubation at 22 °C for 2 hours followed by inactivation at 65 °C for 15 minutes.

4.4.7 Transformation by electroporation

70 μL of SOC medium was thawed and pre heated to 37 °C. Electro competent *E. coli* BL21(DE3) cells were thawed on ice. Just before the transformation the cuvettes were taken out of the -20 °C freezer and hold available dry. After the cells were thawed 1 μL of DNA was added to the cells, mixed carefully and incubated on ice for 1 minute. The cell suspension was then pipetted “bubble free” into the electroporation cuvette. The cuvette was closed, dried with a paper tissue hit three times on the table and pulsed. The time constant was noted.

Table 29: Electroporator settings for different *E. coli* strains

Organism	Voltage [kV]	Resistance [Ω]	Capacity [μF]
<i>E. coli</i> BL21(DE3)	1.38	125	50
<i>E. coli</i> DH10b	2.00	200	25

After pulsing the cell suspension was immediately resuspended in pre heated SOC medium and incubated for 1 hour and 37 °C. The cells were then inoculated onto the agar plates by plating 100 μL of cell suspension as well as by streaking with the inoculation loop.

4.4.8 Selection of transformants

Transformed cells were selected by applying selection pressure using the respective antibiotics. Regarding the cloning, clones were chosen randomly. The plasmids were then analysed by colony PCR.

4.4.9 Colony PCR

To confirm that the grown colonies contain the gene of interest and not only the religated vector pBAD-A itself, 28 colonies were randomly chosen to be analysed. In order to do so, the colony was picked with a sterile toothpick and immersed into the water and then spread onto the numbered backup plate. The rest of the PCR mix was then added and the PCR reaction started.

Table 30: PCR reaction mixture for colony PCR

Compound	Volume [μL]
Water	15
PCR buffer BD 5x	4
10 mM dNTPs	0.4
Primer 732 pBAD-A-fwd	0.2
Primer 733 pBAD-A rev	0.2
Taq-Polymerase	0.2
Total volume	20

The Annealing Temperature was chosen according to the lower melting temperature the primer pair when bound to the molecule minus five degree celsius.

Table 31: Thermocycler setup for colony PCR

Step	Temperature [$^{\circ}\text{C}$]	time [s]	Repeats
Initial denaturation	98	300	1
Denaturation	98	40	30
Annealing	57	40	
Extension	72	150	
Final extension	72	600	1

The PCR products were subjected to Agarose-Gelelectrophoresis to confirm the right fragment size of 1897 bp for a positive clone.

4.4.10 Glycerol stock

For long time storage of the positive clone, 600 μL of sterile 100 % glycerol was added to 600 μL of culture suspension, mixed by inversion and stored at -80°C .

4.4.11 Sequencing

For the sequencing of the VvCCD1 gene on pBAD-VvCCD1 a MiniPrep was prepared from *E. coli* DH10B pBAD-VvCCD1. The sequencing samples were premixed, adding 2 μL 10 μM of the forward primer 732 and reverse primer 733 to 15 μL of plasmid DNA containing 75 $\text{ng}/\mu\text{L}$ giving a total sample volume of 17 μL respectively.

To improve the purity of the VvCCD1 template the region was amplified by Phusion PCR using the primers number 732 and 733 and purified by subsequent gel extraction. The sequencing was conducted using the sequencing primers 760 and 761 by MWG Eurofins in Ebersberg, Germany.

4.5 *In vitro* experiment

The experiment was planned according to (Kato, et al., 2006).

500 mL of LB (Cm) and 500 mL of LB (Cm + Amp) were inoculated with the whole overnight culture of *E. coli* BL21 (DE3) pAC-Epsilon and *E. coli* BL21 (DE3) pAC-Epsilon + pET22b-VvCCD1 respectively. The cultures were incubated at 30 °C, 125 rpm in the dark until the culture with *E. coli* BL21 (DE3) pAC-Epsilon + pET22b-VvCCD1 reached an OD of 0.6 and was then induced with 0.25 mM IPTG. Incubation was continued for 48 hours.

The two samples were centrifuged (5000 g, 15 min. 4 °C) and resuspended in 60 mL vitro buffer 1 each giving a total volume of 120 mL. The cells were decomposed by applying a pressure of 2.4 kbar. The French Press was washed three times with 0.5 M NaOH prior and after the decomposition.

Both decomposed suspensions were brought together in a shaking flask. Since the needle for the air inlet could not reach into the suspension additional buffer was added afterwards. Incubation for 72 hours.

5 Results

5.1 Carotene analysis of *E. coli* BL21(DE3) pAC-Epsilon

5.1.1 Carotene identification

The strain *E. coli* BL21(DE3) pAC-Epsilon provided by Cunningham (CUNNINGHAM FX JR, GANTT E. PLANT J. 2005 FEB;41(3):478-92. 10.1111/j.1365-313X.2004.02309) was investigated for its ϵ -carotene accumulation. The culture was grown at 16 °C for 48 hours, extracted and analysed by HPLC-PDA. The chromatogram is shown in Figure 16. The identification of the peaks is described below.

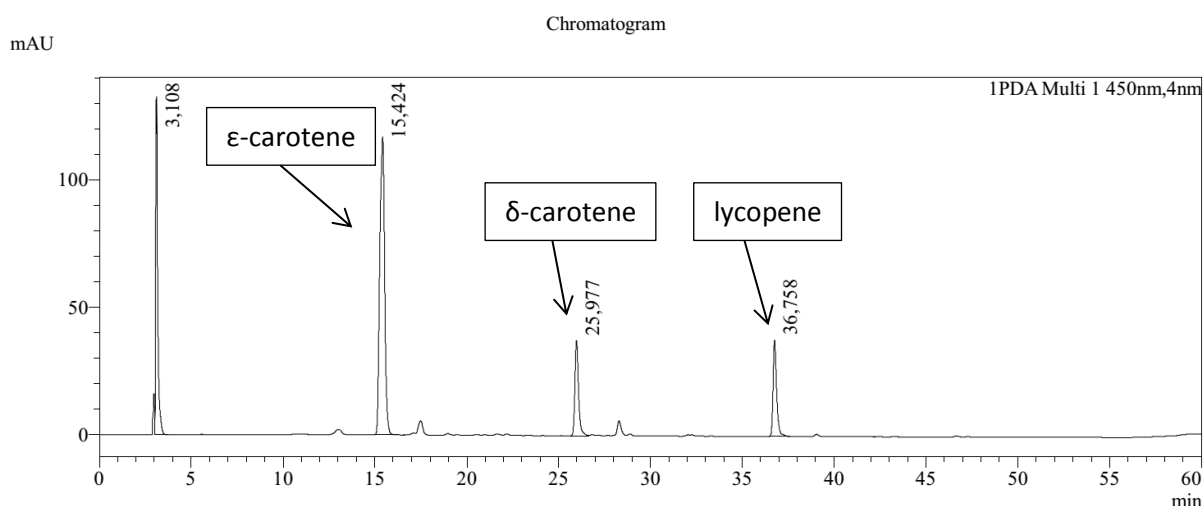


Figure 16: Chromatogram of *E. coli* BL21(DE3) pAC-Epsilon grown at 16 °C for 48 hours.

There are four main peaks visible. The first peak at about 3 minutes is the solvent peak of DCM. The other peaks were identified comparing the absorbance maxima with literature data and retention times of measured standards, if available. The absorbance spectrum of each peak is shown in Table 32.

The fourth peak could be easily identified as lycopene by comparing the retention time with the lycopene standard in Figure 34. The third peak was proposed to be δ -carotene having one ϵ -ring group less than ϵ -carotene hence being in between lycopene and ϵ -carotene in terms of adsorption properties. Due to lack of standards for ϵ -carotene and δ -carotene they were identified by comparing the absorbance maxima with literature data in Table 33.

The absorbance maxima of peak number 2 and 3 fit the literature data very well. Peak 2 and 3 therefore represent most likely ϵ -carotene and δ -carotene.

A confirmation of the identification of the carotenes by mass spectrometry could not be achieved since ESI or APCI is needed for carotene ionisation which was not available. (Oxley, et al., 2014)

Table 32: Absorbance spectra of the extracted compounds of *E. coli* BL21(DE3) pAC-Epsilon

Peak nr.	Retention time [min]	Absorbance spectrum	Absorbance max. in HPLC eluent
2	15.424		417; 440; 470
3	25.977		432; 457; 487
4	36.758		448; 473; 504

Table 33: Absorbance maxima of selected carotenoids in different solvents

Peak Nr.	t _R [min]	Name	Abs. Max. In HPLC eluent	Abs. max. acc. to literature	Source
-	19.70	β-carotene	-; 452; 479	-; 453.2; 478.0 in HPLC eluent	(Fraser, et al., 2000)
2	15.48	ε-carotene	417; 440; 470	416; 440; 470 in petroleum ether 417; 440; 470 in ethanol	(Schwieter, 1965) (Chapman & Haxo, 1963)
3	26.18	δ-carotene	432; 457; 487	431; 456; 489 in petroleum ether	(Rodriguez-Amaya, 2001)
4	37.09	lycopene	448; 473; 504	444; 470; 502 in petroleum ether 446.0; 472.6; 504.2 in HPLC eluent 446; 472; 503 in ethanol	(Rodriguez-Amaya, 2001) (Fraser, et al., 2000) (Rodriguez-Amaya, 2001)

5.2 Carotene and apocarotene analysis of *E. coli* BL21(DE3) pAC-Epsilon + pET22b-VvCCD1

After cotransforming the ε-carotene accumulating *E. coli* clone with pET22b-VvCCD1, *E. coli* BL21(DE3) pAC-Epsilon + pET22b-VvCCD1 was investigated for its carotene accumulation before IPTG induction. For carotene analysis the cells were extracted and analysed by HPLC-PDA. The extracted sample of *E. coli* BL21(DE3) pAC-Epsilon + pET22b-VvCCD1 was totally colourless, while *E. coli* BL21(DE3) pAC-Epsilon was having an orange colour. An exemplary chromatogram is shown in Figure 17.

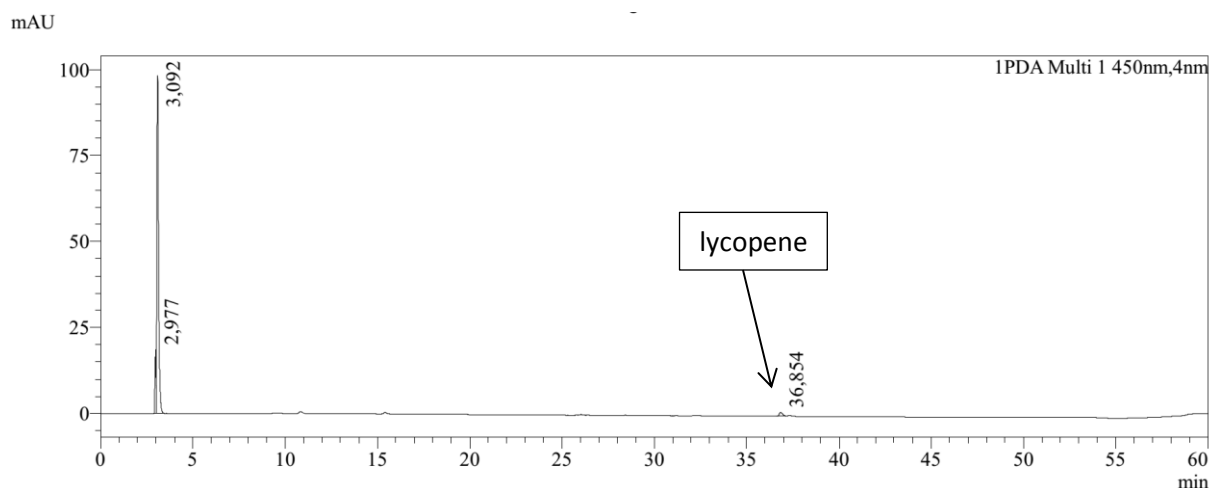


Figure 17: Chromatogram of *E. coli* BL21(DE3) pAC-Epsilon + pET22b-VvCCD1 grown at 30 °C for 41 hours.

Only trace amounts of lycopene could be found. Subsequent experiments with various growing conditions also showed no or only trace amounts of carotenes with or without IPTG induction. (Method 4.1.1.1)

In addition the cultures were analysed for volatile compounds by GC-MS. No product besides indole could be found by extraction from the culture suspension (Method 4.2.3). An exemplary GC-MS chromatogram is shown in Figure 18. The expected retention time of α -ionone is 14.8 min. (see 9.1.2)

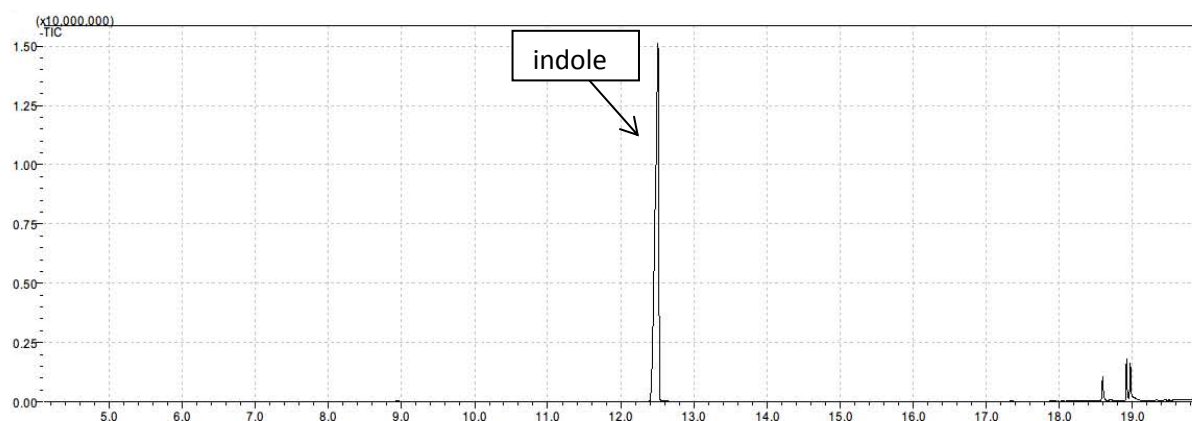


Figure 18: GC-MS chromatogram of the direct extraction of α -ionone from the culture suspension.

Since α -ionone is a volatile substance it could be lost during the incubation duration or during the extraction steps. To examine if the product evaporates from the culture suspension an evaporation test was conducted (Method see 4.2.1.1). After 48 hours of incubation at 30 °C 11 % of the amount of α -ionone was left. The evaporation of α -ionone was tried to prevent by various strategies. The use of a two phase system with n-Hexane (Method 4.2.2) could not capture any product. In case the cells do not tolerate n-Hexane very well it was tried to capture α -ionone by leading the exhaust stream through the solvent (Method 4.2.4). Again no product could be found.

To totally prevent evaporation of α -ionone and other volatile compounds the cultures were grown in SPME vials (Method 0). The results were not reproducible. With one exception, which is shown in chapter 0, no α -ionone could be found. To assess if α -ionone could be degraded while heating to 80 °C during the SPME measurement, heat stability tests with α -ionone and β -ionone were conducted (Method 4.2.1.2). After 72 hours of incubation at 30 °C and heating to 80 °C during the HS-SPME-GC-MS measurement 6 % of the α -ionone sample degraded of which about 2 % was converted to β -ionone. The β -ionone sample was degraded by 15 % of which 13.55 % was converted to β -ionone 5,6-epoxide and 2.61 % to α -ionone.

Though only trace amounts of carotenes could be detected in clones with VvCCD1 the product α -ionone could be found only once and only when growing the cultures in closed SPME vials.

5.3 Influence of pET22b on the carotene production

To find out if the empty vector pET22b influences the carotene synthesis *E. coli* BL21(DE3) pAC-Epsilon was transformed with pET22b, extracted and analysed by HPLC-PDA. It was found that the pET22b vector had an impact on the carotene profile, shifting the accumulation from ϵ -carotene to lycopene instead. The change in carotene accumulation could also be seen visually, while the pellet of *E. coli* BL21(DE3) pAC-Epsilon has a yellow colour *E. coli* BL21(DE3) pAC-Epsilon + pET22b has a red colour. The typical carotene distribution profiles of *E. coli* BL21(DE3) pAC-Epsilon and *E. coli* BL21(DE3) pAC-Epsilon + pET22b are shown in Figure 19 and Figure 20 respectively.

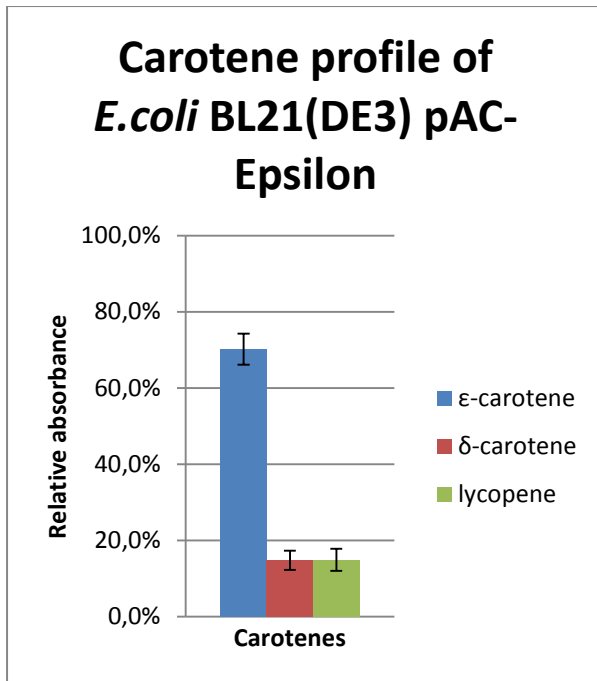


Figure 19: Typical carotene profile for *E. coli* BL21(DE3) pAC-Epsilon (6 data points)

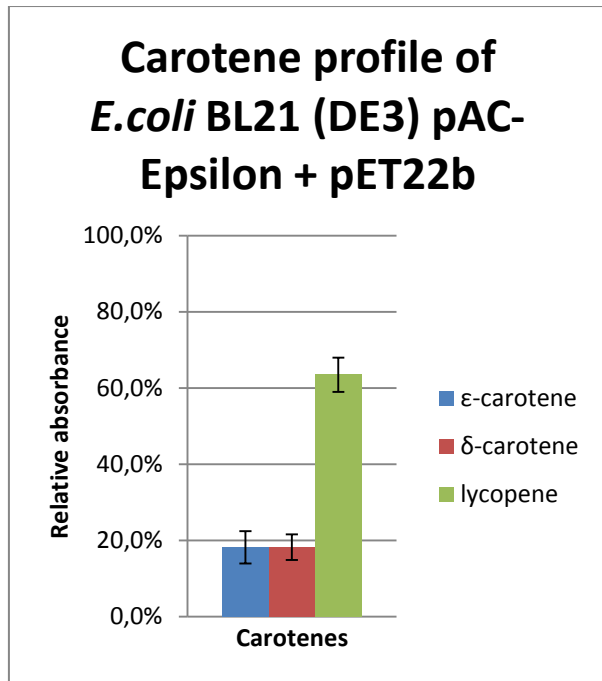


Figure 20: Typical carotene profile for *E. coli* BL21(DE3) pAC-Epsilon + pET22b. (3 data points)

The growing conditions can be found in section 4.1.1). *E. coli* BL21(DE3) pAC-Epsilon primarily accumulated ϵ -carotene. Having a look at the carotene profile of *E. coli* BL21(DE3) pAC-Epsilon + pET22b one could see that the vector pET22b highly influenced the carotene production. The vector reduced the ϵ -carotene production from typically 70 % down to about 17 % preferentially accumulating lycopene instead.

5.4 Background expression

The check if VvCCD1 is properly expressed a protein expression analysis was conducted (Method 4.1.4.1). VvCCD1 has an expected size of 63.4 kDa. The SDS-PAGE is shown in Figure 21.

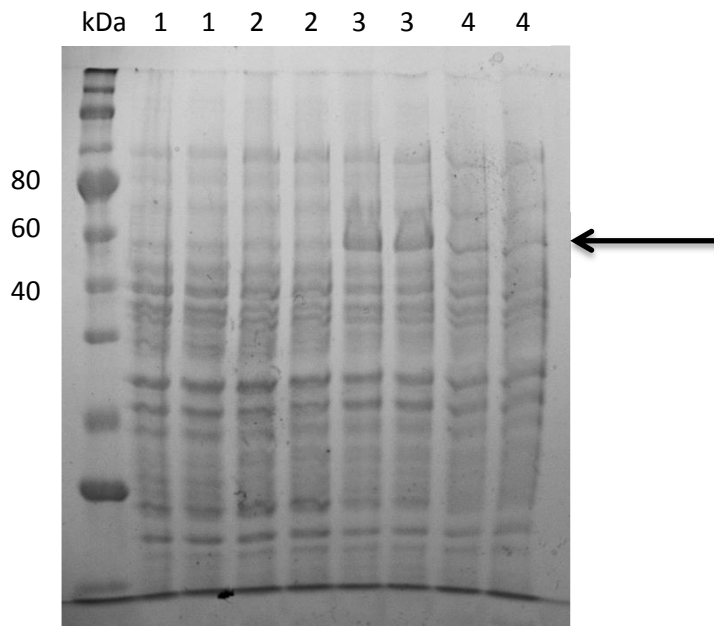


Figure 21: SDS-PAGE of the protein expression analysis of *E. coli* BL21(DE3). The arrow indicates an overexpressed protein of about 60 kDa in both clones containing the VvCCD1 gene. 1: pAC-Epsilon; 2: pAC-Epsilon + pET22b; 3: pAC-Epsilon + pET22b-VvCCD1; 4: pAC-Epsilon + pET22b-VvCCD1 + 0.1 mM IPTG.

The protein expression analysis reveals a band of about 60 kDa in the lanes 3 and 4 of which lane 3 has the largest band. The sample with *E. coli* BL21(DE3) pAC-Epsilon + pET22b-VvCCD1 expressed more VvCCD1 without induction than with IPTG induction. When the experiment was repeated both samples were showing bands of similar intensity. VvCCD1 was therefore highly expressed even without IPTG induction. The sample of *E. coli* BL21(DE3) pAC-Epsilon in lane 1 and the sample of *E. coli* BL21(DE3) pAC-Epsilon + pET22b in lane 2 did not show any distinct difference in the expression pattern to each other.

To reduce the background expression of VvCCD1 from pET22b 1 % glucose was added to the LB medium (Method 4.1.5.1). The effect of glucose was investigated on both clones *E. coli* BL21(DE3) pAC-Epsilon and *E. coli* BL21(DE3) pAC-Epsilon + pET22b-VvCCD1. The carotenes were extracted and analysed by HPLC-PDA.

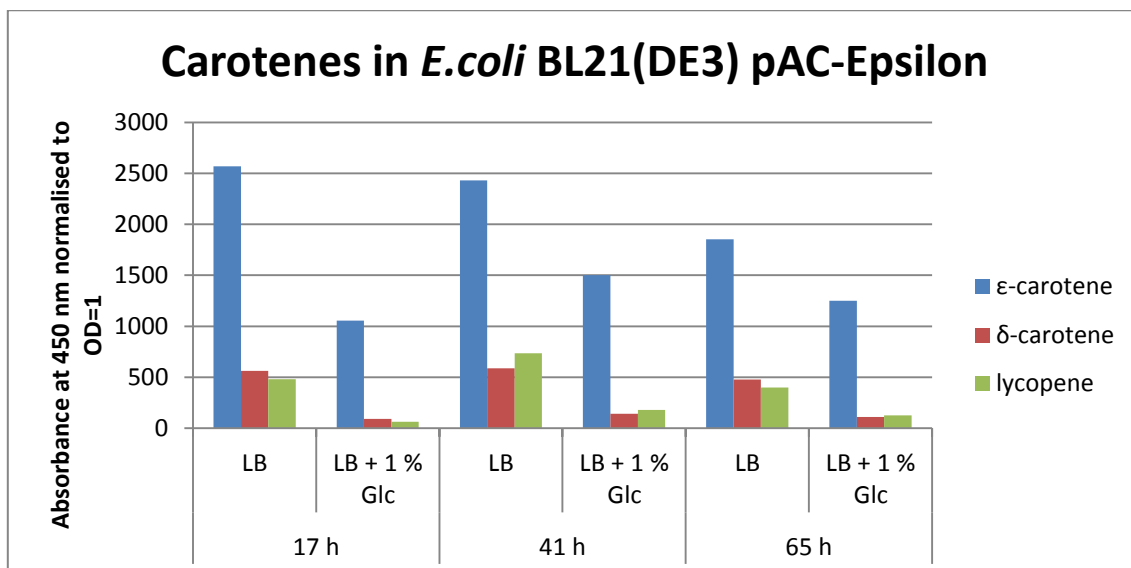


Figure 22: Carotenes in cultures with and without glucose as catabolite repressor.

Figure 22 shows the absorbance of carotenes produced by *E. coli* BL21(DE3) pAC-Epsilon in LB medium compared to the production in LB medium with the addition of 1 % glucose. The addition of 1 % of glucose reduces the maximum amount of ϵ -carotene. While the maximum amount of ϵ -carotene in LB medium is already reached after 17 hours and then slowly decreasing, the maximum with glucose is reached after 41 hours. With the addition of 1 % glucose only about 60 % of the total amount of ϵ -carotene was being produced. Furthermore the addition of glucose increased the relative amount of ϵ -carotene from about 70 % to about 85 % at all time points (data not shown).

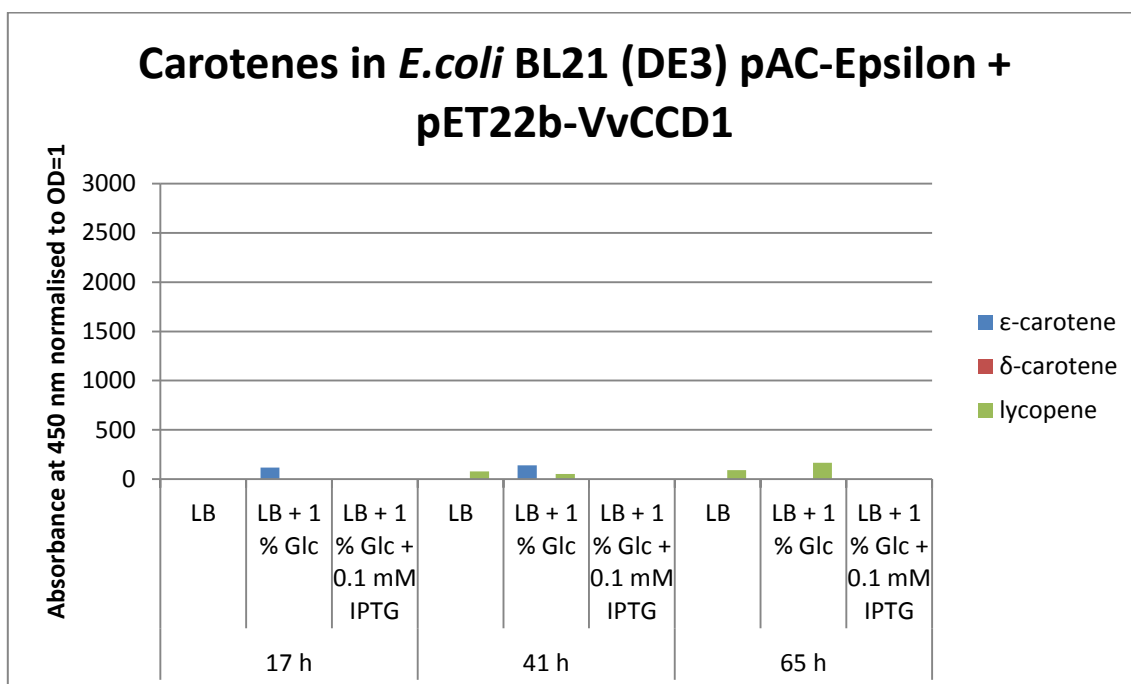


Figure 23: Effect of glucose addition on the amount of carotenes in cultures with VvCCD1

Figure 23 presents a carotene analysis of *E. coli* BL21(DE3) pAC-Epsilon + pET22b-VvCCD1 grown in LB, LB with 1 % glucose and LB with 1 % glucose and 0.1 mM IPTG after different incubation durations. All samples contain no or only trace amounts of carotenes. The addition of 1 % Glucose reduces the background expression of VvCCD1 only to a very low extent.

The influence of pET22b on the carotene production and the high level of background expression renders the pET22b-VvCCD1 plasmid impractical. The VvCCD1 gene was therefore cloned into the pBAD vector. The pBAD vector is described as a vector with very low background expression levels and with very good expression control depending on the L-Arabinose concentration.

To verify that the vector pBAD is not influencing the carotene production *E. coli* BL21(DE3) pAC-Epsilon was transformed with pBAD. The clone was grown at 30 °C for 24 hours, extracted and analysed by HPLC-PDA. The vector pBAD did not influence the carotene accumulation. The comparison of the carotene profiles is shown in Figure 24 and Figure 25.

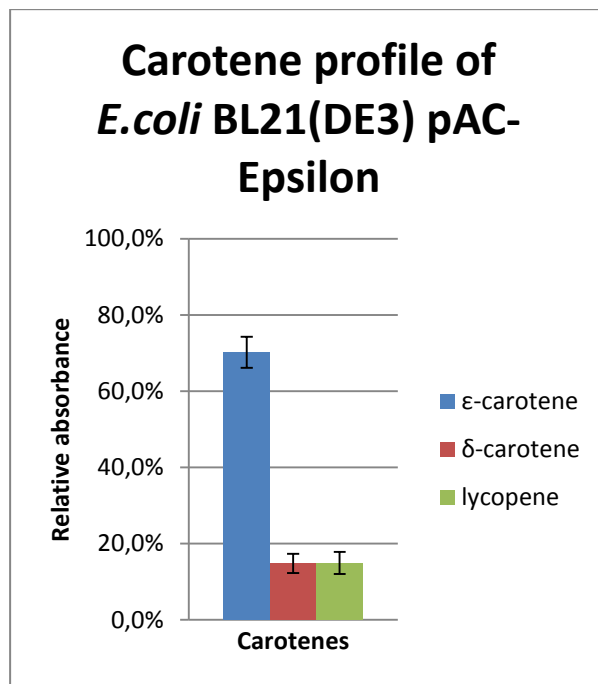


Figure 24: Typical carotene profile for *E. coli* BL21(DE3) pAC-Epsilon (6 data points)

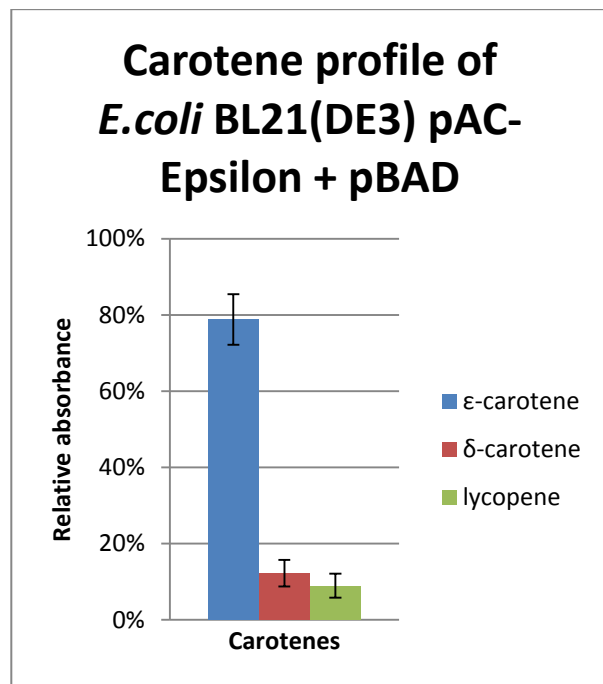


Figure 25: Carotene profile for *E. coli* BL21(DE3) pAC-Epsilon + pBAD grown at 30 °C for 24 hours. (2 data points)

The growing conditions of *E. coli* BL21(DE3) pAC-Epsilon can be found in section 4.1.1.. *E. coli* BL21(DE3) pAC-Epsilon + pBAD accumulates ε-carotene with a relative amount of about 70 % similar to *E. coli* BL21(DE3) pAC-Epsilon. The vector pBAD did not affect the carotene production as the vector pET22b did. The gene VvCCD1 was therefore cloned from pET22b-VvCCD1 into pBAD-A.

5.5 Cloning of VvCCD1 from pET22b-VvCCD1 into pBAD (Method 4.4)

All cloning steps showed the expected fragment sizes. After transforming pBAD-VvCCD1 into *E. coli* DH10b one positive colony among 28 tested colonies could be found.

To verify that the VvCCD1 gene is inserted correctly into the pBAD-A vector the plasmid was sequenced (Method 4.4.11). The alignment (Appendix 9.3) shows, that the VvCCD1 gene is inserted in the correct direction at the initiation ATG position (see multiple cloning site of pBAD-A in section 9.2.2). However only the first 17 bases could be confirmed to be correct, after that the sequence seems to be superimposed by another sequence. The sequencing with the reverse primer resulted in a 100 % alignment with no mismatches or gaps/insertions.

5.6 Carotene and apocarotene analysis of *E. coli* BL21(DE3) pAC-Epsilon + pBAD-VvCCD1

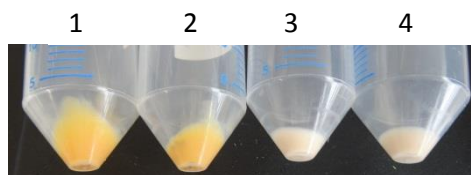


Figure 26: Pellets of *E. coli* BL21(DE3) 1: pAC-Epsilon + pBAD; 2: pAC-Epsilon + pBAD + 0.1 % L-Arabinose; 3: pAC-Epsilon + pBAD-VvCCD1; 4: pAC-Epsilon + pBAD-VvCCD1 + 0.1 % L-Arabinose

Figure 26 shows pelleted *E. coli* BL21(DE3) pAC-Epsilon + pBAD and *E. coli* BL21(DE3) pAC-Epsilon + pBAD-VvCCD1 cells where the respective second sample was induced by 0.1 % L-Arabinose. The *E. coli* (BL21) DE3 pAC-Epsilon + pBAD-VvCCD1 cells are still totally decolourised even without L-Arabinose induction. The carotene analysis of *E. coli* BL21(DE3) pAC-Epsilon + pBAD-VvCCD1 showed no or only trace amounts of carotenes similar to *E. coli* BL21(DE3) pAC-Epsilon + pET22b-VvCCD1.

For a final colour comparison of the cell used in this work, the used *E. coli* strains with different plasmids are shown below in Figure 27.

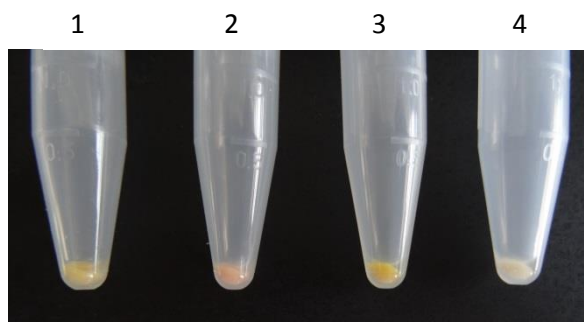


Figure 27: Pellet colour comparison of *E. coli* BL21(DE3) with different plasmids.

1: pAC-Epsilon, 2: pAC-Epsilon + pET22b, 3: pAC-Epsilon + pBAD, 4: pAC-Epsilon + pBAD-VvCCD1

The cultures with pAC-Epsilon and pAC-Epsilon + pBAD resulted in yellow pellets due to ϵ -carotene accumulation. *E. coli* BL21(DE3) pAC-Epsilon + pET22b gave rise to a red pellet due to lycopene accumulation with lower levels of δ -carotene and ϵ -carotene, while *E. coli* BL21(DE3) pAC-Epsilon + pBAD-VvCCD1 is yielding a slightly brown to almost white cell pellet.

The expression of VvCCD1 from pBAD-VvCCD1 was investigated (Method 4.1.5.2). For this reason *E. coli* BL21(DE3) pAC-Epsilon + pBAD was compared to *E. coli* BL21(DE3) pAC-Epsilon + pBAD-VvCCD1 without induction and with L-Arabinose induction over a 10000 fold concentration range from 0.00002 % to 0.2 %. The SDS-PAGE is shown in Figure 28.

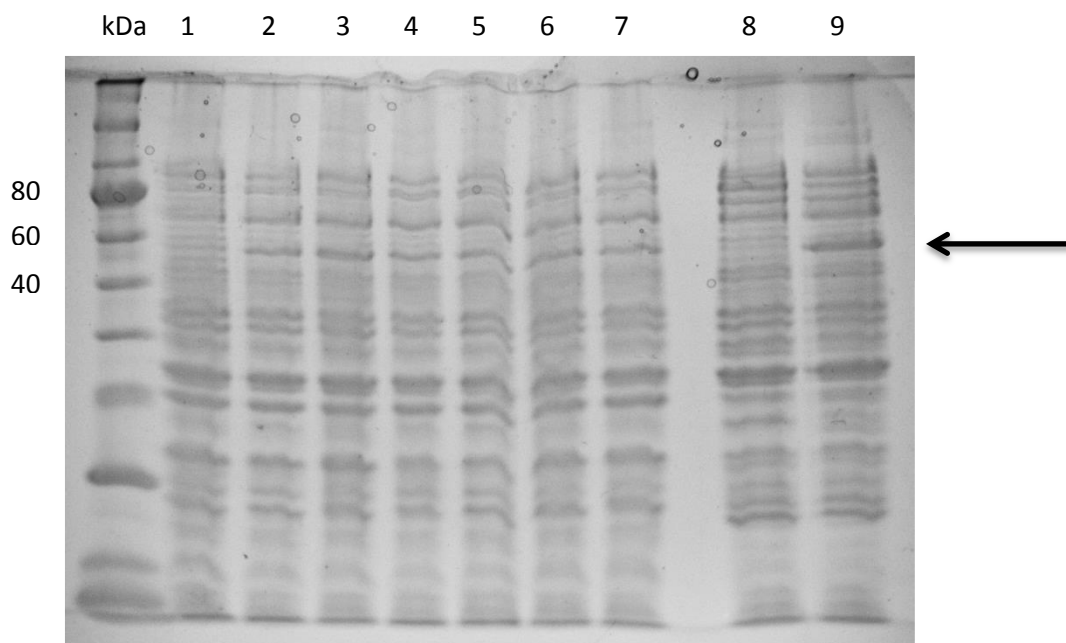


Figure 28: SDS-PAGE of *E. coli* BL21(DE3) pAC-Epsilon + pBAD-VvCCD1 with L-Arabinose concentrations from 0.00002% to 0.2%. The arrow indicates an overexpressed protein of about 60 kDa in clones containing the VvCCD1 gene. 1: negative (*E. coli* BL21(DE3) pAC-Epsilon + pBAD); 2: *E. coli* BL21(DE3) pAC-Epsilon + pBAD-VvCCD1 without L-Arabinose; 3: 0.00002 % L-Arabinose; 4: 0.0002 % L-Arabinose; 5: 0.002 % L-Arabinose; 6: 0.02 % L-Arabinose; 7: 0.2 % L-Arabinose; 8: *E. coli* BL21(DE3) pAC-Epsilon + pBAD in M9; 9: *E. coli* BL21(DE3) pAC-Epsilon + pBAD-VvCCD1 in M9

The expression analysis reveals a protein with about 60 kDa in lanes 2 to 7. The band does not seem to increase in intensity with higher L-Arabinose concentrations. This indicates that VvCCD1 was also highly expressed with the pBAD system even without L-Arabinose induction. Efforts to reduce the background expression of VvCCD1 from pBAD by adding 1 % glucose to the LB medium (Method 4.1.5.2) were as ineffective as previous experiments with pET22b-VvCCD1. As an alternative to the addition of 1 % glucose to the LB medium cells were grown in M9 medium (Method 4.1.5.2.1), which is a defined medium containing glucose as the only carbon source. The cells grew very slowly. After 48 hours of incubation the samples exhibited optical densities of about 0.5. The sample with VvCCD1 but without L-Arabinose induction in lane 9 showed a band at about 60 kDa. With both methods *E. coli* BL21(DE3) pAC-Epsilon + pBAD-VvCCD1 still showed high background expression of VvCCD1.

When growing the cultures in SPME vials and analysing by HS-SPME-GC-MS (Method 0) the results were again not conclusive as α -ionone and other products like β -ionone were produced only in some samples and only in trace amounts.

Since it was not possible to manufacture α -ionone reproducibly with whole cells, the theoretical amount possible with this system was estimated to be about 135 μg ($\pm 22 \mu\text{g}$) of α -ionone per gram dry biomass (Method 4.1.6).

5.7 Unspecific carotene degradation

As previously mentioned (end of Result 5.2 and Result 5.6) the product α -ionone could only be detected twice. The two experiments are shown below and the results are compared.

E. coli BL21(DE3) pAC-Epsilon and *E. coli* BL21(DE3) pAC-Epsilon + pET22b-VvCCD1 were grown in SPME vials at 30 °C, 125 rpm for 72 hours and measured by HS-SPME-GC-MS. The chromatogram is displayed in Figure 29.

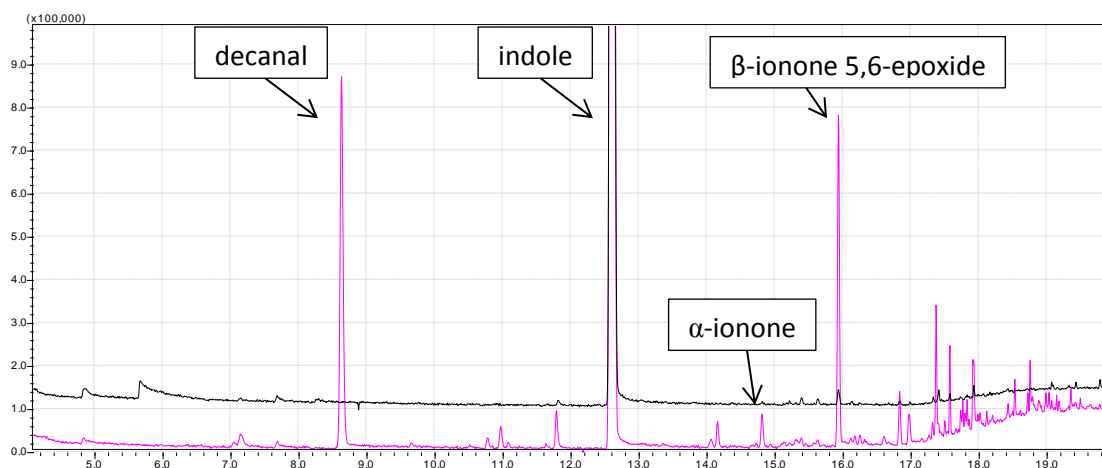


Figure 29: Zoomed in Chromatogram of SPME measurements. From top to bottom: *E. coli* BL21(DE3) pAC-Epsilon and *E. coli* BL21(DE3) pAC-Epsilon + pET22b-VvCCD1 + 0.25 mM IPTG

Figure 29 shows that *E. coli* BL21(DE3) pAC-Epsilon has no other compounds than indole as expected. The *E. coli* BL21(DE3) pAC-Epsilon + pET22b-VvCCD1 sample primarily contains decanal, indole and β -ionone 5,6-epoxide. The product α -ionone and its isomer β -ionone are only present in relatively minor amounts.

The experiment was repeated with the same conditions. The chromatogram is shown in Figure 30.

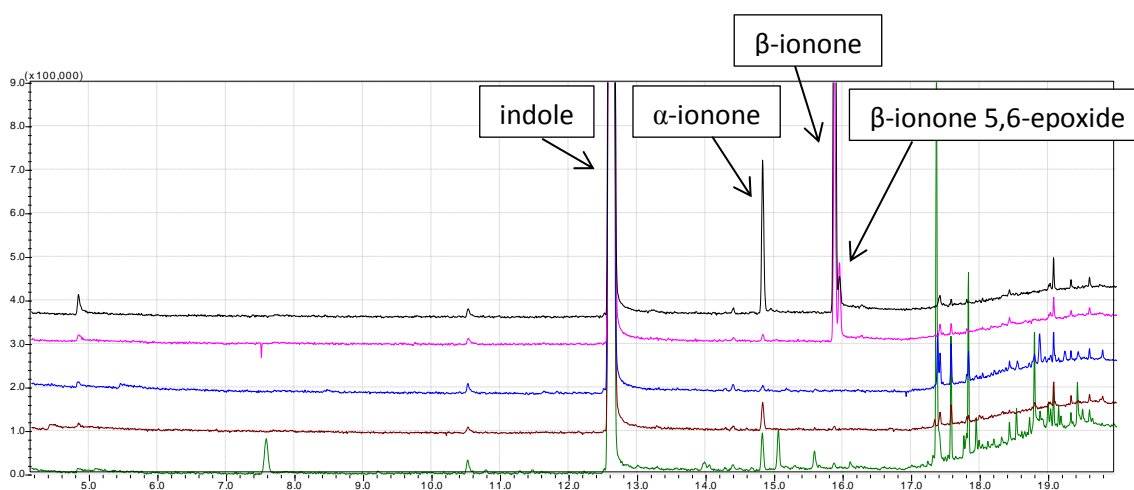


Figure 30: Further zoomed in Chromatogram of SPME measurement of *E. coli* containing different plasmids. From top to bottom: pAC-Epsilon; pAC-Epsilon + pBAD; pAC-Epsilon + pET22b; pAC-Epsilon + pET22b-VvCCD1; pAC-Epsilon + pET22b-VvCCD1 + 0.25 mM IPTG

The first three lanes from the top show *E. coli* BL21(DE3) cultures containing the pAC-Epsilon; pAC-Epsilon + pBAD and pAC-Epsilon + pET22b respectively. Not having the VvCCD1 gene, all three cultures should not show any presence of ionones or other cleavage compounds. However *E. coli* BL21(DE3) pAC-Epsilon did show the presence of α -ionone and an even higher amount of β -ionone as well as β -ionone 5,6-epoxide. *E. coli* BL21(DE3) pAC-Epsilon + pBAD did only have a minor amount of α -ionone besides β -ionone and β -ionone 5,6-epoxide. *E. coli* BL21(DE3) pAC-Epsilon + pET22b contains a minor amount of α -ionone as well.

To test the influence of oxygen on unspecific carotene degradation *E. coli* BL21(DE3) pAC-Epsilon + pBAD was grown 72 hours in SPME vials with either air or nitrogen in the headspace of the SPME vial and measured by HS-SPME-GC-MS.

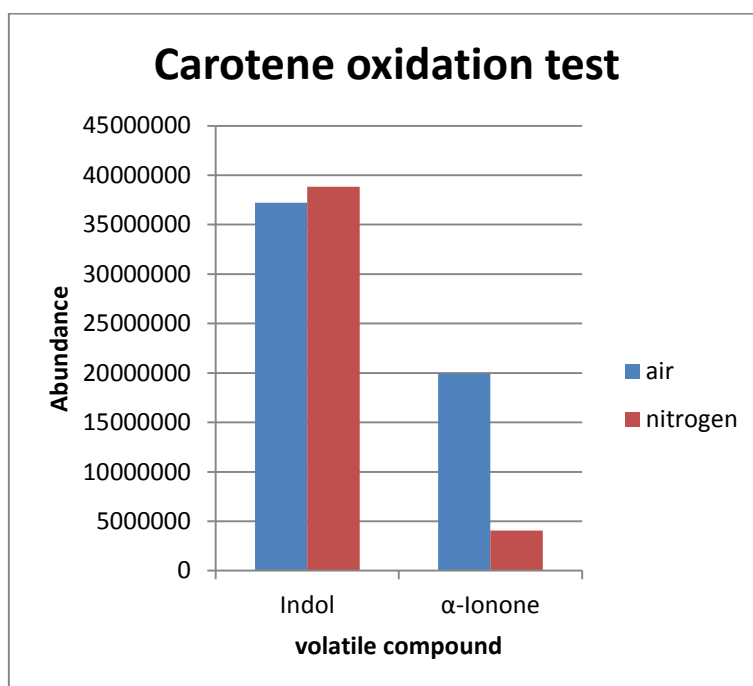


Figure 31: Amount of α -ionone in ϵ -carotene oxidation test. The sample which was grown with nitrogen in the headspace of the SPME vial has about 5 times less α -ionone present.

Figure 31 compares the amount of indole and α -ionone in samples which were grown in SPME vials with either air or nitrogen in the headspace. The comparison of the indole amount ensures that the SPME vial was properly closed which is needed for the comparability of the amounts of α -ionone. After 72 hours of incubation there is about 5 times less α -ionone present in the sample grown with nitrogen compared to the culture grown with air in the headspace. The experiment was repeated with the same parameters. This time indole and α -ionone could be found besides some minor byproducts, showing 50 – 200 times less α -ionone. However in both tests the amount of α -ionone was less in the cultures grown with nitrogen than grown with air.

5.8 *In vitro* experiments

Since an *in vivo* reaction of ϵ -carotene to α -ionone by VvCCD1 is not possible due to the background expression issue, the reaction was tried to perform *in vitro*. In this experiment the carotene producing clones and the VvCCD1 producing clones were separately grown, centrifuged and decomposed. They were then mixed to bring the carotenes in reaction with the enzyme VvCCD1. The experimental setup is equal with the setup for exhaust air collection. (see Method 4.2.4)

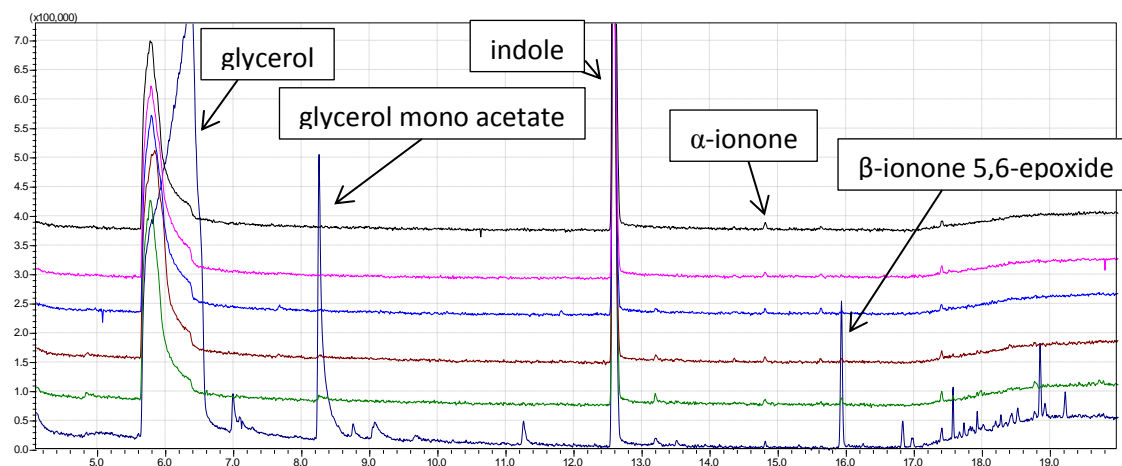


Figure 32: Chromatogram of the *in vitro* assay 1. From top to bottom: 1 mL samples of the reaction suspension were taken at t=0 h; 1 h; 17.5 h; 24 h; 96 h. The last row shows the extracted reaction suspension after 96 hours which was concentrated by vacuum distillation.

Figure 32 shows the chromatogram of the first *in vitro* assay. When extracting the culture suspension, only β -ionone 5,6-epoxide could be found in the concentrated sample besides trace amounts of α -ionone in all samples. No α -ionone could be found in the exhaust air samples of this experiment. The second *in vitro* experiment has been cancelled

6 Discussion

The goals of this work were to develop and optimise a biotransformation process using ϵ -Carotene producing *E. coli* cells to produce α -ionone using the carotenoid cleavage dioxygenase 1 from common grape wine *Vitis vinifera* (VvCCD1) and to determine which α -ionone enantiomer is being produced by VvCCD1. For this reason the ϵ -Carotene accumulating *E. coli* BL21(DE3) pAC-Epsilon was cotransformed with the vector pET22b-VvCCD1.

6.1 Carotene identification

The extracted carotenes were identified by comparing the wavelength of the absorbance maxima of the peaks with literature data of carotenes in petroleum ether and other solvents. The absorbance maxima wavelengths and intensities of a substance are dependent on the medium the substance is dissolved in. This identification method was still chosen since the standards of β -Carotene and Lycopene in the HPLC eluent mixture had very similar absorbance maxima as in the literature, differing only a few nanometers. A confirmation of the identification of the carotenes by mass spectrometry could not be achieved since ESI or APCI is needed for carotene ionisation which was not available (Oxley, et al., 2014).

6.2 Carotene production and analysis

The carotene analysis of the carotene accumulating *E. coli* BL21(DE3) pAC-Epsilon revealed that these cultures contain about 70 % ϵ -Carotene and 15 % each of the precursors δ -Carotene and Lycopene. VvCCD1 has been reported to be able to cleave all three carotenes, ϵ -Carotene yielding two molecules of α -ionone, δ -Carotene yielding one molecule of α -ionone and one molecule of MHO and lycopene yielding two molecules of MHO. The cleavage of the accumulated carotenes would therefore yield 77.5 % of α -ionone and 22.5 % of MHO.

6.2.1 Influence of pET22b

Unlike pBAD, the vector pET22b was shifting the carotene accumulation from ϵ -carotene towards lycopene (Result 0), the reason for that is not known and was not further investigated. Both vectors pET22b and pBAD express the same selection marker β -lactamase, which is expressed into the periplasm for ampicillin resistance. The only difference between the two vectors is that the pET22b vector consists of the lac repressor gene *lacI*, which binds to the operator site to repress the T7 RNA polymerase from binding to the promoter region of the VvCCD1 gene. The lac repressor could possibly influence the carotene production when unspecifically binding to other DNA regions on pAC-Epsilon, thus repressing the expression of proteins involved in carotene synthesis. If the lac repressor protein could bind the promoter region of the lycopene- ϵ -cyclase gene, the protein would be less expressed and the conversion of lycopene to δ -carotene and δ -carotene to ϵ -carotene would be reduced, resulting in a carotene profile as produced by *E. coli* BL21(DE3) pAC-Epsilon + pET22b. In addition there might be some protein-protein interaction between the lac repressor and the lycopene- ϵ -cyclase, reducing its activity and therefore lowering the amount of ϵ -carotene.

6.3 Background expression

Protein expression analysis has shown that VvCCD1 has been highly expressed from both vectors pET22b and pBAD even without induction. The addition of glucose to the medium could not significantly reduce the background expression of VvCCD1 from either vector, which was also found by Vogel using accumulating *E. coli* BL21(DE3) in combination with the pGEX2T vector and a related CCD1 enzyme (Vogel, et al., 2008). Switching to the defined M9 medium containing glucose as the only carbon source could not improve the situation. Another possibility to reduce background

expression levels is through the cotransformation with one of the plasmids pLysS or pLysE. These plasmids express a kind of lysozyme degrading background levels of T7 RNA Polymerases and therefore lowering the background expression of the gene of interest of a T7 expression system. Unfortunately this plasmid could not be used since it contains the same selection marker as pAC-Epsilon to maintain selection pressure. The VvCCD1 gene or one of the pLys genes could be cloned to another vector using a resistance marker complementary to the already used antibiotics. As Lashbrook did not report background expression, the cloning of the carotene accumulating plasmid into *E. coli* TOP10F with additional cloning of VvCCD1 into the pTWIN1 vector system might therefore reduce the background expression levels. Actually they stated that this expression system generates about 85 % of α -ionone from ϵ -Carotene accumulating cells (Lashbrooke, et al., 2013)

The inducibility of the vectors could also be lost when the lac repressor gene or the operator region would be destroyed by cloning mistakes. On pET22b-VvCCD1 the lac promoter region and the lac repressor gene are present as well the T7 promoter and the lac operator region. The lac repressor protein should therefore be expressed and able to inhibit the expression of VvCCD1 by binding the lac operator subsequent to the promoter region of the VvCCD1 gene. On pBAD-VvCCD1 all regions needed for the expression of the regulating protein AraC are present as well the operator regions. Both plasmids should therefore be functional and cloning mistakes can be excluded.

6.4 Apocarotene production and analysis

When analysing VvCCD1 containing cultures, regardless if pET22b or pBAD was used as vector, only trace amounts of carotenes could be found. The carotenes might have been degraded by background expressed VvCCD1. However the inherent C14-dialdehyde which should remain due to the cleavage reaction (Mathieu, et al., 2005) could not be detected by HPLC analysis at 414 nm. Furthermore α -ionone and MHO could usually not be detected by GC-MS. The only compound constantly present was indole, which is most likely produced from tryptophane by endogenous tryptophanase.

When no apocarotenes could be detected by extracting the culture suspension, it was suspected that the volatile compounds might be lost during the purification process. By using a two phase system it was tried to prevent the compounds from evaporating, no products could be found. n-Hexane was chosen as solvent for the two phase system as it has a logP of 3.94, which is above the critical logP of most *E. coli* strains of 3.4 to 3.8 (Venkata & Peeples, 2009). In addition the logP of n-Hexane is very similar to the logP of α -ionone of 3.86 but both compounds having a difference in boiling temperatures of 168 °C. Therefore the cells should tolerate n-Hexane, the product α -ionone should be very soluble in n-Hexane and easily removable by vacuum distillation. In case the cells do not tolerate n-Hexane very well a less polar solvent such as n-Heptane could be chosen. The major drawbacks of this method are though preventing the evaporation of the products, the solvent layer also prevents oxygen to dissolve into the culture suspension, necessary for the cleavage reaction. To circumvent this, the culture suspension could be directly aerated. However direct aeration results in vigorous mixing which is not only increasing the mass transfer between the product and solvent but also increasing the mostly toxic cell-solvent contact. An alternative would be to select a biocompatible solvent and/or to encapsulate the solvent in permeable microcapsules, thereby reducing the toxic cell-solvent contact but simultaneously providing a fast product removal and easy purification setup (Maltzahn, 2004).

Using the volatility of α -ionone as an advantage, it was tried to capture it by leading the exhaust air stream of the culture suspension through a solvent. Again no products could be found. To completely

prevent evaporation the cultures were grown in closed SPME vials. Though this method has already been applied with success (Baldermann, et al., 2010), (Baldermann, et al., 2012), (Ilg, et al., 2014), (Huang, et al., 2009), (Ibdah, et al., 2006) α -ionone could be found only twice whereas MHO could never be detected. The α -ionone present in these two samples was most probably generated by unspecific degradation, discussed in the next subsection. The fact, that α -ionone could not be purified reproducibly using any of the methods described above indicates that the issue lies rather in the production of the apocarotenoids than their loss during purification.

When analysing apocarotenoids in grape wine, most of them were found in their non-volatile glycosylated form (Mathieu, et al., 2005). The cleavage products therefore might have been further degraded by other endogenous *E. coli* enzymes or other cell compounds. This means, that the carotenoids could either be degraded by the background expressed VvCCD1 but then further converted / degraded by endogenous enzymes or the carotenoids were degraded by some other mechanism linked to the expression of VvCCD1. Characterising the activity of AtCCD8 (*Arabidopsis thaliana*) on three carotenoids by *E. coli* BL21-AI containing the respective plasmids for carotene accumulation, Auldridge could show carotene degradation upon L-Arabinose induction with the pDEST15 vector system but could neither find the related products, hypothesising that they were further metabolized by *E. coli* (Auldridge, et al., 2006). This issue has also been observed previously by Lintig and Vogt (Lintig & Vogt, 2000). Interestingly, another study also using *E. coli* BL21-AI cells could detect the cleavage products (Vogel, et al., 2008).

Another possibility is that the analytical methods were not suitable for the detection of MHO and the C14-dialdehyde. The used YMC Carotenoid C30 HPLC column was specifically designed for the analysis of carotenoids, exhibiting a retention time difference of 4 minutes between β -carotene and ϵ -carotene, only having a difference in the position of two electron pairs. The relatively short C14-Dialdehyde might therefore eluate too early to be distinguishable from the solvent peak. All measurements have been checked, no additional peaks to the negative could be found. On the other hand, MHO might not be detectable by the current GC-MS method, as only the detection of α -ionone and β -ionone standards were confirmed (Appendix 9.1.2).

Without MHO and the C14-dialdehyde being detectable, it cannot be proven that the cells cannot accumulate carotenoids due to VvCCD1 activity or if the VvCCD1 expression is influencing the carotene production somehow differently. If VvCCD1 is active, Lycopene could be constantly cleaved to MHO without being noticed, preventing the conversion to δ -Carotene and ϵ -Carotene and thereby also the generation of α -ionone.

A sufficient amount of α -ionone could not be obtained for the investigation of the α -ionone enantiomer produced by VvCCD1 due to previously discussed issues. It is hypothesised that the R-enantiomer is being produced since α -ionone found in various fruit and plant species was found as an almost optically pure R enantiomer (Berger, 2007, p. 22).

6.4.1 Unspecific carotene degradation

There are only two other studies investigating the *in vivo* substrate specificity of VvCCD1 (Vogel, et al., 2008), (Lashbrooke, et al., 2013). Carotene degradation by background expression *in vivo* has also been observed by Vogel (Vogel, et al., 2008) using carotene accumulating *E. coli* BL21(DE3) in combination with a related CCD1 on the pGEX2T vector.

Carotene precursor degradation by non-enzymatic reactions has also been observed by Vogel (Vogel, et al., 2008). The cultivation in SPME-vials with subsequent HS-SPME-GC-MS measurement was the only method where α -ionone could be detected (Result 5.7). However these measurements were inconclusive due to presence of α -ionone in samples of ϵ -Carotene accumulating cultures where it was not expected due to the lack of VvCCD1. In addition the SPME fibre often broke after some measurements which made the subsequent comparison of the results difficult. The measurements were then usually performed one after another to ensure an intact fibre.

The comparatively large amounts of α -ionone, β -ionone and β -ionone 5,6-epoxide in samples without VvCCD1 were most probably caused by the reaction of carotenes with oxygen species and other physical, chemical or unspecific enzymatic degradation processes. For instance, β -carotene can react with oxygen to form 5,6-epoxy- β -carotene which then can be converted to 5,6(5',6')-diepoxy- β -carotene which again might be cleaved to β -ionone 5,6-epoxide which might be converted to β -ionone (Boon, et al., 2010). Similar reactions might have occurred in the cells, but the heat stability test (Result 5.2) suggests that that β -ionone is rather converted to β -ionone 5,6-epoxide than the other way around and that α -ionone is slowly degraded to β -ionone which is further degraded to β -ionone 5,6-epoxide. In general the ionones seem pretty heat stable being degraded only a few percentages after 72 hours of incubation and the heating during the SPME measurement. The products found by (SPME)-GC-MS measurements should therefore not be altered very much, since the degradation process is too slow. The evaporation test suggests that α -ionone is slowly evaporating, but the experimental setup should be improved. The standard was pipetted in one flask of which an aliquot was taken for immediate analysis. Since α -ionone is not water soluble this method is not very accurate. An equal amount of α -ionone should be carefully pipetted in two flasks instead. The products would therefore rather evaporate than degrade over time.

6.4.2 VvCCD1 functionality

The cultures were usually grown in LB medium at 30 °C for about 24 hours with induction when an optical density of 0.6 was reached. Baldermann (Baldermann, et al., 2010) showed that the related OfCCD1 from *Osmanthus fragrans* needs iron (II) to perform the cleavage reaction. In this matter they supplemented the YT medium, which is similar to LB medium, with 5 μ M of FeSO₄ to promote CCD functionality *in vivo*. In addition they included 6 mM ascorbate and 200 U/ mL catalase to prevent the oxidation of the carotenes from non-specific degradation. Former studies on CCDs were already using FeSO₄ (Schwartz, et al., 2004), (Mathieu, et al., 2005), (Vogel, et al., 2008) in *in vitro* assays. Iron (II) is a potential cofactor of CCD1 enzymes, which contain four conserved histidines, which are thought to be necessary for the coordination of the iron (Vogel, et al., 2008). Since the cells with VvCCD1 were not able to accumulate carotenes it was presumed that VvCCD1 is functional without the addition of FeSO₄, which was therefore not added to the LB medium. The addition of ascorbate and catalase might still improve the production of the carotenes by preventing their oxidation. A bleaching of cell pellets was also described by Baldermann (Baldermann, et al., 2012) using *E. coli* XL1 Blue cells containing OfCCD1, however they were still able to detect the corresponding cleavage product. Actually, Baldermann showed that when leaving iron (II) out of the assay, that no cleavage products were formed (Baldermann, et al., 2010). When iron (II) is indeed needed as a cofactor for the cleavage reaction, the *in vivo* assays in this work should have expressed no functional VvCCD1 enzyme or with much less activity, leaving the carotenes intact.

However another study working with carotene accumulating *E. coli* BL21(DE3) pLysS strains from Cunningham which were transformed with an ampicillin inducible plasmid containing the related

ZmCCD1 from maize could not develop the colour of the respective carotene using agar plates with LB medium already containing 1 % glucose to reduce background expression of ZmCCD1 (Sun, et al., 2008). So even while containing the pLysS plasmid, which is used to reduce the background expression from T7 expression systems, and additional glucose to further reduce background expression, the colonies were not able to develop the carotenes. The plates were incubated at 21 °C for 4 – 7 days with no statement about ampicillin induction. This study basically shows the same issue as in this work that the cells with the CCD1 gene could not accumulate the carotenes without induction, but the reason for this was not discussed. Cultivation in liquid LB medium, again without the addition of iron (II), overnight at 30 °C with subsequent extraction and GC-MS analysis could, in contrast to this work, identify the corresponding cleavage products in reasonable relative amounts (Sun, et al., 2008). Auldridge could also observe carotene degradation upon L-Arabinose induction without iron (II) addition (Auldridge, et al., 2006).

6.5 Cloning

Only 1 out of 28 colony PCRs was positive, showing the expected fragment size. The vector could have recirculised leaving mostly empty vectors behind. An additional alkaline phosphatase step prior to ligation might improve this situation. This step is designed to prevent self-ligation of the vector without the insert. The colony PCR did also show four colonies with smaller inserts than expected, suggesting that the restriction digest of the insert lead to some unspecific reactions inside the insert resulting in smaller fragments which then ligated with the vector. However the DNA taken for ligation was purified by gelexttraction in advance, which did not show any smaller fragments and which should eliminate all unspecific fragments anyway.

The sequencing alignment (Appendix 9.3) of pBAD-VvCCD1 could only confirm the second half of the gene and that the VvCCD1 gene is correctly inserted into the pBAD-A vector at the initiation ATG position (Appendix 9.2.2) in the correct direction. The forward sequencing however could only confirm the first 17 base pairs. From this position starting, the sequence seems to be superimposed by another sequence. This might be caused by primers unspecifically binding inside the gene producing additional templates during the PCR reaction. The amplification of the VvCCD1 region by Phusion PCR with subsequent gel extraction and newly designed sequencing primers could not improve the sequencing result.

A comparison of the cDNA sequence of the presumably used VvCCD1 from *V. vinifera* L. cv Pinotage obtained by Lashbrooke (Lashbrooke, et al., 2013) with the obtained DNA sequence by sequencing and the pET22b multiple cloning site (Appendix 9.2.1) revealed that the first 17 base pairs resemble the beginning of the *pelB* sequence of 66 bp prior to VvCCD1, which is a leader sequence commonly used for periplasmic protein expression in *E. coli*.

Translated VvCCD1 feature of pET22b-VvCCD1:

**MKYLPTAAAGLLLLAAQPAMAMAEKEEQGGAGVAVVDPKPSKGFTSKAVDWLEKLIVKLMYDSSQPLHYLSGN
FAPVRDETPPCKNLPVIGYLPECLNGEFVVRVGPVNPVAGYHWFDDGMIHGLHIKDGKATYVSRYVRSRLKQ
EEYFGGAKFMRIGDLKGLFGLLMVNMQMLRAKLIKLDVSYGTGTGNTALVFHRGKLLALSEADKPYVLKVLLEDGDL
QTLGMLDYDKRLTHSFTAHPKVDPFTGEMFSFGYSHTPPYITYRVISKDGFMHVPITISDPIMMHDFAITENYAI
MDLPLYFRPKEMVKEKLIFFDATKKARFGVLPYAKNELHIKWFELPNCIFIHANAWEEDEEVLLITCRLEHPDL
DLVGGDVKEKLENFGNELYEMRFNMKTGIASQRKLSASSVDFPRVNESYTGKQRYVYGTILDSIAKVTGIIKFDLHA
EPDTGKSKLEVGGNVQGIFFDLGVGRFGSEAVFVPREPGITSEEDDGYLIFFVHDEKTGKSYVNVDAKTMSPDPIAIV
ELPNRVYPYGFHAFVTEEQLEQAKL** **pelB VvCCD1 (underlined part was confirmed by sequencing)**

However since the *pelB* leader sequence is removed with periplasmic expression (Sokolosky & Szoka, 2013) it should not influence the translated amino acid sequence of VvCCD1.

Table 34: Sizes of genes and corresponding proteins

	Gene size [bp]	Protein size [kDa]
pelB + VvCCD1	1695	63
VvCCD1	1629	60

The VvCCD1 gene without *pelB* leader sequence results in a protein of a size of 60 kDa. Unfortunately this small difference is not clearly distinguishable on a 12 % SDS-PAGE. Obviously periplasmic expression could have most likely influenced the folding and activity of VvCCD1. The periplasm is rather reducing, promoting the formation of disulphide double bonds, whereas VvCCD1 has a predicted cytosolic localisation in plants (Lashbrooke, et al., 2013). The apocarotenes produced inside the periplasm might also be more quickly degraded than a production in the cytoplasm.

The cloning of VvCCD1 from pET22b to the pBAD vector, which is known as a vector with very low basal expression levels and tight regulation (Balzer, et al., 2013), could not reduce background expression levels of VvCCD1 (Result 5.4). Cultures with pBAD-VvCCD1 were still totally decolourised even without induction (Result 5.6).

6.6 *In vitro* experiments

To circumvent the issue of background expression *in vitro* experiments were conducted. (Result 0) *In vitro* assays have been performed showing the presence of glycerol, glycerol- α -monoacetate, 5,6-epoxy- β -ionone only in the concentrated sample and a similar low amount of α -ionone in all samples. However this low amount of α -ionone should be much higher in the concentrated sample, indicating a probable contamination by α -ionone.

A second experiment was cancelled because of the unsuccessful cell decomposition by sonication. It cannot be ensured that the cell decomposition in the first experiment was successful since there was no protein expression analysis conducted. The 5,6-epoxy- β -ionone might also have been created by unspecific carotene degradation.

In general an *in vitro* conversion of ϵ -Carotene to α -ionone might be a more efficient way to produce α -ionone. With ϵ -Carotene production separated from the production of VvCCD1 there is no issue with background expressed VvCCD1 degrading the carotene precursors leading to less byproducts and therefore a higher yield of α -ionone. Even if the background expression could be controlled very well, the amount of ϵ -Carotene produced until this point would be cleaved rather quickly after induction of VvCCD1. To produce new ϵ -Carotene by these cells one could try to use fresh medium without inducer present, but the already expressed VvCCD1 would most likely still be present continuing to cleave the carotene precursors.

7 Summary and future prospect

The production of α -ionone from ϵ -Carotene by VvCCD1 cleavage could not be established neither *in vivo* nor *in vitro*. Whenever the enzyme VvCCD1 on either vector pET22b or pBAD was transformed into the ϵ -Carotene accumulating *E. coli* strains, the cell pellets turned brownish to almost white without IPTG or L-Arabinose induction. A Carotene analysis could only find trace amounts of carotenes in these cultures. It was assumed that background expressed VvCCD1 was cleaving the carotenes. A protein expression analysis confirmed high VvCCD1 expression even without induction. However the resulting cleavage products could not be found. Besides background expression, it was found that the pET22b vector influences the carotene profile shifting the accumulation from ϵ -Carotene towards Lycopene instead. The VvCCD1 gene was then cloned from pET22b-VvCCD1 to the vector pBAD, which is supposed to be a very tight regulated vector and which did not influence the carotene profile. However the background expression issue still persisted and the product α -ionone could still not be produced controllably. The addition of 1 % Glucose to the medium could not reduce the background expression of VvCCD1 with either vector. The product α -ionone could be found in only two measurements. However in these measurements the product was also present in samples without VvCCD1 where it was not expected and was accompanied by other apocarotenes like β -ionone and β -ionone 5,6-epoxide, which should not be generated by the cleavage of VvCCD1. It was therefore assumed that these apocarotenoids were rather generated by unspecific mechanisms. In subsequent research it was found that the VvCCD1 gene still has a pelB leader sequence, which results in periplasmic expression of VvCCD1. This is most probably influencing the activity or even the folding of VvCCD1 since it has a cytosolic localisation in plants. Since the production of α -ionone could not be established, further aims of this work could not be followed.

In the future the background expression must be reduced to ensure an inducible and therefore controllable production process. The first step in cloning is to remove the pelB sequence at the beginning of the VvCCD1 gene to provide cytoplasmic expression. Secondly *E. coli* BL21 and related strains should be avoided for carotenoid production as they were found to frequently produce colonies not able to accumulate carotenoids (Cunningham & Gantt, 2007). The *E. coli* TOP10F strain in combination with the pTWIN1 vector should be chosen as this system has been shown to produce about 85 % of α -ionone from ϵ -Carotene accumulating cells (Lashbrooke, et al., 2013). The medium composition and growing conditions of this paper should be chosen as a starting point. From there the temperature, time of induction, growing duration and oxygen input for the maximum amount of α -ionone is reached should be established. As VvCCD1 can also cleave the ϵ -Carotene precursors a good time of induction might be when the maximum amount of ϵ -Carotene is reached. In addition the necessity of the medium supplements of this study should be evaluated, as they were simply adopted from another study.

When the production of α -ionone is optimised some purification methods should be evaluated. Due to the broad substrate specificity of VvCCD1 and therefore ϵ -Carotene precursor degradation, the production can only be performed batch wise. Since most of the carotenes are probably cleaved within hours after induction, one needs to examine how much α -ionone evaporates in this amount of time, or if most of the product remains in the culture suspension. If the product is evaporating fast enough, one could lead the exhaust air stream through a solvent and thereby collecting the product. When the carotenes are cleaved, the culture suspension could be supplemented with sodium chloride to stop further metabolism of *E. coli* and to promote the evaporation of the volatile products with subsequent vacuum distillation. If the product is not evaporating fast enough one

could use a micro encapsulated solvent for continuous product removal and easy extraction with subsequent filtering, elution and vacuum distillation.

The investigation of the α -ionone enantiomer produced by VvCCD1 could be easily accomplished by a GC-MS analysis. The chiral GC column Restek Rt- β DEXsm (30 m, 0.32 mm ID, 0.25 μ m (cat.# 13104)) provides a resolution factor of 6.40 (Restek, Technical Guide: A Guide to the Analysis of Chiral Compounds by GC, 1997). The method is also provided in their manual.

8 References

- Ansari, M. S. & Ansari, S., 2005. Lycopene and prostate cancer. *Future Oncology (London, England)*, 1(3), p. 425–430.
- Auldrige, M. E. et al., 2006. Characterization of three members of the Arabidopsis carotenoid cleavage dioxygenase family demonstrates the divergent roles of this multifunctional enzyme family. *The Plant Journal : For Cell and Molecular Biology*, 45(6), p. 982–993.
- Auldrige, M. E., McCarty, D. R. & Klee, H. J., 2006. Plant carotenoid cleavage oxygenases and their apocarotenoid products. *Current Opinion in Plant Biology*, 9(3), p. 315–321.
- Baldermann, S., Kato, M., Fleischmann, P. & Watanabe, N., 2012. Biosynthesis of α - and β -ionone, prominent scent compounds, in flowers of *Osmanthus fragrans*. *Acta Biochimica Polonica*, 59(1), p. 79–81.
- Baldermann, S. et al., 2010. Functional characterization of a carotenoid cleavage dioxygenase 1 and its relation to the carotenoid accumulation and volatile emission during the floral development of *Osmanthus fragrans* Lour. *Journal of Experimental Botany*, 61(11), p. 2967–2977.
- Balzer, S. et al., 2013. A comparative analysis of the properties of regulated promoter systems commonly used for recombinant gene expression in *Escherichia coli*. *Microbial Cell Factories*, Volume 12, p. 26.
- Barbosa-Filho, J. M. et al., 2008. Sources of alpha-, beta-, gamma-, delta- and epsilon-carotenes. *Revista Brasileira de Farmacognosia*, 18(1), p. 135–154.
- BBC Research, 2014. *Global Markets for Flavors and Fragrances*, s.l.: BBC Research.
- Berger, R. G., 2007. *Flavours and Fragrances: Chemistry, Bioprocessing and Sustainability*. London: Springer London, Limited.
- Bicas, J. L., Silva, J. C., Dionísio, A. P. & Pastore, G. M., 2010. Biotechnological production of bioflavors and functional sugars. *Ciênc. Tecnol. Aliment. (Ciência e Tecnologia de Alimentos)*, 30(1).
- Biswal, B., 1995. Carotenoid catabolism during leaf senescence and its control by light. *Journal of Photochemistry and Photobiology B: Biology*, 30(1), p. 3–13.
- Boon, C. S., McClements, D. J., Weiss, J. & Decker, E. A., 2010. Factors influencing the chemical stability of carotenoids in foods. *Critical Reviews in Food Science and Nutrition*, 50(6), p. 515–532.
- Brenna, E., Funganti, C., Serra, S. & Kraft, P., 2002. Optically Active Ionones and Derivatives: Preparation and Olfactory Properties. *European Journal of Organic Chemistry*, pp. 967-978.
- Britton, G., Liaaen-Jensen, S. & Pfander, H., 2004. *Carotenoids*. Basel: Birkhäuser Basel;Imprint;Birkhäuser.
- Cardozo, M. T. et al., 2011. Chemopreventive effects of β -ionone and geraniol during rat hepatocarcinogenesis promotion: distinct actions on cell proliferation, apoptosis, HMGCoA reductase, and RhoA. *The Journal of Nutritional Biochemistry*, 22(2), pp. 130-135.
- Chapman, D. & Haxo, F., 1963. *Plant Cell Physiology*, 4(57).

- Chernys, J. T. & Zeevaart, J. A., 2000. Characterization of the 9-Cis-Epoxy-carotenoid Dioxygenase Gene Family and the Regulation of Abscisic Acid Biosynthesis in Avocado. *Plant Physiology*, 124(1), p. 343–354.
- Council, E. P. a. o. t., 2008. *REGULATION (EC) No 1334/2008*, s.l.: European Parliament and of the Council.
- Crane, C. M. et al., 2008. Synthesis and characterization of cytidine derivatives that inhibit the kinase IspE of the non-mevalonate pathway for isoprenoid biosynthesis. *ChemMedChem*, 3(1), p. 91–101.
- Cunningham, F. X. & Gantt, E., 2001. One ring or two? Determination of ring number in carotenoids by lycopene epsilon-cyclases. *Proceedings of the National Academy of Sciences of the United States of America*, 98(5), p. 2905–2910.
- Cunningham, F. X. & Gantt, E., 2005. A study in scarlet: enzymes of ketocarotenoid biosynthesis in the flowers of *Adonis aestivalis*. *The Plant Journal : For Cell and Molecular Biology*, 41(3), p. 478–492.
- Cunningham, F. X. & Gantt, E., 2007. A portfolio of plasmids for identification and analysis of carotenoid pathway enzymes: *Adonis aestivalis* as a case study. *Photosynthesis Research*, 92(2), p. 245–259.
- Cunningham, F. X. et al., 1996. Functional analysis of the beta and epsilon lycopene cyclase enzymes of *Arabidopsis* reveals a mechanism for control of cyclic carotenoid formation. *The Plant Cell*, 8(9), p. 1613–1626.
- Cunningham, F. X. et al., 1994. Molecular structure and enzymatic function of lycopene cyclase from the cyanobacterium *Synechococcus* sp strain PCC7942. *The Plant cell*, 6(8), p. 1107–1121.
- de la Rosa, Laura A., Alvarez-Parrilla, E. & González-Aguilar, G. A., 2009. *Fruit and Vegetable Phytochemicals*. Ames, Iowa: Wiley-Blackwell.
- Dun, E. A., Brewer, P. B. & Beveridge, C. A., 2009. Strigolactones: discovery of the elusive shoot branching hormone. *Trends in plant science*, 14(7), p. 364–372.
- Fraser, P. D., Pinto, M. E. S., Holloway, D. E. & Bramley, P. M., 2000. Application of high-performance liquid chromatography with photodiode array detection to the metabolic profiling of plant isoprenoids. *The Plant Journal*, 24(4), pp. 551-558.
- Henry, L. K. et al., 2000. Effects of Ozone and Oxygen on the Degradation of Carotenoids in an Aqueous Model System. *Journal of Agricultural and Food Chemistry*, 48(10), p. 5008–5013.
- Huang, F.-C. et al., 2009. Substrate promiscuity of RdCCD1, a carotenoid cleavage oxygenase from *Rosa damascena*. *Phytochemistry*, 70(4), p. 457–464.
- Huang, F.-C., Molnár, P. & Schwab, W., 2009. Cloning and functional characterization of carotenoid cleavage dioxygenase 4 genes. *Journal of Experimental Botany*, 60(11), p. 3011–3022.
- Ibdah, M. et al., 2006. Functional characterization of CmCCD1, a carotenoid cleavage dioxygenase from melon. *Phytochemistry*, 67(15), p. 1579–1589.

Ilg, A., Bruno, M., Beyer, P. & Al-Babili, S., 2014. Tomato carotenoid cleavage dioxygenases 1A and 1B: Relaxed double bond specificity leads to a plentitude of dialdehydes, mono-apocarotenoids and isoprenoid volatiles. *FEBS Open Bio*, Volume 4, p. 584–593.

Isler, O. L. H., Montavon, M., Rüegg, R. & Zeller, P., 1956. Synthesen in der Carotenoid-Reihe. 1. Mitteilung. Die technische Synthese von β -Carotin.. *Helvetica Chimica Acta*, 39(1), pp. 249-259.

IUPAC, 1974. Nomenclature of Carotenoids. p. 26.

Kanehisa Laboratories, 2015. *KEGG - Terpenoid backbone biosynthesis - Escherichia coli BL21(DE3)*. [Online]

Available at: http://www.genome.jp/kegg-bin/show_pathway?org_name=ecb&mapno=00900&mapscale=&show_description=show [Accessed 12 November 2015].

Kato, M. et al., 2006. The role of carotenoid cleavage dioxygenases in the regulation of carotenoid profiles during maturation in citrus fruit. *Journal of Experimental Botany*, 57(10), p. 2153–2164.

Krings, U. & Berger, R. G., 1998. Biotechnological production of flavours and fragrances. *Applied Microbiology and Biotechnology*, 49(1), p. 1–8.

Lashbrooke, J. G. et al., 2013. Functional characterisation of three members of the *Vitis vinifera* L. carotenoid cleavage dioxygenase gene family. *BMC Plant Biology*, Volume 13, p. 156.

Lashbrooke, J., Young, P., Dockrall, S. & Vasanth, K. V. M., 2013. *National Center for Biotechnology Information*. [Online]

Available at: <http://www.ncbi.nlm.nih.gov/nuccore/KF008001.1> [Accessed 12 November 2015].

Lintig, J. v. & Vogt, K., 2000. Filling the gap in vitamin A research. Molecular identification of an enzyme cleaving beta-carotene to retinal. *The Journal of Biological Chemistry*, 275(16), p. 11915–11920.

Lin, Y.-C., 2013. *The expression of carotenoid cleavage dioxygenases 1, 4a, and 4b in berries of Vitis vinifera throughout ripening and in vitro substrate specificity*, Davis, Calif.: University of California.

Maltzahn, B., 2004. *Design und Modellierung eines integrierten Bioprozesses zur Produktion natürlicher Aromastoffe*. Erlangen: Technische Fakultät der Universität Erlangen-Nürnberg.

Marasco, E. K., Vay, K. & Schmidt-Dannert, C., 2006. Identification of carotenoid cleavage dioxygenases from *Nostoc* sp. PCC 7120 with different cleavage activities. *The Journal of Biological Chemistry*, 281(42), p. 31583–31593.

Mathieu, S. et al., 2005. A carotenoid cleavage dioxygenase from *Vitis vinifera* L.: functional characterization and expression during grape berry development in relation to C13-norisoprenoid accumulation. *Journal of Experimental Botany*, 56(420), p. 2721–2731.

Meckenstock, D. H., 2005. *Breeding red irises*. Hays, KS: Dan H. Meckenstock.

Menary, R. C. & Garland, S. M., 1999. *Authenticating essential oil flavours and fragrances*. Barton, A.C.T.: Rural Industries Research and Development Corporation.

- Noda, C. et al., 1998. Aldol Condensation of Citral with Acetone on Basic Solid Catalysts. *Brazilian Journal of Chemical Engineering*, 15(2).
- Oxley, A. et al., 2014. An LC/MS/MS method for stable isotope dilution studies of β -carotene bioavailability, bioconversion, and vitamin A status in humans. *Journal of Lipid Research*, 55(2), p. 319–328.
- Poucher, W. A. & Jouhar, A. J., 1991. *Poucher's Perfumes, Cosmetics and Soaps -- Volume 1: The Raw Materials of Perfumery 9.th Ed.*. 9th ed. ed. London; New York: Chapman & Hall.
- Qin, X. & Zeevaart, J. A., 1999. The 9-cis-epoxycarotenoid cleavage reaction is the key regulatory step of abscisic acid biosynthesis in water-stressed bean. *Proceedings of the National Academy of Sciences of the United States of America*, 96(26), p. 15354–15361.
- Qin, X. & Zeevaart, J. A. D., 2002. Overexpression of a 9-cis-epoxycarotenoid dioxygenase gene in *Nicotiana plumbaginifolia* increases abscisic acid and phaseic acid levels and enhances drought tolerance. *Plant Physiology*, 128(2), p. 544–551.
- Rodriguez-Amaya, D. B., 2001. *A guide to carotenoid analysis in foods*. Washington, D.C.: ILSI Press.
- Rodríguez-Ávila, N. L. et al., 2011. Identification and expression pattern of a new carotenoid cleavage dioxygenase gene member from *Bixa orellana*. *Journal of Experimental Botany*, 62(15), p. 5385–5395.
- Rosati, C., Diretto, G. & Giuliano, G., 2009. Biosynthesis and Engineering of Carotenoids and Apocarotenoids in Plants. *Biotechnology and Genetic Engineering Reviews*, 26(1), p. 139–162.
- Salter, G. J. & Kell, D. B., 1995. Solvent selection for whole cell biotransformations in organic media. *Critical Reviews in Biotechnology*, 15(2), p. 139–177.
- Schaefer, B., 2007. *Naturstoffe der chemischen Industrie*. 1. Aufl. ed. Heidelberg: Elsevier, Spektrum Akad. Verl..
- Schwartz, S. H., Qin, X. & Loewen, M. C., 2004. The biochemical characterization of two carotenoid cleavage enzymes from *Arabidopsis* indicates that a carotenoid-derived compound inhibits lateral branching. *The Journal of Biological Chemistry*, 279(45), p. 46940–46945.
- Schwartz, S. H., Qin, X. & Zeevaart, J. A., 2001. Characterization of a novel carotenoid cleavage dioxygenase from plants. *The Journal of Biological Chemistry*, 276(27), p. 25208–25211.
- Schwieter, U. B. H. C.-d.-J. L. E. G. K. M. K. A. P., 1965. Synthesen in der Carotinoid-Reihe 19. Mitteilung: Physikalische Eigenschaften der Carotine. *Helvetica Chimia Acta*, Volume 19, pp. 294-302.
- Seo, M. et al., 2000. The *Arabidopsis* aldehyde oxidase 3 (AAO3) gene product catalyzes the final step in abscisic acid biosynthesis in leaves. *roceedings of the National Academy of Sciences of the United States of America*, 97(23), p. 12908–12913.
- Sharma, V. et al., 2012. Synthesis of β -ionone derived chalcones as potent antimicrobial agents. *Bioorganic & medicinal chemistry letters*, 22(20), p. 6343–6346.

- Simkin, A. J. et al., 2004. The tomato carotenoid cleavage dioxygenase 1 genes contribute to the formation of the flavor volatiles beta-ionone, pseudoionone, and geranylacetone. *The Plant journal : for cell and molecular biology*, 40(6), p. 882–892.
- Sokolosky, J. T. & Szoka, F. C., 2013. Periplasmic production via the pET expression system of soluble, bioactive human growth hormone. *Protein Expression and Purification*, 87(2), p. 129–135.
- Srivastava, A. K., Dohare, P., Ray, M. & Panda, G., 2010. Design, synthesis and biological evaluation of new ionone derivatives as potential neuroprotective agents in cerebral ischemia. *European journal of medicinal chemistry*, 45(5), p. 1964–1971.
- Sun, Z., Gantt, E. & Cunningham, F. X., 1996. Cloning and Functional Analysis of the β -Carotene Hydroxylase of *Arabidopsis thaliana*. *Journal of Biological Chemistry*, 271(40), p. 24349–24352.
- Sun, Z. et al., 2008. Cloning and characterisation of a maize carotenoid cleavage dioxygenase (ZmCCD1) and its involvement in the biosynthesis of apocarotenoids with various roles in mutualistic and parasitic interactions. *Planta*, 228(5), p. 789–801.
- Tan, B. C., Schwartz, S. H., Zeevaart, J. A. & McCarty, D. R., 1997. Genetic control of abscisic acid biosynthesis in maize. *Proceedings of the National Academy of Sciences of the United States of America*, 94(22), p. 12235–12240.
- Tan, B.-C. et al., 2003. Molecular characterization of the *Arabidopsis* 9-cis epoxy-carotenoid dioxygenase gene family. *The Plant Journal*, 35(1), p. 44–56.
- Thompson, A. J. et al., 2000. Ectopic expression of a tomato 9-cis epoxy-carotenoid dioxygenase gene causes over-production of abscisic acid. *The Plant Journal*, 23(3), p. 363–374.
- Venkata, B. J. G. S. & Peeples, T. L., 2009. *Biocatalysis for oxidation of naphthalene to 1-naphthol: liquid-liquid biphasic systems and solvent tolerant strains*, s.l.: University of Iowa.
- Vogel, J. T., Tan, B.-C., McCarty, D. R. & Klee, H. J., 2008. The carotenoid cleavage dioxygenase 1 enzyme has broad substrate specificity, cleaving multiple carotenoids at two different bond positions. *The Journal of biological chemistry*, 283(17), p. 11364–11373.
- Yahyaa, M. et al., 2013. Formation of norisoprenoid flavor compounds in carrot (*Daucus carota* L.) roots: characterization of a cyclic-specific carotenoid cleavage dioxygenase 1 gene. *Journal of agricultural and food chemistry*, 61(50), p. 12244–12252.
- Zhou, J., Geng, G., Batist, G. & Wu, J. H., 2009. Syntheses and potential anti-prostate cancer activities of ionone-based chalcones. *Bioorganic & medicinal chemistry letters*, 19(4), p. 1183–1186.

9 Appendix

9.1 Standard measurements

9.1.1 Carotene analysis by HPLC-PDA

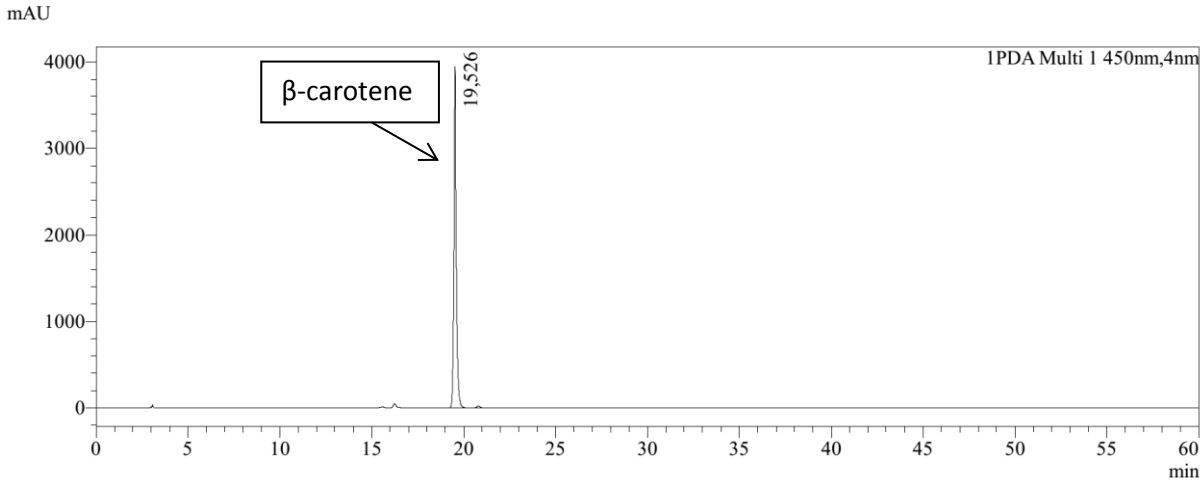


Figure 33: β-carotene standard

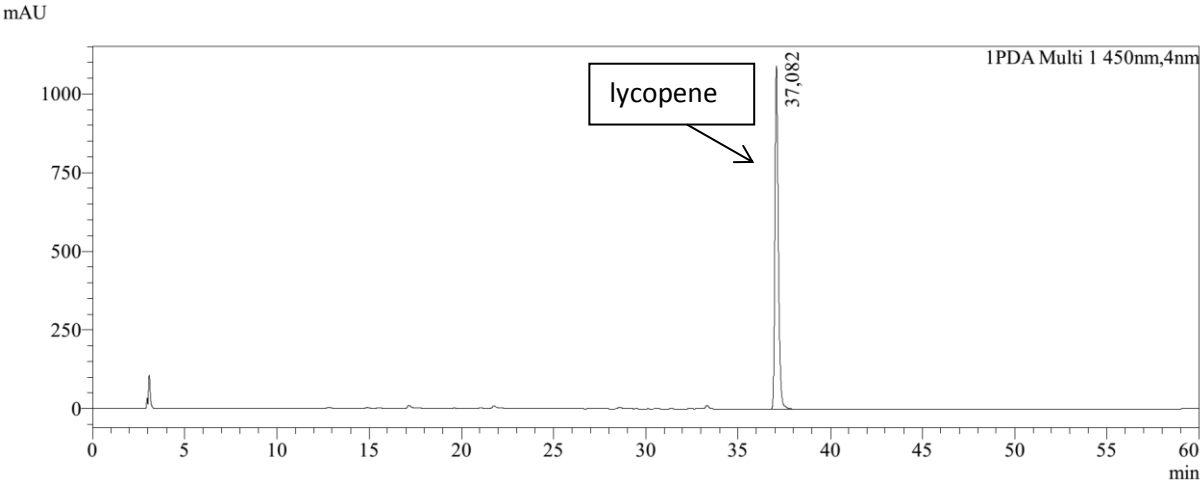


Figure 34: Chromatogram of the lycopene standard

9.1.2 Ionone analysis by GC-MS

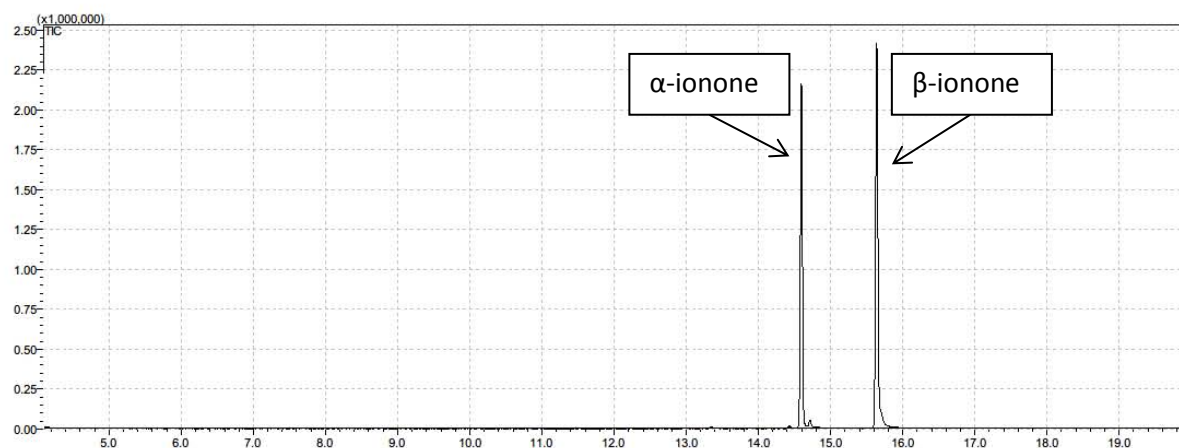


Figure 35: Chromatogram of the α -ionone and β -ionone standards

The method provides separation of the very similar compounds α -ionone and β -ionone with a difference in retention time of about 1 minute. When the GC column was exchanged by a new one, the retention times changed slightly. The new retention times were 14.8 min. for α -ionone and 15.8 min. for β -ionone.

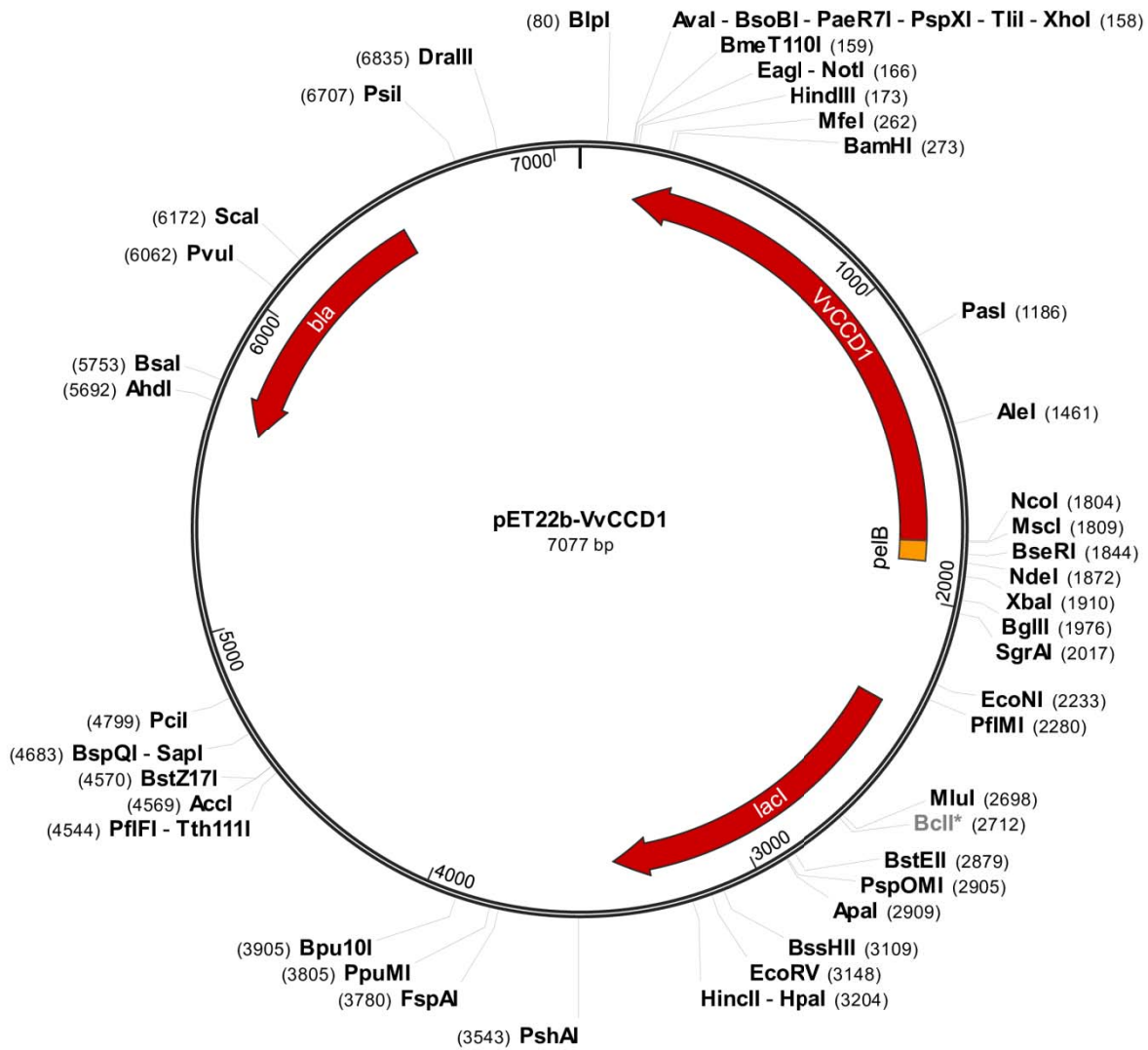


Figure 37: Vector map of pET22b-VvCCD1

9.2.2 pBAD-A

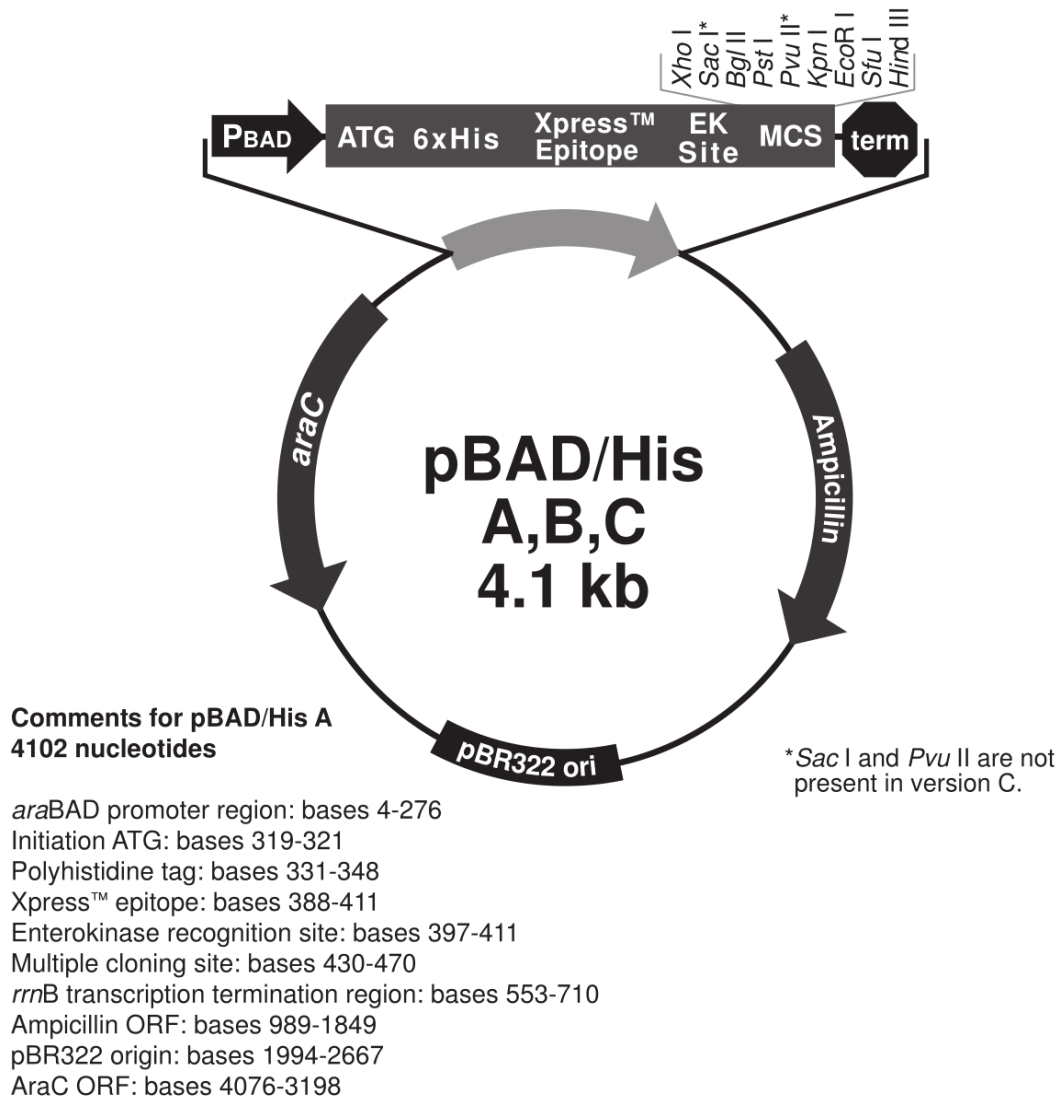


Figure 38: pBAD vector map (Invitrogen pBAD User Manual, 2010)

pBAD/His A Multiple Cloning Site

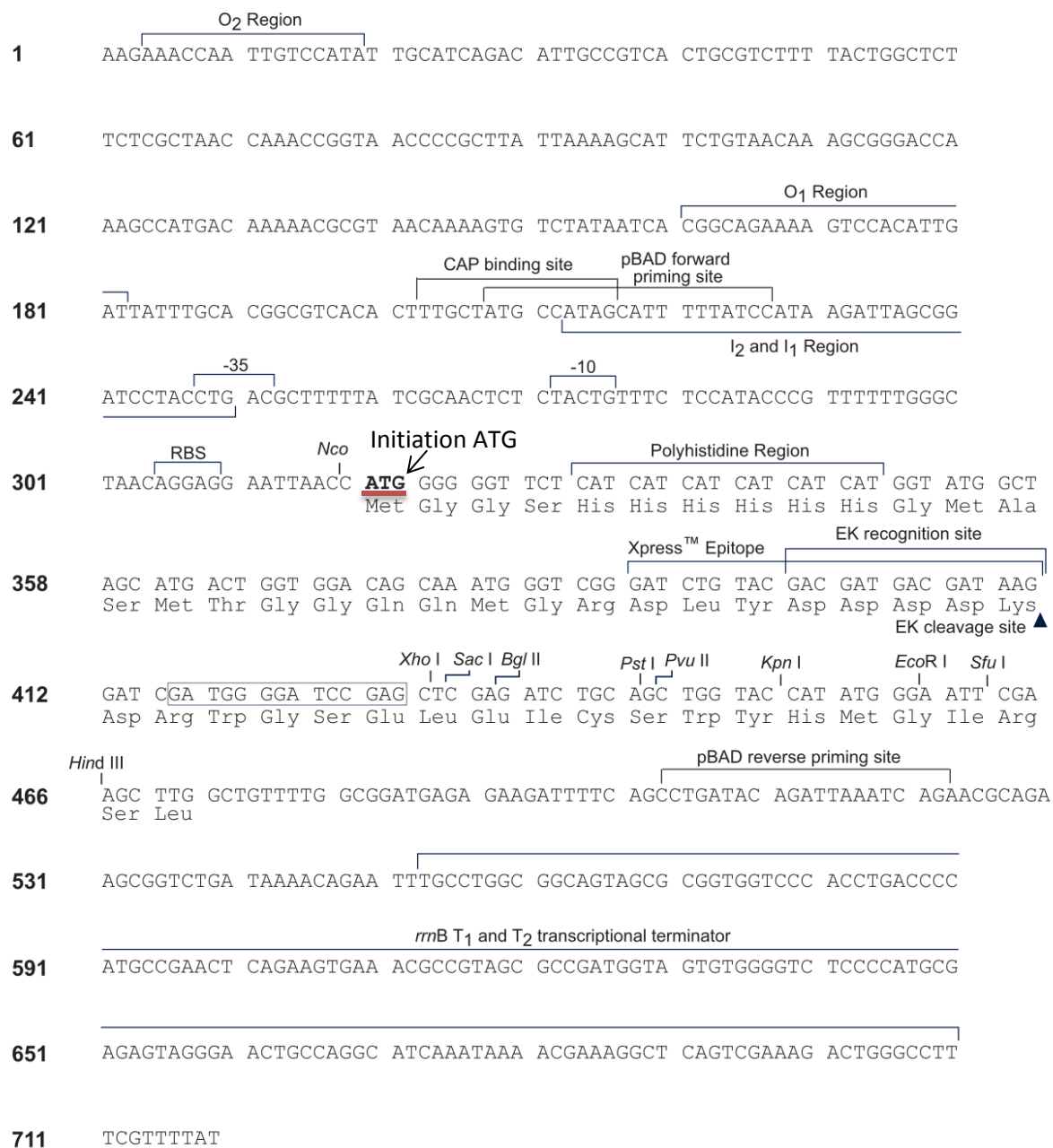


Figure 39: pBAD vector multiple cloning site. Row 301 shows the initiation ATG where VvCCD1 was cloned into.

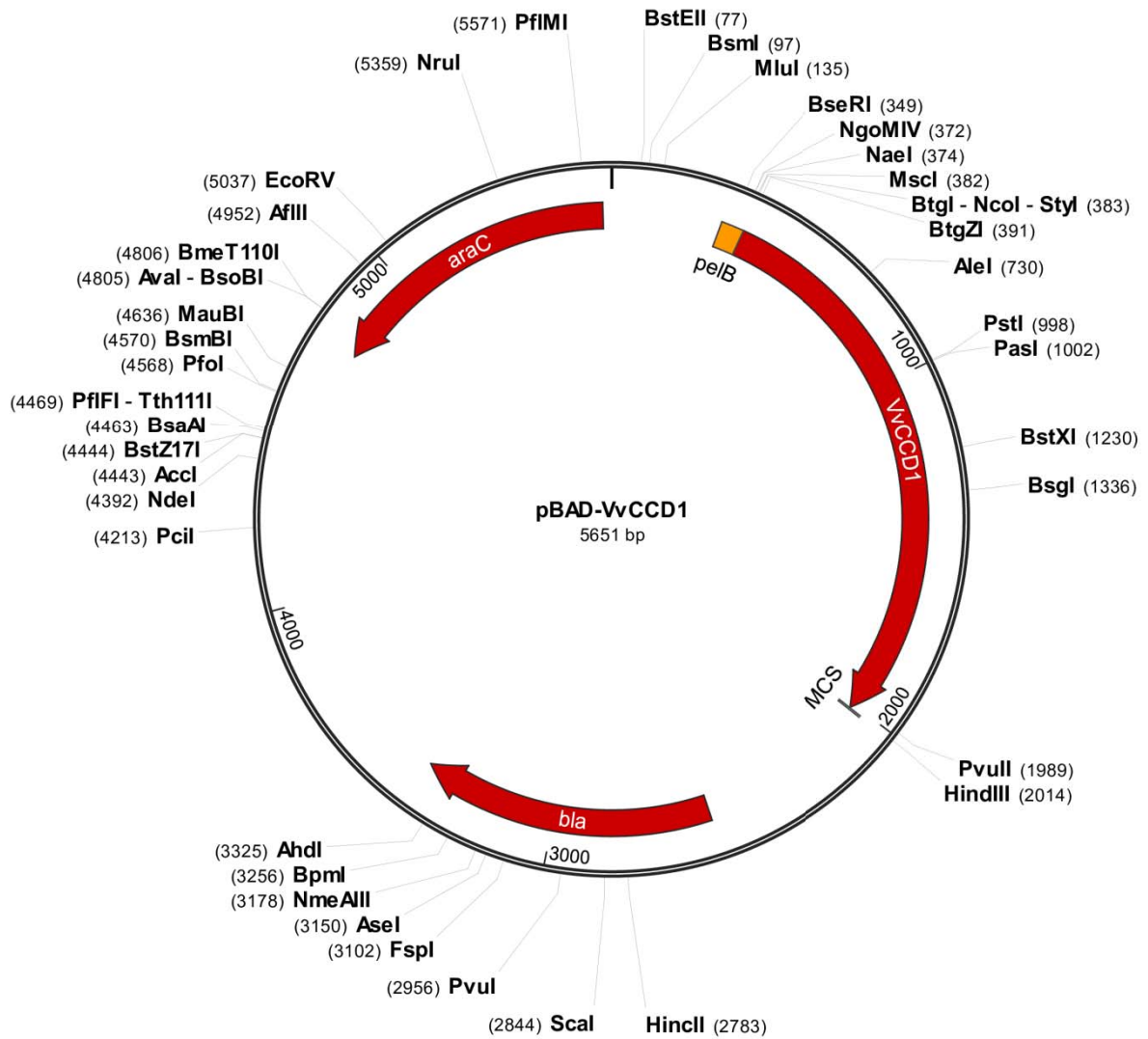
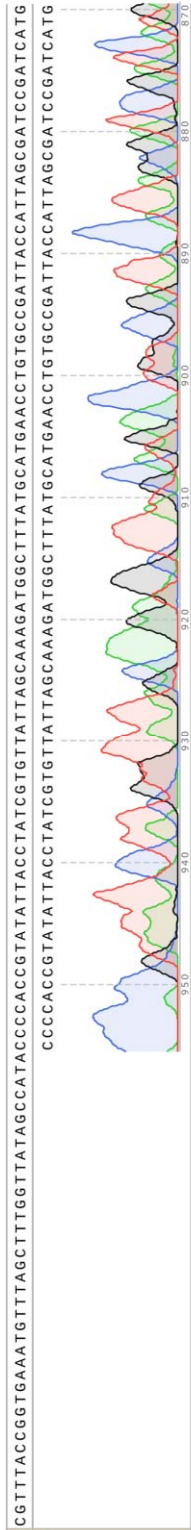
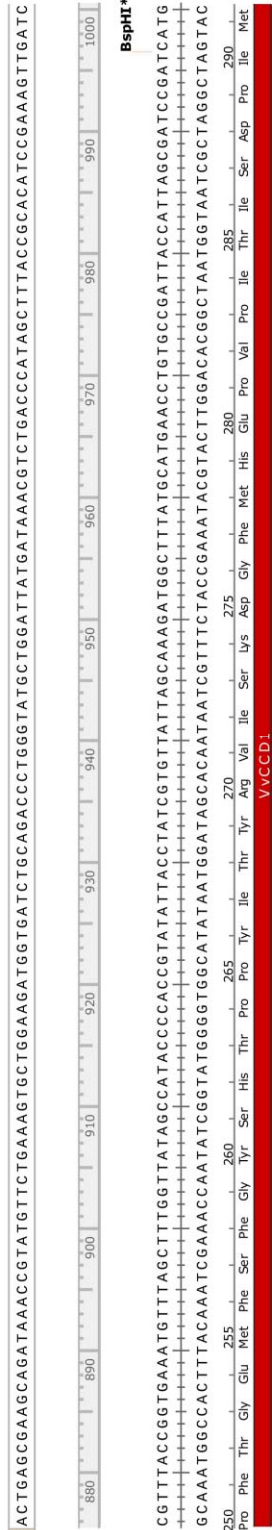
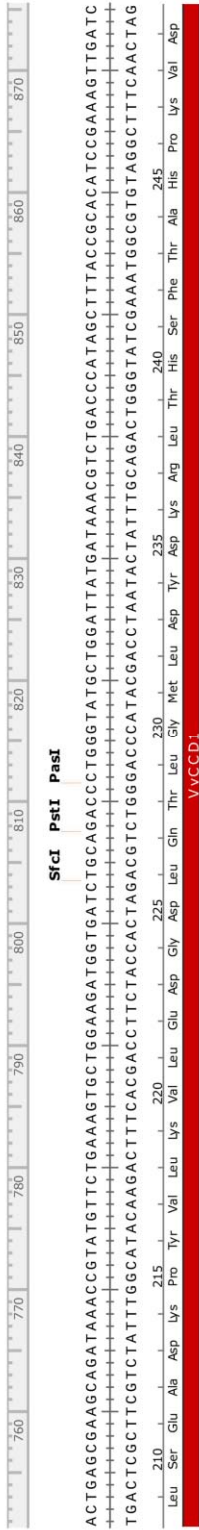
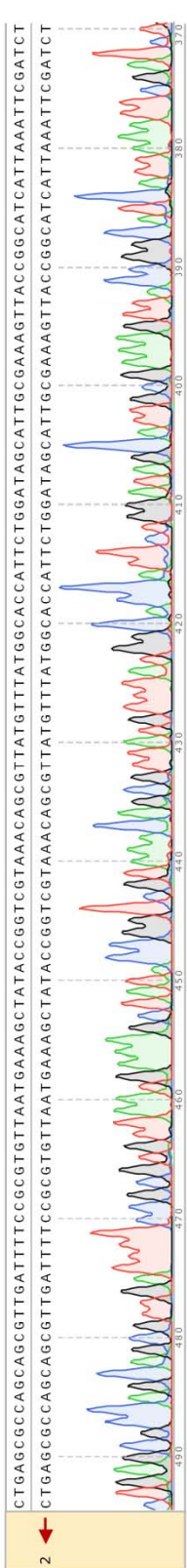
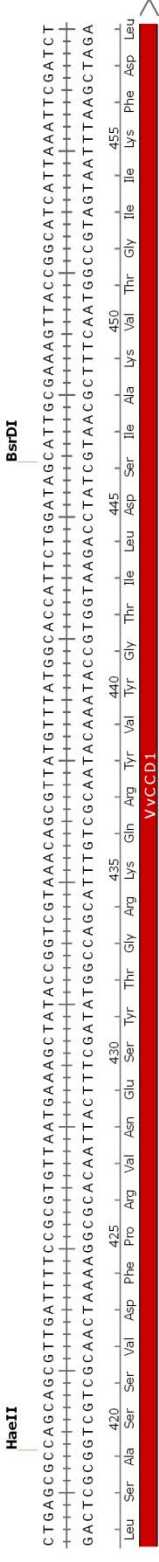
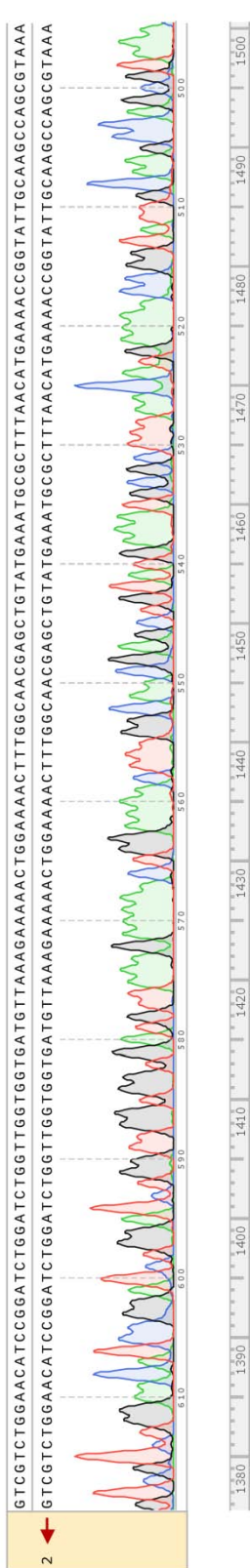
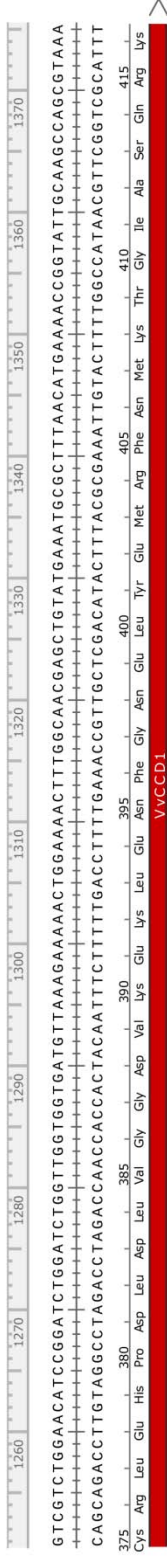
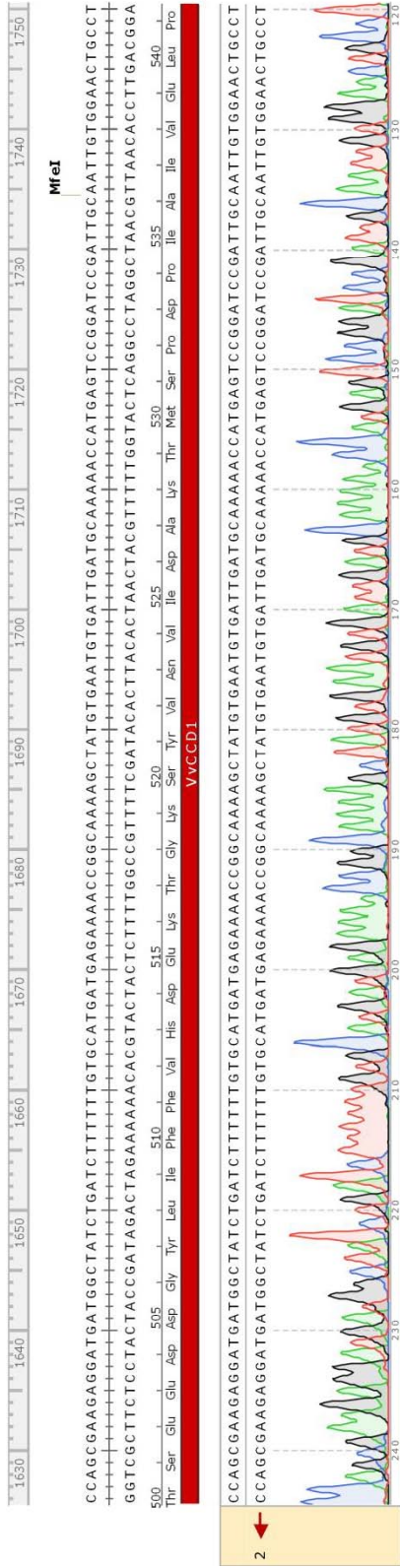
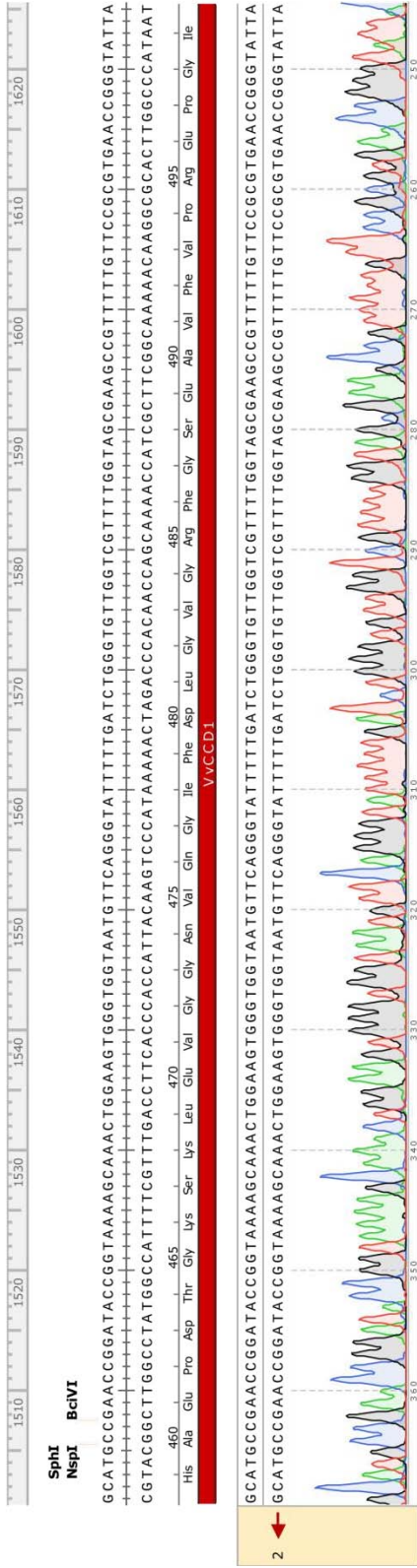


Figure 40: Vector map of pBAD-VvCCD1







10 Affirmation

I certify, that this master thesis “**Biotechnological production of flavourings**” was written by me, not using sources and tools other than quoted and without use of any other illegitimate support.

Furthermore, I confirm that I have not submitted this master thesis either nationally or internationally in any form.

Vienna, 08 February 2016

Marcel Hans